DESIGN STRATEGY FOR AND IMPLEMENTATION OF ELECTROSTATIC CONTROL OF DIESEL EXHAUST

by

Mark C. Zaretsky

S.B., Massachusetts Institute of Technology
June 1980

SUBMITTED IN PARTIAL FULFILLMENT OF THE
REQUIREMENTS FOR THE DEGREE OF

MASTER OF SCIENCE

at the

MASSACHUSETTS INSTITUTE OF TECHNOLOGY

June 1982

Signature of Author . . . . . .
Department of Electrical Engineering
and Computer Science, May 21, 1982

Certified by . . . . . .
James R. Melcher
Thesis Supervisor

Accepted by . . . . . .
Arthur C. Smith
Chairman, Departmental Committee
on Graduate Students

Design Strategy For and Implementation Of Electrostatic Control of Diesel Exhaust

by Mark C. Zaretsky

Submitted to the Department of Electrical Engineering and Computer Science in partial fulfillment of the requirements for the degree of Master of Science
May 21, 1982

ABSTRACT

Diesel soot is a highly conducting, submicron, fluffy particulate. Problems with electrostatic collection of soot due to its physical nature are separated as follows: (1) fouling of the corona element, (2) fouling of the high voltage insulation, (3) reentrainment due to induction charging, (4) lengthy residence times for efficient collection, (5) transport of collected soot to a storage area and (6) storage of collected soot. Various solutions to each problem are suggested and two, in particular, were investigated.

One solution dealt with the reentrainment problem by trapping soot in a field free region. With the traps as the collection electrode, a single stage ESP was tested on a single cylinder diesel engine. Treatment of 13.1 acfm at flow velocities of 3.2 m/s at collection efficiencies of 92.5% when clean and 76.9% after 4 hours (measured by impactor sampling) was accomplished. Power consumption of the device was between 18-27 W, however, no attempt had been made to prevent fouling of either the corona element or the high voltage insulation. Minimum residence time in the ESP was 150 ms. Scaling up the ESP to handle the total output of an 8 cylinder engine, 340 acfm at 600°F, implied a total collection surface area of 10.2 sq. ft.

Electrofluidized beds (EFB's) can operate at comparable efficiencies with a large savings on volume. The second scheme investigated involved a liquid enhanced EFB (LEEFB). Introduction of the proper liquid into the bed would serve three, possibly four, purposes: (1) insulate the bed particles by adequate dispersion of the collected soot, (2) insure adhesion of soot to the bed particles, (3) compact the soot and (4) provide a possible transport medium for removal of collected soot from the bed. This device treated the entire output of a single cylinder, 23 acfm. When using a bed mixture of #2 sand and Shell 10W-40 motor oil (7.1% loading by mass), steady state collection efficiencies of 60%-65% were measured using a light extinction method. Stable operation (below current limit of power supply) was maintained for a period of 75 minutes. Over this time power consumption doubled from 3.5-7 W.

Two major limitations were temperature and power consumption. The exhaust was cooled to 200°F to prevent volatilization of the motor oil. Application of the LEEFB to

diesel cars requires an economical exhaust cooling system, an oil with much beter thermal stability or a combination of the two. The Dow Corning 710H silicone oil has a usable temperature range of up to 600°F but, in experiments performed at 200°F, resulted in greater power consumption and shorter stable bed operation times.

Thesis supervisor: James R. Melcher
Title: Professor of Electrical Engineering
Massachusetts Institute of Technology

ACKNOWLEDGEMENTS

First of all, I would like to express my extreme gratitude for the opportunity to work with Professor James Melcher. I greatly appreciate the time and effort he has put into this project. He has been a strong, positive influence on my intellectual growth and maturation.

General Motors generously funded this project and provided a most interesting experience in attempting to design a practical device. Carleton Speck was very helpful with providing information and opinions - I hope he accomplishes what has been attempted here. Thanks are due to Dr. Joe Rife and the Sloan Automotive Lab, particularly to Don Fitzgerald and Sal Albano, for help in using the diesel engine.

Frank Beunick did most of the machining for which I can only offer praise. He is someone who is never at a loss for a suggestion and was a great asset. Paul Warren provided much needed third and fourth hands as well as good company. The Continuum E. lab group were a fine bunch of people to work with. Special thanks go to Eliot and Sol, without whom this page probably would never have seen the light of day, and to Rick - whose drive will never cease to amaze me and encourages me to push on as best I can. My friends, both in and out of Baker House, were always able to somehow ease the pressure. I will miss them dearly.

Finally, to my parents I wish to say thank-you for all you have done and may I prove to be worthy of it.

TABLE OF CONTENTS

LIST OF FIGURES

LIST OF TABLES

LIST OF SYMBOLS

Q_v - volume flow rate

V - voltage

A - cross-sectional area

τ_{ESP} - ESP characteristic collection time

s - ESP electrode spacing

b - mobility

E - electric field

η - efficiency

c - experimental constant for EFB's

ℓ_o - unfluidized bed height

R - bed particle radius

U - mean gas velocity

τ - characteristic time of a process

τ_{EFB} - EFB characteristic collection time

τ_e - ion relaxation time

$V_{col.}$ - volume of collection region

τ_{gc} - gas residence time in collection region

n_{in} - particulate density in exhaust

b_ℓ - liquid mobility

E_w - average electric field strength normal to A_w

A_w - electrophoresis collection surfaces

n_ℓ - particulate density in liquid

ρ_s - soot mass density

a - radius of soot particle

C_d - discharge coefficient

d - diameter of orifice

g - gravitational constant

Δp - pressure drop

ρ - gas density

I - light intensity

σ - scattering cross-section

n - particulate density in exhaust

ε_o - permittivity of free space

F_ℓ - Lebedev lift-off force

F_H - van der Waal's forces

m_s - mass of soot particle

Chapter 1: Introduction

1.1 Motivation

Due to a growing awareness of a worldwide energy crisis and, more directly, uncertainty in oil supplies, the American auto industry and public has begun to look towards more fuel efficient automobiles. A step in this direction has been made by General Motors in the form of a large commitment to light duty diesel vehicles. Projections have been made by GM predicting diesels to comprise 20%-25% of the car market by 1990 (1). Diesel engines, due to higher compression ratios, higher combustion temperatures and longer duration of combustion during power stroke, are inherently 25% more fuel efficient than gasoline engines (2).

Among the negative aspects of diesels is the vast amount of solid emissions exhausted. Diesels emit 50-100 times as much solid emissions as comparable gasoline engines. Up until the late 1970's recognition of this fact was evidenced only by smokemeter tests and complaints of "smelly" diesels. No mention of particulates is made in an SAE paper released in 1976 studying diesel emissions (3). However, in 1977, quantitative measurements of particulates in grams/mile were presented (4).

Originally, proposed legislation would have set particulate levels for light-duty diesel vehicles at .6 g/mi by 1981 and .2 g/mi by 1983 (5). From the industrial point

of view, the 1981 deadline was "stretching existing technology" and the 1983 deadline "not yet feasible"(6). Extensions were granted and the deadlines were pushed back to 1982 and 1985 respectively (7). The 1982 standard has been met but a satisfactory solution to the 1985 deadline has not yet been achieved (8).

Just how bad is diesel soot? (Note that the terms soot, particulate and solid emissions are taken to be the same in this thesis and will be used interchangeably). With a mean diameter of .1-.3 microns the soot is of the right size to penetrate to the depths of the lungs and reside there (9). It is known that many carcinogenic hydrocarbons are adsorbed onto the surfaces of the soot (10,11). The questions are: (1) can these hydrocarbons enter the internal systems and (2) how much of a factor is soot in t e overall picture of pollutants inhaled? The answer to the first question appears to be yes - there are chemicals in the body which can remove the hydrocarbons from the soot. At least two known mechanisms can account for this: (1) the soot is small enough to be engulfed by the lung tissue and then enter the bloodstream or (2) eventually (after many months) soot is coughed out of the lungs, most of it enters the gastrointestinal tract where biosalts, which remove PAHs well, are produced (9). One epidemiological study has shown a correlation between mortality from cancer, especially stomach cancer, and suspended particulate matter (12). Also shown was a disappearance of benzo(a)pyrene, a known

carcinogen, from soot recovered from human lungs. However, the answer to the second question is unknown due to the variety of pollutants which contribute to the suspended particulate matter. What is clear is that an increase in soot levels due to poor emission controls combined with increased use of diesel cars would result in an increase of carcinogenic material in the air.

Another potential hazard of diesel emissions is its affect upon the local atmosphere. The small particles will tend to remain suspended in the air for long periods of time, thus raising smog and visibility problems. In some cities, a failure to control diesel exhaust emissions and an increased percentage of diesels on the road could lead to reductions in visibility from 20%-50% (8).

For an eight cylinder, 350 cubic inch Oldsmobile diesel engine, GM has set forth requirements which call for reducing solid emissions to meet the 1985 EPA regulation of .2 g/mi. Using .6 g/mi as the rate of solid particulate emissions, a filter collection efficiency of 60% is required. Limitations on filter design are also placed on maintenance frequency and complexity, power consumption, loss of fuel economy and cost. These criteria are examined in more detail further on.

1.2 Electrostatic Control and Alternatives

The successful application of electrostatic fields in controlling industrial solid emissions has a long history. An excellent account may be found in H.J. White's Industrial Electrostatic Precipitation along with many theoretical and experimental explanations of the technology (13). Electrostatic precipitators (ESP's) are very attractive because of their energy efficiency and simplicity. The electrical forces act directly on the particulate and not through any intermediary medium. ESP's are passive in that there are very little, if any, moving parts and the gas flow is relatively unrestricted as it traverses the device. Application of ESP's in controlling diesel exhaust leads to different problems than those traditionally encountered.

Two known attempts at electrostatic control of diesel soot should be mentioned. One was by a group in Japan headed by Professor Masuda (14). The idea was to precipitate the charged soot onto a moving belt collection electrode. The soot was compressed onto the belt by rollers and then scraped off into a hopper. Collection efficiencies of 93% at an exhaust flow velocity of 1.5 m/sec were observed. Actual tests were performed using soot generated from burning city gas. A mean diameter of 1 micron was characteristic of this soot, three times that of soot produced by a diesel engine. Also, the temperature of the gas passing through the device was 104°F, much lower than typical engine exhaust temperatures.

The second attempt was by Professor Stuart A. Hoenig at University of Arizona at Tucson (15). A cylindrical ESP was hooked up to a three cylinder diesel engine. Effective cleaning of the gas was reported although no efficiencies were stated. The device was rather large, approximately 4 ft. in length with a 6 in. radius. Application of the device was geared towards cleaning up exhaust from stationary sources, i.e. fixed farm machinery. Exhaust flow velocities were 3 or 4 m/s and 300°-400° F (16).

A large effort has been concentrated on developing a purely mechanical collection of diesel soot. There were two basic approaches taken here. One was to mechanically collect the soot on metallic or fabric fibers and allow them to agglomerate. Once agglomerated, to approximately 1 micron in diameter, they were then blown off into a secondary collector, such as a cyclone.

This mode of collection was investigated by Karl Springer and Ralph Stahman (17). The primary collector, used as an agglomerator, was a cylindrical tube packed with Texaco alumina coated steel wool. A separator called TAVs, for single tangential anchored Vortex, served as the secondary collector. After tests performed over many Federal driving cycles the device effectiveness decreased to about 6% from a $66\frac{2}{3}$% efficiency when new. The alumina coated steel wool initially performed as traps. After 1227 miles they were agglomerating, their initial function. The inertial separator operated at an efficiency of 6% - not enough to

make its inclusion worthwhile. The conclusion was that the agglomeration must produce heavier and bigger particles.

A way of judging whether or not a particular device is 'worthwhile' is to judge its adverse affects, if any, upon car operation. The steel wool was a physical obstruction to exhaust flow - the engine had to work against an increased back pressure. The results would be reduced fuel economy and longer acceleration times. In the above project acceleration times, already a problem with diesels, were up to 20 percent longer and engine exhaust back pressures were about 11 times the standard of 25 mm Hg at 55 mi/hr. No measurable decrease in economy was reported.

A similar device, called an Aut-Ainer, was developed by Eikosha Company, Ltd. (18). The primary collector, originally designed to function as a particulate trap, was a 3-stage throttle-plate with the regions in between the plates packed with metal wool. It was reported that cleaning must occur every 1200 miles or the device acted solely as an agglomerator and did not collect (10). A later version had the primary stage functioning as an agglomerator and the second stage, a cyclone, functioning as an inertial separator. In preliminary tests on a diesel engine no plugging was mentioned and an increase in back pressure of only 12 inches H_2O was reported. No further mention of this device has turned up in the literature.

The other philosophy in mechanical collection involves a cellular ceramic filter whose walls are porous. As exhaust

passes through the pores, they are increasingly plugged up with soot and thus, collect more and more efficiently. However, the increased plugging also means increased back pressure. Regeneration of the filter by oxidizing the soot eliminates the problem of excessive soot buildup. The development of a monolithic cellular ceramic filter composed of cordierite by Corning Glass Works has focused much attention towards this approach (19,20,21).

In contrast with the agglomerator/inertial separator scheme (fig. 1.1c) the efficiencies of ceramic filters tend to start out low and increase over ti me depending on pore size (fig. 1.1b) (17,19). Also shown is the time dependence of the back pressure (fig. 1.1a) (19). In addition to pore size, wall thickness plays an important part in determining the time scale over which operation can be called satisfactory. For example, a doubling of wall thickness for a 12.5 micron mean pore size filter halves the time to achieve a pressure drop of 55.1 in. H_2O across the filter. After experimenting with many cell geometries one design was singled out based on efficiency and capacity requirements. This design was capable of greater than 80% efficiencies and operating times of over 2 hours with maximum filter pressure drop less than 55.1 in. H_2O (19).

For continuous operation of the filter, regeneration by oxidation of the soot must take place. An average trap pressure rise rate of 44.6 in. H_2O/100 mi. at a cruise condition of 40 mi/hr. has been observed (20). The effect of

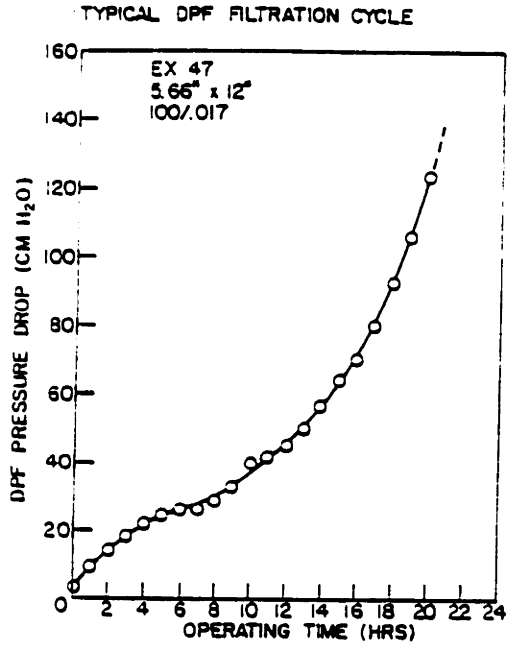

(a)

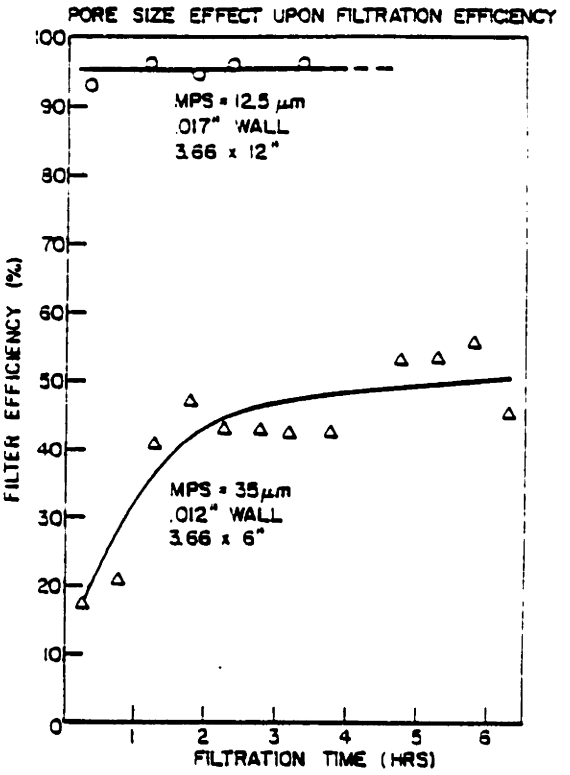

(b)

Data using Corning Glass ceramic filter

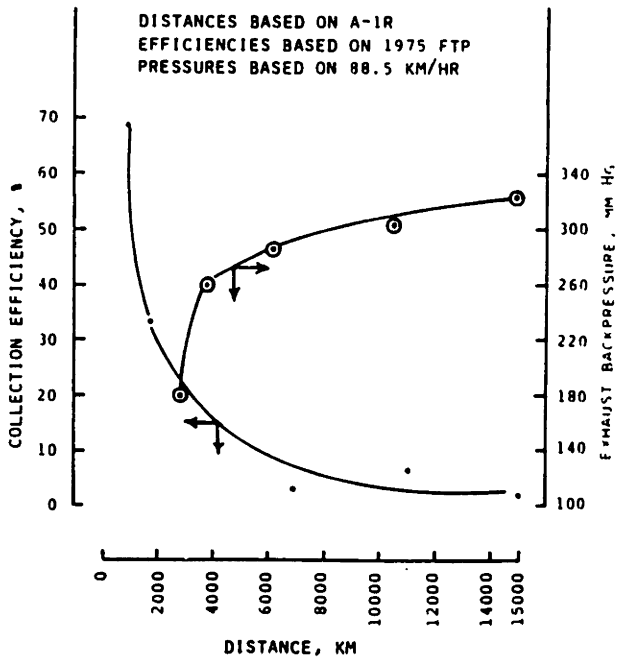

(c)

Data using Alumina coated steel wool filter

Figure 1.1

this increased back pressure was a 1% loss in fuel economy for every increase of 13 in. H_2O. Based upon particulate economy, the frequency of regeneration would be every 90 to 120 miles. The lower mileage limit arises when fuel economy loss reaches 3% - probably the overriding factor determining regeneration frequency.

The three major requirements for oxidation to occur are high exhaust temperatures (above 900°F at trap inlet), sufficient oxygen concentration (above 2%) and adequate time to complete combustion. As shown in an exhaust temperature map for a 2.3L engine, temperatures above 900°F are reached only for very short periods of time during high speed/high load conditions (fig. 1.2) (20). Various combustion strategies have been outlined and investigated (20-22). They include the use of catalysts, either in the diesel fuel or on the filter surface, which would lower the ignition temperature of the soot. Fuel additives, such as lead, lowered the ignition temperature by as much as 300°F but may have adverse effects upon the engine, fuel injection system and the trap and may introduce yet another pollutant into the atmosphere. Catalysts impregnated in the trap produced no effect, possibly due to the exposure of relatively little soot to the catalyst. Throttling the engine produced higher exhaust temperatures and caused oxidation to occur at a 55 mi/hr. cruise condition. Fuel consumption and exhaust emissions increased as a result of the lowered air/fuel ratios. If overthrottling occurs (a lack of sufficient

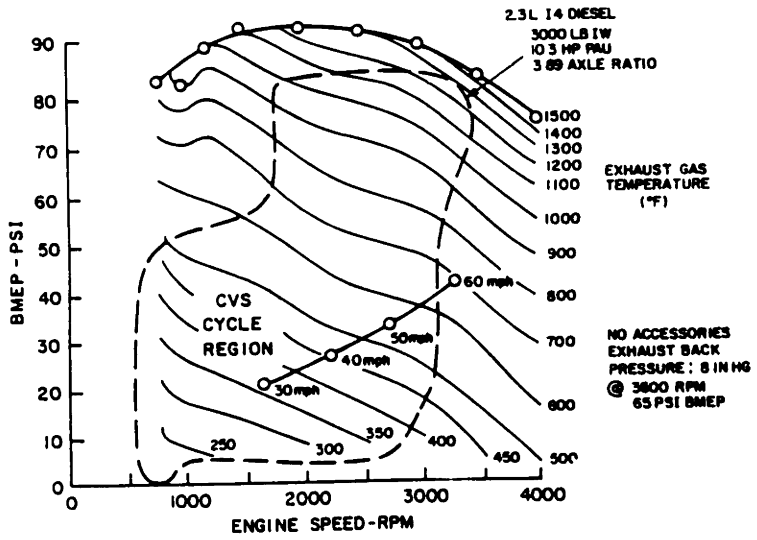

Exhaust temperature map

Figure 1.2

oxygen for combustion producing super-heated particulates) a "run-away" regeneration occurs and the filter melts.

The next option is to place a burner just upstream of the filter which would heat the exhaust and produce the needed regeneration conditions. A burner using the exhaust gas as the combustion oxygen supply has achieved regeneration at the 55 mi/hr. cruise condition but increased fuel consumption by 5% . An air-fed burner consumed only 2.5% additional fuel but requires a complex air-pump system.

Each regeneration scheme increases and decreases various pollutants such as HC, CO, and NO_x . Indeed, a major problem is the fact that the combustion conditions which produce less particulates will, by nature, produce more NO_x emissions (23). Another problem is the necessity for even distribution, axially and radially, of the thermal stresses as heating of the filter occurs. Thus the filter must be very durable, both mechanically and thermally.

Recent work at Texaco has attempted to use the alumina coated steel wool as a complete trapping system, as opposed to the agglomerator mode studied by Springer and Stahman (24). This step is a logical one since high trapping efficiencies due to the steel wool had been reported. At a 50 mph cruise condition collection efficiencies of 65% were attained. The engine used was a 1980 Oldsmobile diesel 350 V-8 so it is unusual that reported particulate emissions with no exhaust gas recirculation or muffler was .133 g/mi, way below the normally quoted value of .6-.8 g/mi. A

decrease in fuel economy of 1.8% due to the pressure drop across the filter was measured. Regeneration of the filter was accomplished with a catalytic torch using propane gas. The torch introduces a hydrocarbon into the exhaust and catalytically oxidizes it, providing the heat necessary to regenerate the soot. After 100 regenerations, at intervals of 150-200 miles the filter still performed satisfactorily.

It is interesting to note that the majority of these designs originated as possible solutions to the emissions problems of a gasoline engine (25). There, all the surfaces over which the exhaust passed, either steel wool, fibers or ceramic filter, were impregnated with catalysts.

A novel approach taken by FIAT was to use a fluidized bed as an agglomerator and a cyclone as a collector (26). Efficiencies of up to 90% soot removal were reported. An increase of 4% to 10% in fuel consumption due to increased exhaust back pressure was also reported. Evidence of agglomeration was given as a visual examination of soot collected by the cyclone. This soot was actually separated out of the flow because it was still deposited on sand fines that, through attrittion or otherwise, had been elutriated from the bed. Soot itself was not being agglomerated to large enough sizes to be removed inertially. It should be noted that this system was designed to improve heat recovery from exhaust gases in an effort to conserve energy. A cooling coil exposed to the exhaust became fouled with soot, greatly reducing its heat transfer ability. The fluidized

bed particles scrub the soot off the coil walls thus improving heat transfer as well as serving as surfaces upon which soot agglomerates.

The main adverse effect with all these schemes is the loss of fuel economy, generally due to an increase in exhaust back pressure. For the ceramic filters, this back pressure increase necessitates the regeneration of the collected soot. Regeneration can be achieved using a burner upstream of the filter with the consequence of a greater reduction in fuel economy. At this writing, the problems of durability and cost of such a filtering scheme have not been resolved satisfactorily. It is clear that any electrostatic control scheme must minimize exhaust back pressure.

1.3 Diesel Soot

In a sentence, diesel soot is a highly conducting (electrically), submicron particulate. An elemental chemical analysis shows carbon to be the main constituent, approximately 85% by mass, with traces of sulfur, zinc, phosphorus, calcium, iron, silicon and chromium also present (27). Many of these elements are found in the diesel fuel or lubricating oil additives. The large amount of carbon present accounts for the high electrical conductivity. There are also polynuclear aromatic hydrocarbons (PAH) adsorbed onto the surface of a soot particle. Many of the PAH are known carcinogens and are the cause of much controversy when the health effects of soot are considered.

More than 50% of the soot particles, by mass, are under .3 microns in diameter. The particles are irregularly shaped, as borne out by the fact that a range of 2-13 for the ratio of measured to superficial surface area has been observed (27). When collected, as in schemes mentioned previously, the soot was described as having a flour-like consistency. The soot particles are fluffy, not dense, and pack with a density of about .1 g/cc^3 . There are many physical similarities between diesel soot and carbon blacks produced as pigments for the rubber industry and for ink, coating and plastics applications (28).

A great deal of industrial usage of ESP's has been for collecting flyash, a substance which is highly resistive in the temperature range in which the ESP operates. Treatment of a highly conducting particulate is bound to introduce unique problems which will adversely affect collector efficiency and power consumption. These problems have been encountered when designing ESP's for treatment of exhaust from oil-fired boilers. Collection of particulate was effected by modifying existing ESP's designed to collect flyash. Additional insulator bushings cleansed by air-injection, increased amperage capability of power supply and control technology for current limiting were necessary additions due to the low resistivity of the particulate (29). ESP's have also been operated as agglomerators preceding an inertial separation collector stage. A pilot plant study for enhanced scrubbing of black liquor boiler

fumes utilized this system and reported increased efficiencies due to the agglomeration (30). It was also concluded that the agglomeration occurred mainly at the collection surfaces and resulted in an increase in particle diameter of one to two orders of magnitude. However, due to frequent shut-downs to allow cleaning of fouled surfaces and increased power consumption, interest in this scheme has diminished (31) and been replaced with a multi-stage inertial agglomerator/separator i.e. cyclones.

Generally, the smaller the particulate being collected the larger the ESP must be to operate at similar efficiencies. For particulate below 1 micron in diameter the size of an ESP becomes prohibitive. These problems will be discussed more fully in the next chapter.

1.4 Goals

There are two major purposes of this project. The first is to develop a cohesive strategy for electrostatically collecting highly conducting, submicron particulate (i.e. diesel soot). As noted above, there are new problems that may arise due to the physical nature of the soot. By breaking down the various functions necessary for collection into separate, though not independent, categories, the basic building blocks for a design strategy will become clear. It will be instructive to build an ESP and observe its shortcomings firsthand in an effort to clarify the problems

that must be contended with.

The second purpose will be to actually follow through one set of options that emerge from the above strategies. That is, design, build and test a collection device which also meets constraints that are amenable to installation on a diesel automobile. Obviously, the device will also justify whether or not the design strategy evolved is a reasonable one.

Chapter 2: Design Strategy

2.1 Design Strategy

All ESP's operate using the same basic concepts although the particular implementation may vary from one to another. The idea is to charge the particulate being collected and then use a basic coulombic attraction to precipitate the charged particulate onto a collection electrode of opposite polarity. As shown in figure 2.1 , ESP's can be single stage or two stage. The advantage to a two stage design is the flexibility of having separate power supplies for the charging and collection stages. The advantage to single stage is the presence of space charge throughout the device thus, reentrainment of once precipitated soot can be countered by subsequent charging and precipitation. For a more complete explanation of ESP operation and design see reference 13. It will be assumed from here on that this basic understanding is present.

Qualitative experiments using a single stage ESP with a modified collection electrode were conducted. Details of the design are presented in chapter 5. For now, attention is focused on the problems associated with long-term operation of the ESP. A major problem is the reentrainment of precipitated particulate. Upon precipitation the highly conducting soot immediately reverses its charge, through conduction, and recharges with the same polarity as the collecting electrode. While residing on the collecting

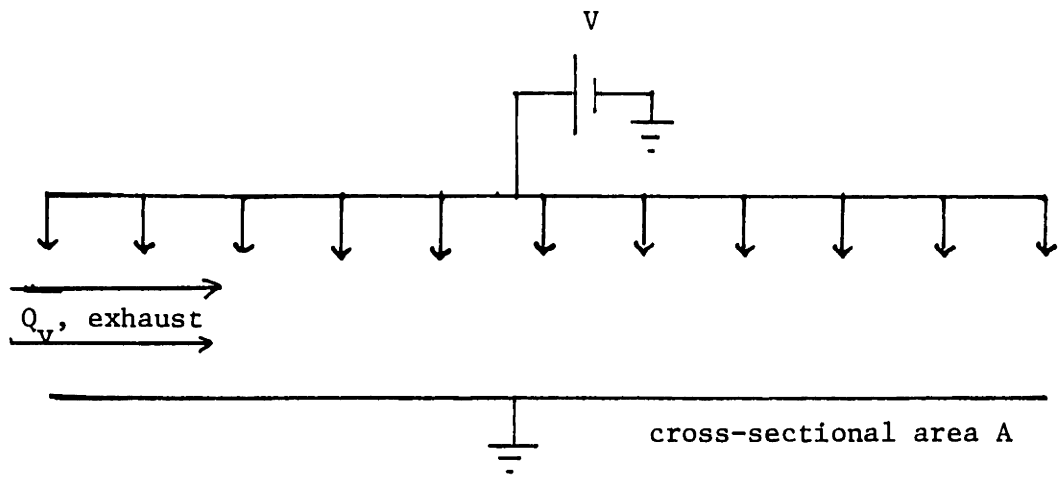

Single stage

(a)

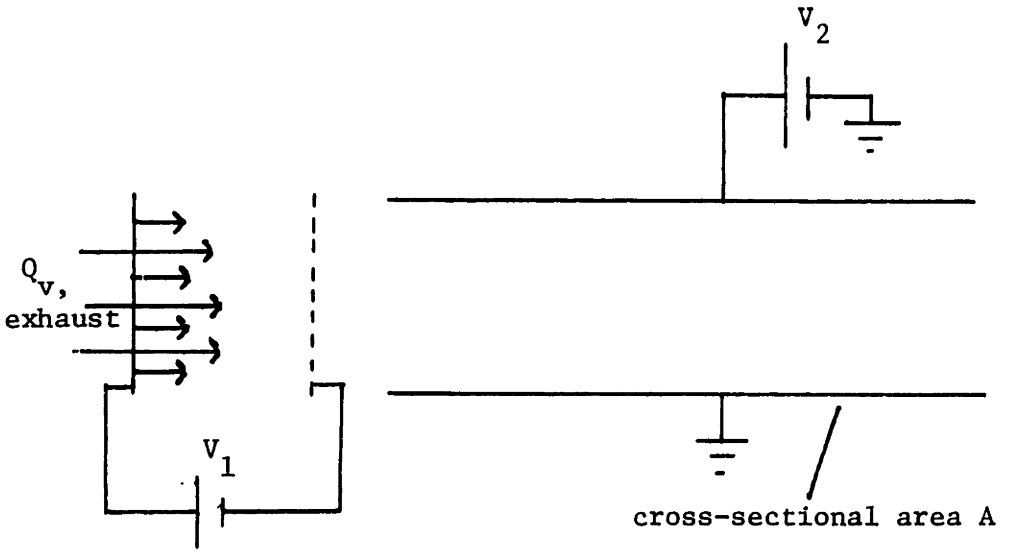

Two stage

(b)

Electrostatic Precipitators

Figure 2.1

electrode the soot also agglomerates with other precipitated soot particles. When the conditions are right, i.e. there is sufficient mass and charge for an agglomerate to overcome the surface forces, reentrainment occurs, and a pith-ball type particle motion is possible. Over long periods of time, sufficient for agglomerates to form, efficiencies of the ESP's used for diesel exhaust typically drop significantly. Part of the reason is due to this reentrainment of highly conducting particulate.

Reentrainment not only reduces efficiency through the particulate "bouncing" its way through the ESP, but also through fouling of the charger. After several hours of operation the corona elements are thickly coated with soot. Apparently, agglomerates of sufficient mass and charge are able to penetrate through the entire space charge region surrounding a corona element without becoming completely neutralized, and precipitate onto the corona element. Why don't these particles reentrain? It appears that the space charge region tends to shield the agglomerates. The field that would be responsible for pulling a particle back into the gas in the absence of corona is terminated on the corona space charge. Over a period of time, sufficient amounts of soot have precipitated onto the corona element to cause a more even distribution of the field lines, a sort of rounding off of sharp edges or points, thus tending to turn the corona off. This results in reduced particulate charging.

Another important consideration is the power requirement. Power consumption typically increased anywhere between 2-10 times, to a steady state level of 18-27 watts. The cause of this increase lies in the fact that any surface exposed to the exhaust will become coated with at least a thin layer of soot. Conducting paths between ground and the high voltage will form within this fine layer. These leakage currents will become more and more noticeable with time as the soot deposited increases. The power loss due to these leakage currents makes it imperative that great care be taken to insulate the location of the high voltage feedthrough.

With regards to capacity, the ESP handled a reduced flow of 4-8 scfm (an exhaust flow velocity of 1-2 m/s) at efficiencies of 70%-90% . The exhaust residence time in the ESP was 150-300 ms. At higher flow rates efficiencies dropped drastically as the gas residence time decreased. For practical application on a car, this would imply a large device to handle the full exhaust flow rate. A rough estimate as to the actual volume is obtained from the product of the gas residence time and the volume flow rate. At 600°F, the volume flow rate is 340 acfm or 5.67 ft^3/s . Using a 150 ms residence time implies a collection volume of .85 ft^3. With electrode spacings on the order of 1", a total collection surface area of 10.2 ft^2 is required.

There is a limit to the amount of soot that can be stored in an ESP while maintaining high collection

efficiencies. Therefore, the collected soot must be removed to a storage area to provide room in the ESP for continued optimal operation.

2.2 Design Strategy

Based upon these observations a separation of processes may be made. They represent the building blocks from which, it is hoped, a complete and practical system for collection and storage of diesel soot may be constructed.

A. The charging element must be kept clean. Needle tips or thin wires which are in corona must be swept free of deposited soot. One method is to provide air-injection at the corona points, continuously blowing air across the element. If the device is a fluidized bed, the bed particles could possibly be used to "scrub" the element. In both cases it is assumed the corona element is immobile. A mobile element (barbed chain or wire on pulleys) could also be cleaned by air-injection or by scraping the soot off in an area outside the charging region.

B. Reentrainment of the soot from the collection electrode, due to the pith-ball effect, must be eliminated. Trapping the soot in a field-free collection region would negate this effect. Another way to ensure adhesion is a "wet-wall" approach. In this case, the collecting electrode has a sticky surface so the precipitated soot will not reentrain.

C. The collection volume must be large enough to obtain a high efficiency yet small enough to be practical. Comparing gas residence times with the characteristic time with which collection occurs is a particularly useful method for rating various devices. A good overview of this subject with regards to electrostatic control devices is provided in a paper by Melcher, Sachar and Warren (32).

D. For long-term continuous operation the collecting surfaces must always be cleansed of collected soot. A means of transporting the collected soot to a storage region must be provided. For an ESP, the collection electrode may be either scraped clean (with either scraper or electrode in motion) or mechanically rapped clean. There are a

variety of options for an electrofluidized bed (EFB) - these will be discussed later.

E. There must be a storage region where the soot will be held until servicing. Over a period of 3,000 miles 1.2 kg of soot is to be collected. At a density of $.1x10^3$ kg/m^3, a dry volume of .012 m^3 must be stored, approximately the volume of a 9" cube. A vast compression of this soot, from its original dry volume, must be accomplished. Using a factor of 20 increase in the packing density, equivalent to the compression achieved by Masuda's ESP, a volume of $6x10^{-4}$ m^3, or a 3.3" cube, is required for storage. Also, care must be taken to prevent stored soot from reentraining. Storing the soot in a liquid is a possibility, compaction levels should be at least as much as a dry volume compression.

F. The device must have a reasonable power consumption. This requires high voltage feedthroughs that will minimize the formation of conducting paths between electrodes. The options here are the same as those for keeping the corona elements clean, namely

air-injection or bed particle scrubbing. For EFB's, care must be taken to insure low bed conductivities even when loaded with soot.

An important set of constraints not yet mentioned are those imposed by the automobile manufacturers and the particular engine the device is to be designed for. In this case, the engine is a 350 cubic inch, 8 cylinder 1979 Oldsmobile diesel.

Table 1: Automobile Manufacturer's Constraints

Temperature in exhaust train	900°-450° F
Flow rate	170 scfm
Tolerable pressure drop	27 in. H_2O ?
Gas residence time	50-100 ms
Particle size (mean diameter)	.1-.3 micron
Particle loading	.7-.8 g/mi
Desired clean-up efficiency	80%
Maintenance	once per 3,000 miles minimum

A question mark has been placed next to the tolerable pressure drop requirement since this number should relate directly to loss in fuel economy. As mentioned earlier, pressure drops of 55 in. H_2O were being considered as the maximum allowable for the same model engine (20). As to the

maintenance requirement, it must be a minimum type of service maintenance of the same order of complexity as an oil or oil filter change.

2.3 Motivation for Alternatives to an ESP

Examining the work done by Professor Masuda's group reveals a big push on attacking the problem of reentrainment and, to a lesser degree, on storage. An approach of scraping the soot off of a mobile collection electrode before it agglomerates enough to reentrain has been taken. Also, mechanical compression of the soot to 1/20 of its original density has greatly reduced the storage volume necessary. What is not mentioned is how the corona elements and high voltage feedthroughs are kept free of soot deposits and what increase, if any, in power consumption is observed.

The ESP developed by Professor Hoenig has emphasized the prevention of fouling of both the charger and high voltage insulator. Both problems are overcome by the use of air-injection to keep surfaces free of soot. It is believed that reentrainment is reduced by shaping the collection electrode properly so that field free regions are obtained. The ESP is rather large in size due to the particular application it was designed for - fixed farm machines. Development of the device has been temporarily halted (16).

While the scraping idea is simple enough it introduces a mechanical complexity in the need for moving parts. In

such a hostile environment, with soot getting into every corner and crack, it would be difficult to keep a smooth motion for a long period of time. Excessive amounts of soot buildup in bearings and the like would have a detrimental effect. This problem also arises in operating a mobile charging unit which could be cleaned outside of the collection region. Here, also, is the additional problem of bringing in the high voltage to a mobile unit.

An alternative to scraping, trapping in a field-free region, was utilized in the ESP experiments mentioned earlier. Shown in figure 2.2a is the collection stage of a two stage ESP. The charged particulate is precipitated out, agglomerated and reentrained, thus "bouncing" its way through the device. Note that the particle trajectory increasingly resembles an electric field line as the particle bounces downstream. After each precipitation, the resulting agglomeration yields particles with higher mobilities, thus the electrical forces dominate the fluid mechanical forces. In figure 2.2b collection electrodes with traps are shown. With this configuration the particulate's trajectory stands a good chance of eventually following the electric field lines into the trap. Once inside the trap the particulate will not reentrain due to the extremely low electric field strengths at the trap's surface.

What determines the probability of particulate entering a trap? The pertinent parameters are position in the flow, the amount of charge accumulated, mass and aerodynamic

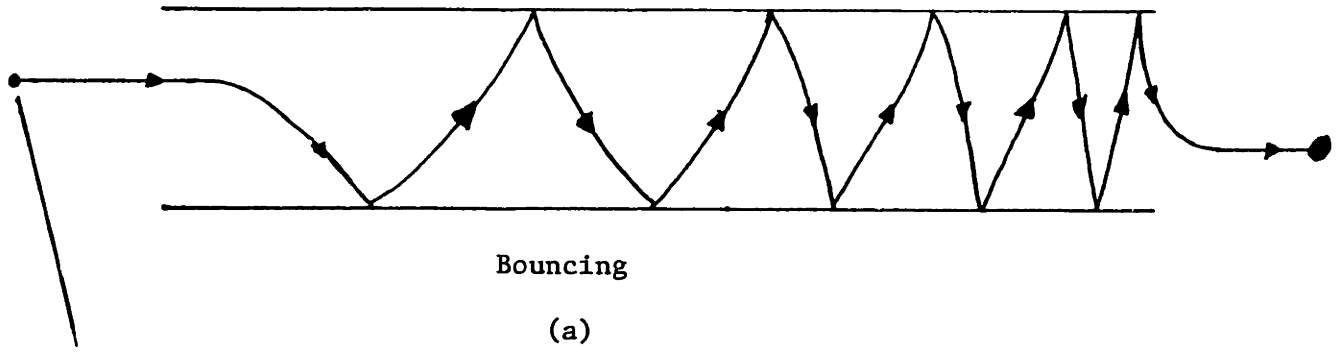

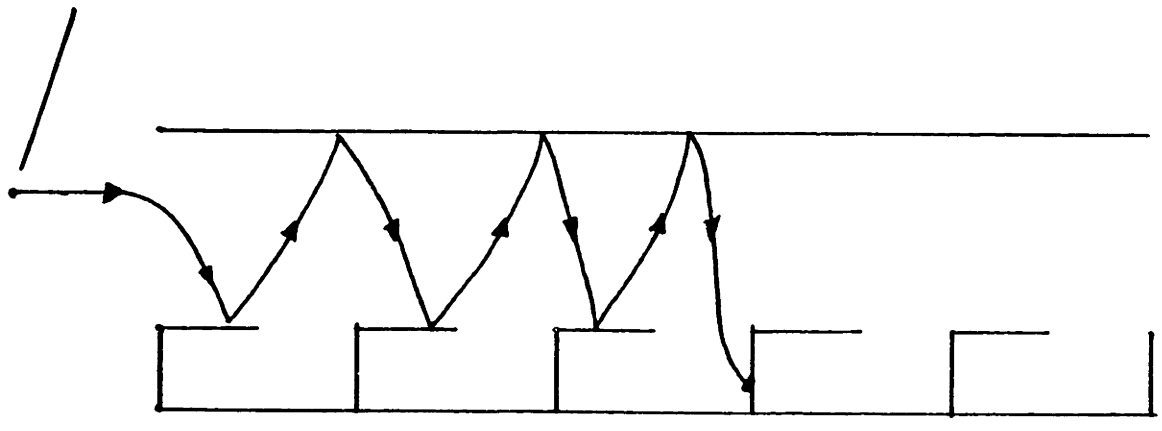

Figure 2.2

diameter. In section 5.2 an attempt is made to qualitatively account for the efficiency of the traps. It is important to point out here that the idea of trapping works. Pictorial evidence shows soot accumulating inside the traps. Furthermore, the trapped soot appears to be big agglomerates whereas those on the upper, or bounce, surface, appear to be fine particles. This fits in well with the concept of particles bouncing between collection electrodes and agglomerating before entering the traps. In a single stage ESP the process of bouncing is slightly more complicated. The reentrained particulate loses its charge in the space charge region and is then charged up again oppositely, its trajectory arcing back towards the collection electrodes.

Again the problem of agglomerated soot not being completely neutralized and making its way back to fouling the corona element is present. In the experiments no attempt was made to alleviate this problem. Thus efficiencies dropped and power consumption increased as fouling increased. The solution to this problem must be air-injection, requiring unwanted machinery in the form of air pumps.

A wet-wall approach, running liquid down the collection electrode, would ideally take care of the reentrainment problem and also the fouling problem. New problems introduced are the mechanics of circulating a liquid and the possible environmental hazards of the liquid such as odor and disposal.

An ESP with traps and air-injection is still not a complete system. Transport and storage of the soot introduce even more size and mechanical complexity. However, the ultimate obstacle to ESP design is the actual volume of the sections devoted to charging and collection.

A useful technique in evaluating the physical size and operating efficiency of a device is to examine the characteristic time with which collection occurs. In an ESP the collection time is on the order of the time required for particulate with a migration velocity bE to travel the plate spacing distance s,

$$\tau_{ESP} = \frac{s}{bE} \cdot \qquad 2.3.1$$

For the ESP used, s is 2 cm and bE, for a .1-.3 micron particle, is 2 cm/s (at room temperature). Thus τ_{ESP} = 1 sec implying a very large device either in length or in cross-sectional area.

The next device to consider is an electrofluidized bed (EFB). The efficiency of an EFB in collecting a submicron aerosol has been documented to have an exponential behavior (33),

$$\eta = 1 - e^{\frac{-3\pi}{8} c \frac{\ell_o}{R} \frac{bE}{U}} = 1 - e^{\frac{-3\pi}{8} c \tau/\tau_{EFB}} \qquad 2.3.2$$

where c - constant determined by experiment, dependent upon state of fluidization and orientation of electric field to gas flow - on the order of unity

ℓ_o - unfluidized bed height

R - radius of bed particles

U - mean gas velocity

$\tau = \frac{\ell_o}{U}$ - gas residence time and

τ_{EFB} - collection time in EFB .

Using a completely mixed model for turbulent flow in a precipitator, its efficiency is,

$$\eta = 1 - e^{\frac{-\ell}{s}\frac{bE}{U}} = 1 - e^{-\tau/\tau_{ESP}} \qquad 2.3.3$$

where ℓ - collection length of ESP and

s - corona to plate spacing for a single stage device .

Taking $\frac{3\pi}{8}$ c to be approximately unity, the key difference between τ_{EFB} and τ_{ESP} is the fact that R can be made much smaller than s. The limit on bed particle size is elutriation whereas the limit on s is electrical breakdown of air. With flow velocities on the order of 1-2 m/s, R can be on the order of 1 mm. For comparable efficiencies an EFB can therefore be 1/10 the length of an ESP, a considerable savings on size.

2.4 Conventional Electrofluidized Beds

At its best, an electrofluidized bed is an extremely efficient ESP. The collection surfaces in an EFB are the surfaces of the bed particles, as opposed to an essentially planar collection electrode. The greater amount of collection surface area per unit volume in an EFB is reflected in the difference between τ_{EFB} and τ_{ESP}.

Understanding the operation of an EFB requires a familiarity with fluidized beds. A fluidized bed is a bed of particles with a gas or liquid passing through with sufficient velocity so as to support the weight of the bed. This is the condition for minimum fluidization. The upper bound on the gas velocity is set by the terminal velocity of the bed particles, above which elutriation occurs (34). Some characteristics of a gas fluidized bed are: buoyancy - light objects will float to the top of the bed and the upper bed surface remains horizontal when the container is tipped - properties exhibited by fluids. When properly fluidized, the gas is distributed evenly throughout the bed resulting in high gas-to-bed particle surface contact, ideal for chemical reactions. Even when the gas is distributed evenly, bubbling will occur.

The short residence times implied by a high gas-to-bed particle surface contact makes the idea of collection with an applied electric field appealing. If an electric field is applied across the bed then the bed particles will become

polarized and will collect appropriately charged particulate over some portion of their surface area (see figure 2.3) . This "window" for collection can be determined using the Whipple-Chalmers model for impact charging combined with imposed field and flow conditions (35). Research conducted by Zahedi, Alexander and Zieve has resulted in the characterization of EFB's according to several basic parameters and the utilization of EFB's in several air pollution cleanup schemes (33,36,37).

There are many problems, new and old, associated with the typical EFB when combined with the design constraints listed earlier. Old problems that are still present include preventing fouling of the charger and bringing in the high voltage properly. Also still present are the transport and storage problems exacerbated by the additional fact that the collected soot will rapidly accumulate in the bed to the point where conduction through the bed becomes a dominant power loss mechanism. Reentrainment is still a problem too. In the research cited investigating EFB collection efficiencies an aerosol, DOP, was used as the pollutant. Besides its ability to be generated in a spherical, fairly monodisperslike form, it is also a liquid which will adhere well to the surface of a bed particle. The diesel soot will adhere to the surface for a while and agglomerate but will eventually flake off. This will depend greatly upon the violence of the fluidization but the end result is the same, solids will not adhere to the bed particles forever. This

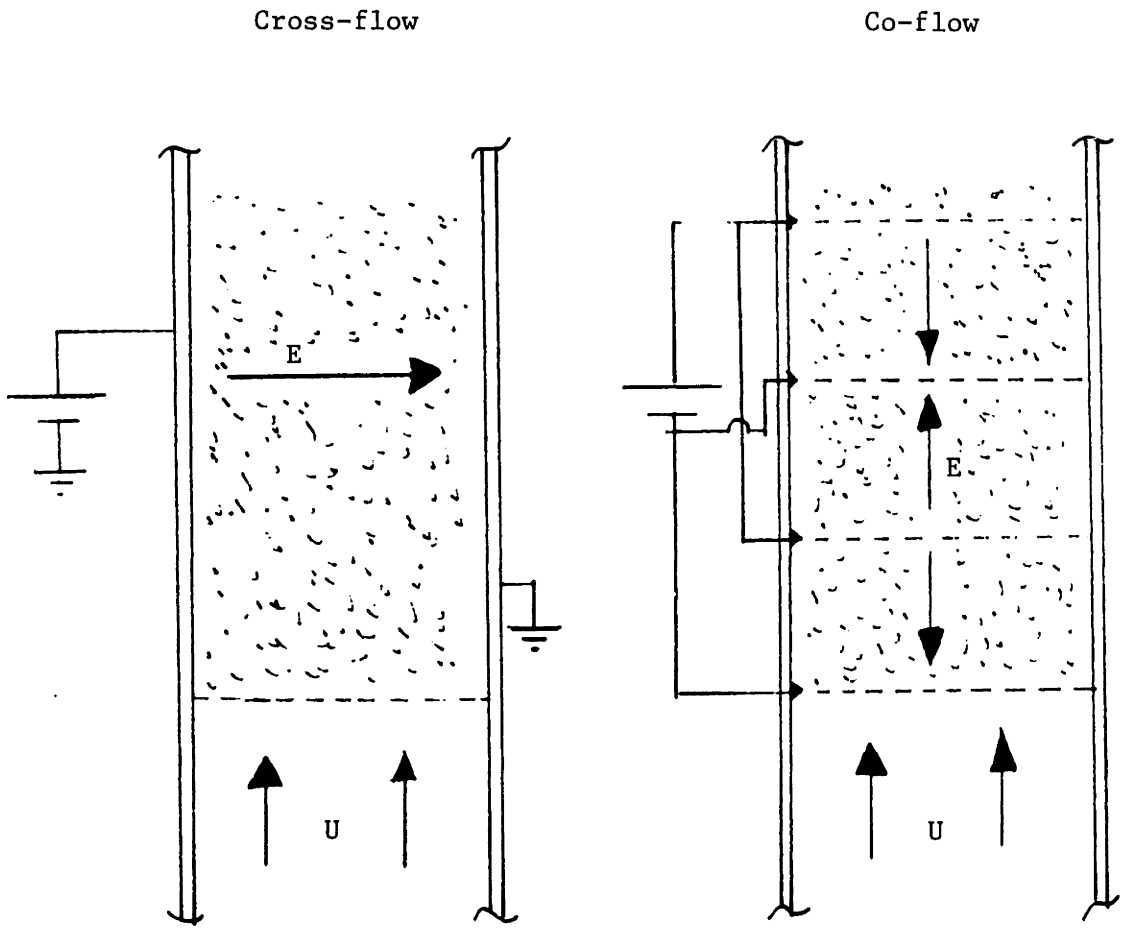

Collection efficiency

$$\eta = 1 - e^{-\ell_f/\ell_c} \; ; \quad \ell_f/\ell_c = \frac{3\pi}{8}\, c\, \frac{\ell_o}{R}\, \frac{bE}{U} \qquad (c \sim 1)$$

Conventional EFB's

Figure 2.3

does lead to the possibility of using the EFB as an agglomerating stage and, in fact, has been used as such (see section 1.2). A distributor plate is required to provide bed support. This introduces large pressure drops, especially if the plate gets clogged with soot. It seems as if the only advantage to an EFB is the reduction in collection volume, not insignificant but not enough for a total solution. However, as outlined in section 2.2, the possible options given a bed of fluidized particles suggests alterations to a conventional EFB design that have potential for overcoming these problems.

Chapter 3: Liquid Enhanced EFB Design (LEEFB)

3.1 Description of LEEFB

In figure 3.1 is shown a unit cell of the LEEFB. The exhaust enters from a plenum below the bed (A) and passes through a bubble-cap (B) into the bed (C). There are corona points along one of the coaxial surfaces within the bubble-cap. It is in this region that charging of the particulate, both by impact and diffusion, occurs. The exhaust then rises through the bed and exits through the freeboard region (D). As the exhaust passes through the bed note that the gas flow is always perpendicular to the electric field, even when the gas is "turning the corner" at the bottom of the bubble-cap. Recent investigations have shown that this cross-flow orientation is most efficient for collection of particulate (38).

Due to the geometry of the design, the bulk of the gas flow is through an annular section of the bed adjacent to the high voltage electrode. This causes the bed particles to circulate upward near the center of the bed and downward in the outer region of the bed.

In order to overcome the historical problem with EFB's, adhesion, the bed is composed of a mixture of bed particles such as sand, with a liquid. It has been shown that a liquid additive will guarantee adhesion of fine particulate (37). This was the motivation for measuring EFB collection efficiencies with an aerosol such as DOP.

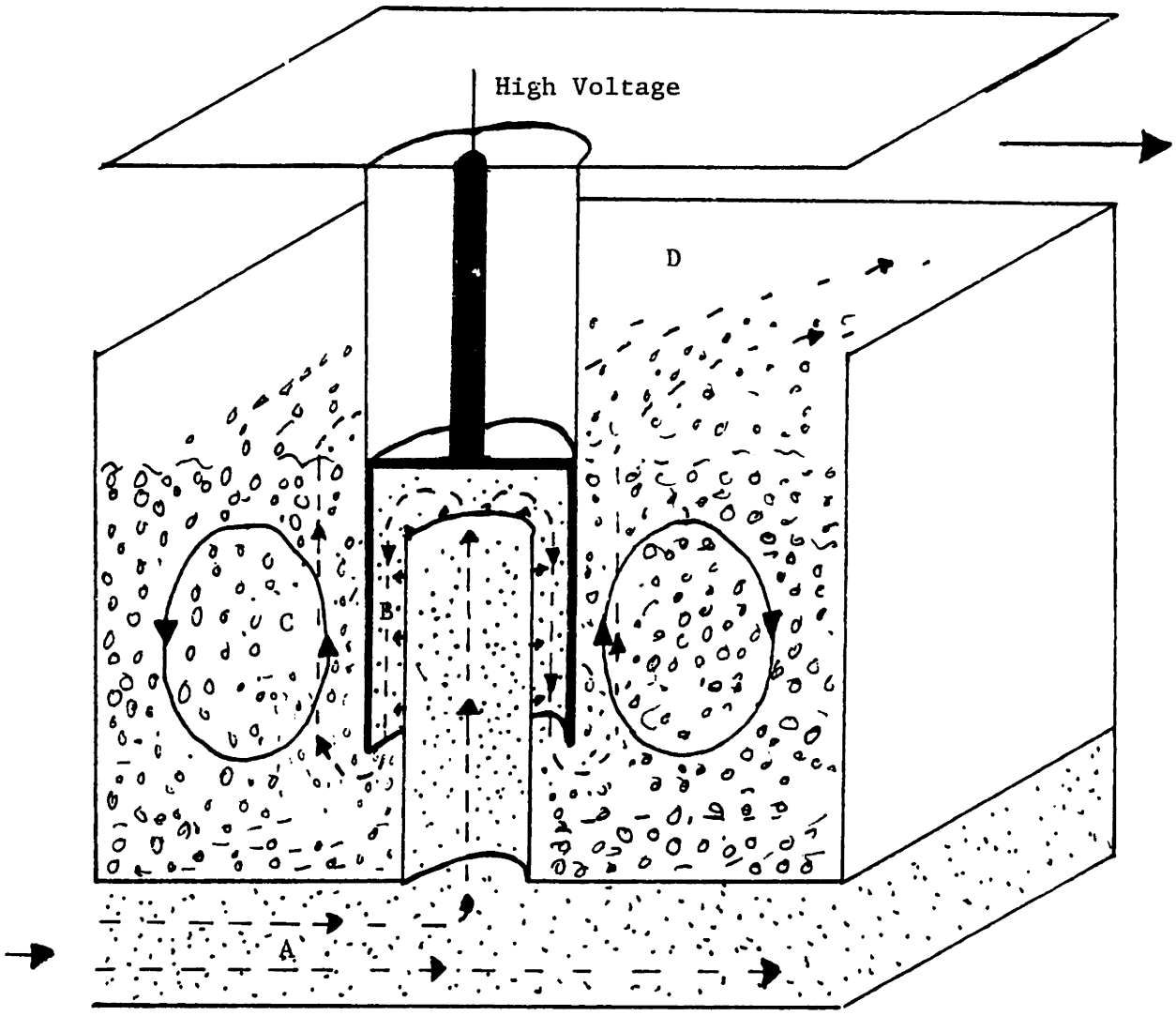

A - inlet plenum

B - bubble-cap charger

C - cleaning volume

D - free-board

Unit Cell - LEEFB

Figure 3.1

The liquid serves two, possibly three, other functions. One important property is the vast reduction in bed conductivity as an appropriately selected liquid insulates soot coated bed particles from one another. Assuming the liquid itself is insulating and that the chemistry of the particles and liquid is right, the problem of conducting paths forming across the bed shouldn't occur until the mass loading of soot in the liquid reaches a critical point.

The second purpose of the liquid is to compact the soot. A sludgy mixture of liquid and soot will reside in a volume much reduced from that of the original, dry soot.

A third function the liquid could possibly serve is as a transport mechanism for soot removal from the bed. Electrophoresis of soot through diesel oil has been observed in experiments performed at GM (39). If the liquid used in the bed was such that double layers formed around immersed soot particles, then the fields used for collection could also be used to electrophorese the soot out of the bed. Using the correct polarity for the high voltage, the soot would migrate to the outer wall and bottom of the bed and the outer wall of the inlet duct. The mobility of the soot in the liquid is much less than its mobility in the exhaust. However, the soot density in the liquid is much greater. Using a completely mixed model for bed fluidization, it will be shown that, given reported mobilities (mobilities corroborated by our experiments as well), removal of soot from the bed can keep up with the collection rate.

A possible configuration for putting the unit cells together is shown in figure 3.2 . A parallel arrangement of 2 rows of 4 unit cells each is shown. The exhaust enters a plenum at the bottom of the unit and flows through the cells to the freeboard region and is exhausted to the right. The inlet plenum decreases in size as the exhaust travels downstream resulting in an even distribution of the exhaust. A possibility of the system also serving as a muffler exists. The bed particle continuum will act as a damping medium which may, in consort with the arrangement of cells, sufficiently reduce exhaust noise.

Consider now how these alterations to a conventional EFB satisfy the criteria listed in sec. 2.2. With proper design of the bubble-cap region, exhaust will travel past the corona points at high velocities, thus blowing off any major accumulation of soot. Also, as exhaust output varies, the bed particle-exhaust interface within the bubble-cap region will vary. These fluctuations allow the interface to move up and down in this region, scrubbing the corona points. At high velocities, more points are exposed than at low velocities, thus compensating for the shorter gas residence time in the charging region.

Introducing the exhaust to the bed through a bubble-cap as opposed to a distributor plate will reduce the back pressure that the engine must work against. Elimination of any clogging problem is also accomplished with this design.

The problem of reentrainment has been eliminated with

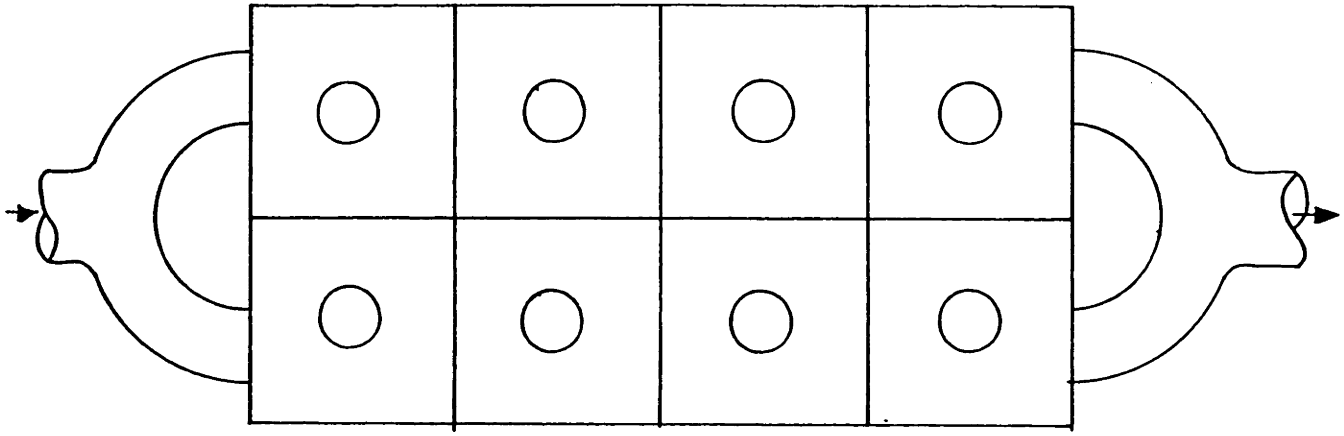

Top view

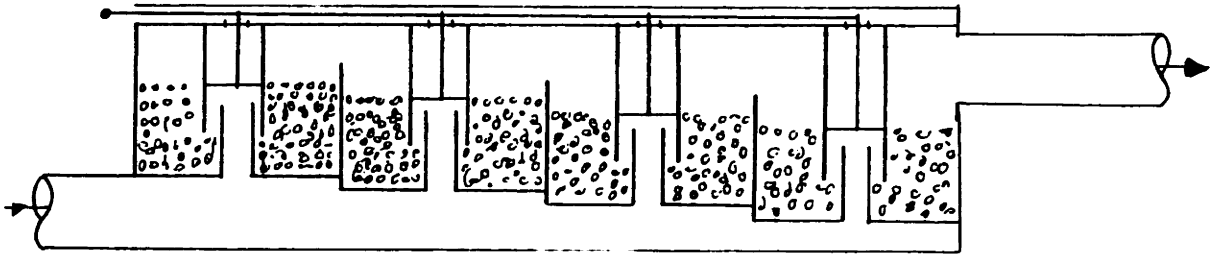

Cutaway side view

Complete device for installation on an 8 cylinder diesel engine

Figure 3.2

the use of a liquid in the bed. In a way, the LEEFB can be looked at as a wet-wall ESP. The unfavorable aspect of such a mode - due to the mechanical complexity of pumping - may remain. Environmental problems will depend upon the volatility of the liquid and whether there is any industrial use for soot immersed in that particular liquid.

The pumping question is part of the transport question. Transport of the soot in the bed is accomplished through bed particle circulation and migration of the soot through thin films of liquid on the bed particles and liquid bridges at points of contact between the bed particles. Once collected at the bottom, the sludgy mixture of liquid and soot could be drained off. If the amount of liquid required between services is small enough, then a once through mode of liquid cycling would be enough. If not, then cycling of the liquid through a filter and reintroduction of the cleansed liquid into the bed must take place. The cleansing could be through a common oil filter (doubtful) or through a filtering process using electrophoresis to remove the soot. Pumping the liquid with an electric field might also be possible since all that is required is a low volume flow rate of liquid. This cycling of the liquid will also serve to wash off bed particles, removing the dirty soot and liquid film and replacing it with a clean film, thus cutting down on bed conductivity and power consumption.

The problem of storage is solved by the compaction of the soot by the liquid. As with the compression of soot

mentioned earlier, a reduction of soot volume by 1/20 seems to be reasonable.

Fouling of the high voltage insulation is taken care of in two ways. To begin with, there is only one place in which the high voltage is brought in and it is located on the clean side of the bed. This greatly reduces the opportunity for fouling. One mechanism for cleaning is the scrubbing action of the bed particles at the metal-insulator interface. Any conducting path due to a coating of a liquid/soot/bed particle combination will be broken up and removed. Also, electrophoresis of the soot upward along the insulator will lead to formation of a clean zone on the insulator surface adjacent to the high voltage. This upward motion corresponds to the outward and downward motion of soot particle electrophoresis in the bed. The direction will be determined by the polarity of the double layer surrounding a soot particle dispersed in the liquid. Given the correct liquid additives (if necessary) and polarity of the high voltage power supply, the direction of the electrophoresis will be as described above.

The problem of excessive bed conductivity is also taken care of by the liquid. Insulation of soot coated bed particles by the liquid will greatly increase the amount of soot that can be retained in the bed before power loss through bed conduction necessitates liquid and bed particle cleaning.

The issue of collection volume has been treated before.

It was the initial motivation for seeking an alternative solution to an ESP and for selecting an EFB. The size of a device with eight unit cells (one for each cylinder output) is envisioned to be about two to three times the size of a muffler.

3.2 Design

To get a rough idea of the dimensions of the bed the following design parameters are used.

Table 2: LEEFB Design Parameters

Q_v - actual volume flow rate for one unit (since each unit will handle one cylinder's output and the total volume flow rate is 340 acfm, Q_v=42.5 acfm=.02 am^3/s

U_a - gas velocity in inlet center duct = 50 m/s

U - mean gas velocity in fluidized bed = 2 m/s

R - bed particle radius = .5 mm

bE - .05 m/s

η - efficiency of filter = 95%

V - 10 kV

τ_e - ion "relaxation time" $\frac{\varepsilon_0}{n_i b_i q_i}$ = 1 ms

The bed is broken up into various regimes. A charging region is defined by a length ℓ_3 and an annulus bounded by r_2 and r_3. An effective annular collection region has inner and outer radii r_3 and r_1 respectively and a length ℓ_1. Application of geometrical and mass conservation constraints lead to the following analysis (see figure 3.3) .

By mass conservation the volume flow rate through the

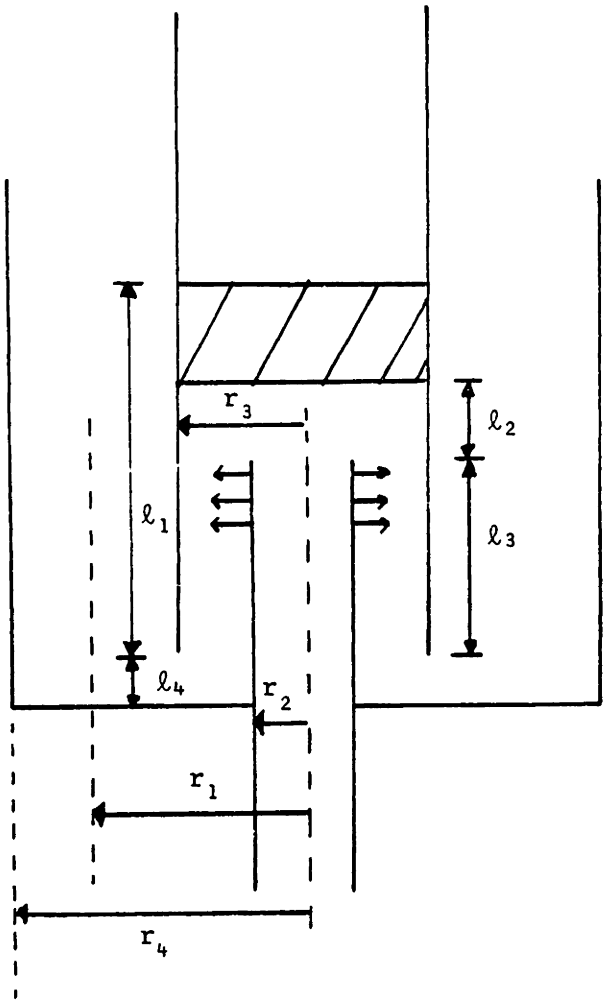

LEEFB geometry and design parameters

Figure 3.3

inlet duct is

$$Q_v = U_a \pi r_2^2 \quad . \qquad 3.2.1$$

With all of the exhaust passing through the annular collection region the volume flow rate is related to the mean gas velocity in the bed by

$$Q_v = U\pi(r_1^2 - r_3^2) \quad . \qquad 3.2.2$$

To allow time for sufficient charging to occur the charging region should be large enough to allow a gas residence time of, say, 5 relaxation times. Thus

$$Q_v = \pi[\ell_3 r_3^2 - \ell_3 r_2^2]/5\tau_e \quad . \qquad 3.2.3$$

The volume of the collection region is

$$V_{col.} = \pi(r_1^2 - r_3^2)\ell_1 \quad . \qquad 3.2.4$$

Using a completely mixed model to describe bed fluidization allows the use of the previously mentioned efficiency equation, adapted here by multiplying the numerator and denominator of the exponent by the cross-sectional area of the collection zone. Rewriting the efficiency equation yields

$$\frac{V_{col.}}{Q_v} = \frac{-8R}{3\pi cbE} \ln(1-\eta) \quad . \qquad 3.2.5$$

The right-hand side of 3.2.5 is known. Thus the gas residence time in the collection region is known,

$$\tau_{gc} = \frac{V_{col.}}{Q_v} = \frac{\ell_1}{U} \quad . \qquad 3.2.6$$

As to estimating bed particle circulation, the cross-sectional area for particle recirculation is set equal to that of the collection zone,

$$\pi(r_4^2 - r_1^2) = \pi(r_1^2 - r_3^2) \quad . \qquad 3.2.7$$

At this point there are 8 unknowns and 5 useful equations. The last equations come from a good guess as to how much space is "wasted" in the bubble-cap region, i.e. let

$$\ell_3 = 2\ell_2 \quad , \qquad 3.2.8$$

a limiting value for spacing between the high-voltage and ground,

$$\ell_4 = r_3 - r_2 \quad , \qquad 3.2.9$$

and the requirement of electric fields on the order of breakdown within the charging region. For a coaxial geometry,

$$E_{II} = \frac{V}{r\ \ell n(r_3/r_2)} \qquad 3.2.10$$

so $E_{II}\Big|_{r=r_2} = 10^6$ V/m . Solving for the unknowns yields the

values shown in Table 3.

Table 3: Dimensions of LEEFB (in cm)

$r_1 = 6.27$	$\ell_1 = 5.09$
$r_2 = 1.13$	$\ell_2 = 2.55$
$r_3 = 2.74$	$\ell_3 = 5.11$
$r_4 = 8.44$	$\ell_4 = 1.61$

If R = 1 mm, use bigger sand particles to reduce elutriation, the only change is in the length of the collection region, ℓ_1 becomes 10.17 cm.

To derive an equilibrium condition for the rate of electrophoretic removal of soot from the bed, assume a worst-case condition of complete mixing within the bed. The migration velocity of the soot in the liquid is $b_\ell E_w$ where b_ℓ is the electrophoretic mobility and E_w is an average electric field strength normal to a surface A_w, the surfaces toward which the soot particles migrate. Basically, A_w is the area of the outer wall and bottom of the bed. The last factor is the number density of particulate in the liquid films, n_ℓ.

The rate at which particulate enters the bed (assuming a "worst-case" of complete collection) is the product of the exhaust volume flow rate, Q_v, and the density of soot particles in the exhaust, n_{in}. Equating the two rates yields,

$$Q_v n_{in} = b_\ell E_w A_w n_\ell \ . \qquad 3.2.11$$

A typical soot loading is 10^{-4} kg/m^3 . Modeling the soot as spheres of .2 micron diameter with a density of .1x10^3 kg/m^3 , ρ_s, gives

$$n_{in} = \frac{10^{-4}}{\frac{4}{3}\pi a^3 \rho_s} = 3.0\text{x}10^{13} \text{ particles/m}^3 \ .$$

With a liquid loading of .25 g of soot per cm^3 of liquid, the number density in the liquid is

$$n_\ell = \frac{.25\text{x}10^3}{\frac{4}{3}\pi a^3 \rho_s} = 7.4\text{x}10^{19} \text{ particles/m}^3\text{(liquid)} \ .$$

Thus, in order for 3.2.11 to hold, the electrophoretic mobility must be

$$b_\ell = \frac{Q_v n_{in}}{E_w A_w n_\ell} = \frac{(.02)(3.0\text{x}10^{13})}{10^5(3.5\text{x}10^{-2})(7.4\text{x}10^{19})} = 2.3\text{x}10^{-12} \ \frac{m^2}{V\text{-}s}$$

where $A_w = 2\pi r_4(\ell_1+\ell_4)$ and E_w is the field intensity adjacent to the outer wall of the bed. Here, only the outer wall has been used as the collection surface area but the bottom of the bed could be considered as a part of this surface area too. The picture derived from this model is that of soot particles within a thin layer along the outer wall migrating out of the bed before its carrier bed particle reenters the collection region.

3.3 Modifications

When actual experiments were performed using the LEEFB certain problems in the original design showed up immediately. One was the poor fluidization of the bed. Due to the "gloopiness" of the liquid-sand bed the exhaust would tend to break through the bed in one region and bypass the rest of the bed. This bubbling, limited to one region of the bed, resulted in lowered efficiencies. For a better gas distribution a greater pressure drop must be presented to the exhaust before it leaves the bubble-cap region and enters the bed. Flow visualization experiments were performed using a system which was very similar in geometry but a half-cell version of the LEEFB (figure 3.4) . This allowed a cross-sectional view of the fluidization. Flexibility in the dimensions of the bubble-cap region was provided by using plexiglass tubes cut in half lengthwise. These were attached to the planar plexiglass cover piece (parallel to plane of figure 3.4) by paraffin. The method of melting the paraffin, pouring it onto the places where the tubes met the planar surface and allowing it to cool and harden provided a good seal combined with ease of removal and redesign.

Compressed air was sent through the bed at rates of 10-20 scfm, half the full output of one cylinder at 300°F. For a realistic modeling at room temperature of an experiment run at much higher temperatures, silicone oil of

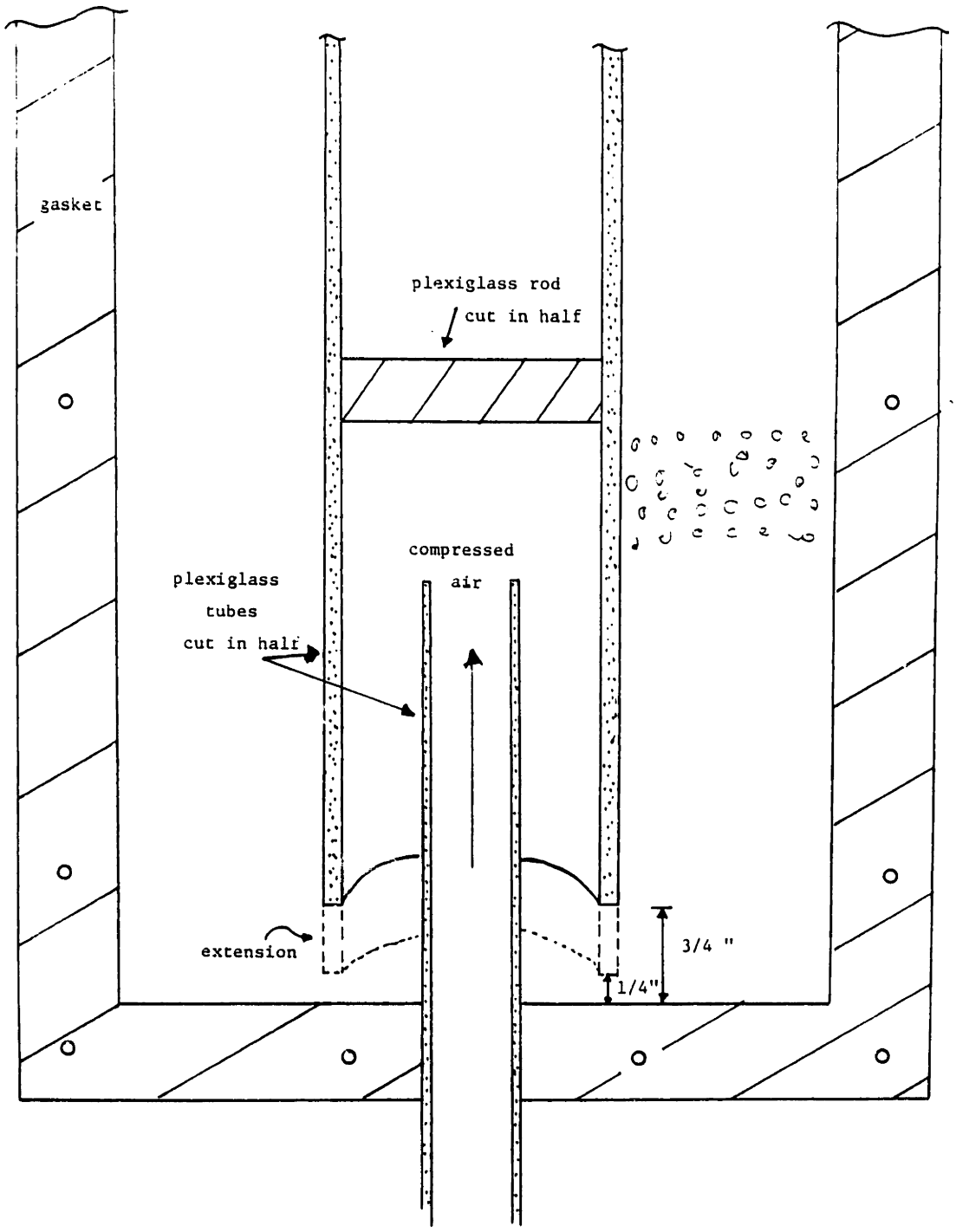

Flow visualization set-up

Figure 3.4

3 cs was used to match the 6 cs viscosity of the Shell 10W-40 motor oil at 300°F. No correction was made for the increased viscosity of air at higher temperatures. Extending the length, ℓ_1, of the high voltage electrode didn't result in enough of a pressure drop to either reduce bubbling or engage more of the bed. It was felt that the exhaust was turning the corner and running up the outside wall of the high voltage electrode to break through the bed. Once through, the exhaust would continue to bubble up solely through that region. In order to break up this path and get the exhaust further out into the bed a protruding lip was placed at the bottom of the bubble-cap (see figure 4.4). This results in a better gas distribution, utilizing more of the bed volume. Also r_3, the inner diameter of the bubble-cap, was increased to reduce the problem of alignment. The length of the high voltage insulator was $19\frac{1}{2}$" and was not exactly plumb to the horizontal.

Another question was how much scrubbing of the corona points was accomplished by the bed particles? The flow visualization experiments showed that the angle of repose of the bed mixture was large enough such that the bed particles never really came back into the charging region. Thus, cleaning of the charger is only due to the high exhaust velocities in the bubble-cap. If bed particle scrubbing is no longer being counted upon, there are less restrictions as to the size and shape of the protruding lip.

The original charger consisted of three rows of

needles, each row containing four needles equally spaced around the circumference. The second row of needles was shifted 45° with respect to the other needles on the circumference. Spacing between rows was $\frac{1}{4}$" with the first row beginning $\frac{1}{4}$" down from the top of the inlet duct. The needles extended $\frac{1}{4}$" out from the inlet duct to which they were soft soldered. In order to increase both the charging volume and the probability of saturation charging of soot an improved charger (see figure 4.4) was used. Improving the charger amounted to increasing the number of rows to twelve, still spaced $\frac{1}{4}$" apart, and increasing to eight the number of needles per row. Now every other row was rotated 22.5° to minimize sneakage regions. Thus, ℓ_3 was effectively increased.

Chapter 4: Experiments With LEEFB

4.1 Set-up and Procedures

Diesel Engine

The engine was a 1979 V-8 350 cubic inch Oldsmobile diesel engine. Seven of the cylinders have been blanked off and all the pistons removed except for the one in the live rear left-hand cylinder (No. 7) and its balance piston in No. 8. The seven unused injectors were mounted in a dummy injection block so as to realistically account for the injection pressure. A dynamometer was connected to the drive shaft to allow running of the engine at steady state conditions. Engine speed was controlled by adjusting the amount of power absorbed by the dyno and the rate of fuel consumption was determined by adjusting the fuel rack. Heat exchangers allowed control of the oil and coolant temperatures. For a more complete description of the engine see reference 40.

The typical run procedure was to heat the coolant to between 150°F-165°F, the oil to >165°F and then turn the dynamometer on. When the engine RPM reached 1450 the fuel rack was opened. At the equilibrium conditions of 1900 RPM and an air-to-fuel ratio of 36 (a fuel rate of .35 g/s), the exhaust was diverted through a set of ball valves to the experimental device, ESP or LEEFB.

Water-Bath

Relatively high exhaust temperatures proved to be a major problem when running the LEEFB. Water-cooling of the exhaust was very effective in reducing the temperature. Approximately 4 feet of 2" pipe was immersed in an oil barrel filled with water which was continually being replenished. A control of exhaust temperature from 500°F to 200°F was achieved with this system.

Freeboard Region

Topping the LEEFB was a Corning Glass 6" diameter pyrex tee (figure 4.1) . The tee afforded a partial view of the bed fluidization. A disadvantage of the large freeboard region was the initial condensation of water upon the walls of the pyrex tee when the exhaust first entered the bed. This water would drip down into the bed and sometimes affect the power supply operating conditions owing to increased bed conductivity. It is also an unrealistic representation of the real size of the freeboard region in a practical device. The rather lengthy insulator does not allow a fair judgement as to leakage currents due to fouling of the high voltage feedthrough.

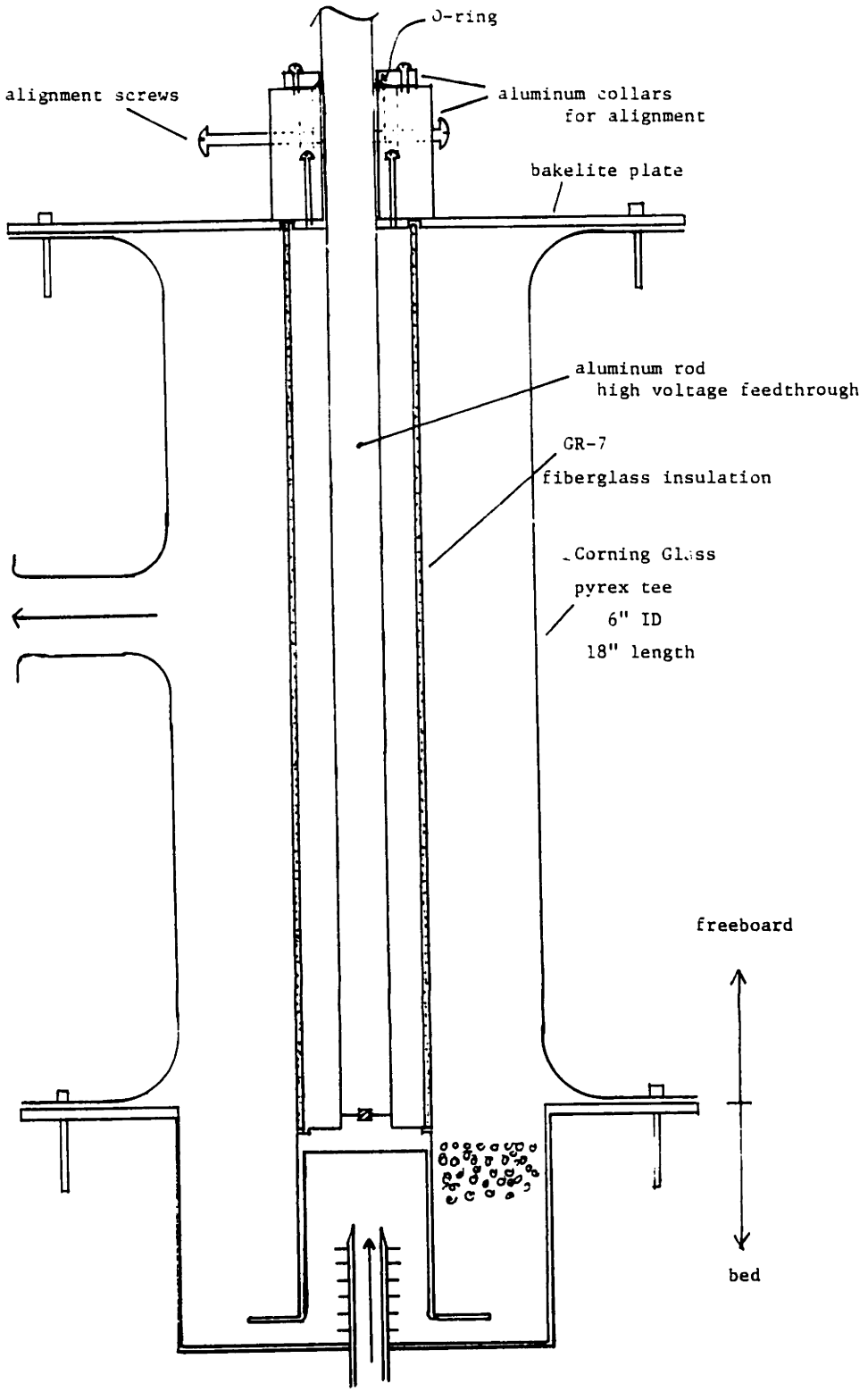

Freeboard of LEEFB

Figure 4.1

Orifice Plate

An orifice plate was constructed and placed downstream of the LEEFB. Measurements of both the pressure drop using taps placed $1\frac{1}{2}$ pipe diameters upstream and downstream of the plate and the temperature using a thermocouple placed upstream yielded the exhaust volume flow rate. Using a standard orifice plate calculation resulted in a hole of $\frac{3}{4}$" diameter within a 2" ID pipe giving rise to pressure drops of approximately 9" H_2O (41).

$$Q_v = 60 C_d \frac{\pi d^2}{4} \sqrt{\frac{2g\ \Delta p}{\rho}} \qquad 4.1.1$$

where
- C_d - discharge coefficient = .635
- d - diameter of orifice = $\frac{3}{4}$" = .0625 ft.
- ρ - gas density (lb/ft^3) = $.075 \frac{T}{529}$
- T - temperature at orifice (°R)
- g - gravitational acceleration = 32.2 ft/s^2
- Δp - pressure drop (in. H_2O)
- Q_v - volume flow rate (ft^3/min)

For a Δp of 9" H_2O at a temperature of 106°F, Q_v = 22.7 acfm. Note that the orifice plate is located about 4 feet downstream of the LEEFB.

Light-Extinction

One method of measuring the collection efficiency of

the bed was to use light-extinction. A source of light was placed at one end of a dilution tunnel and a phototube connected to an oscilloscope was placed at the other end (figure 4.2a) . The dilution tunnel construction and dimensions can also be found in reference 40. A Radiant Lamp projection medium prefocus bulb was used as the light source. The phototube was an RCA 929 vacuum phototube.

Given a physical situation as shown in figure 4.2b the light-extinction theory is as follows (13). Assuming the soot particles are monodisperse and act as independent scatterers then

$$I(z+\Delta z) \simeq I(z) - \sigma n I(z) \Delta z \qquad 4.1.2$$

or

$$dI = -\sigma n I dz \qquad 4.1.3$$

where σ - scattering cross-section (m^2/particle) and
n - particulate density (particles/m^3) .

Integrating 4.1.3 yields

$$I = I_o e^{-\sigma n z} \qquad 4.1.4$$

where I_o is the intensity for n=0. If the soot concentration is dilute, $\sigma n \ell << 1$, then

$$I \simeq I_o(1 - \sigma n \ell) \qquad 4.1.5$$

or

$$n = \frac{1}{\sigma \ell}(I_o - I) \; . \qquad 4.1.6$$

An efficiency is defined as

$$\eta = 1 - \frac{n_1}{n_2} = 1 - \frac{I_o - I_1}{I_o - I_2} \; . \qquad 4.1.7$$

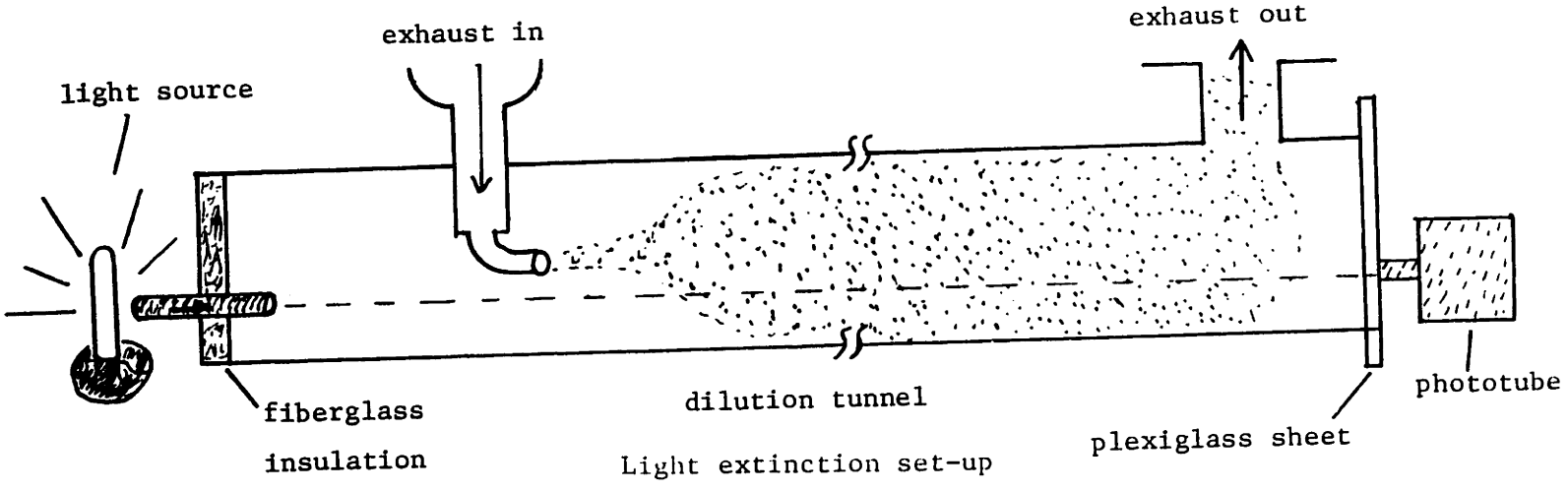

Light extinction set-up

(a)

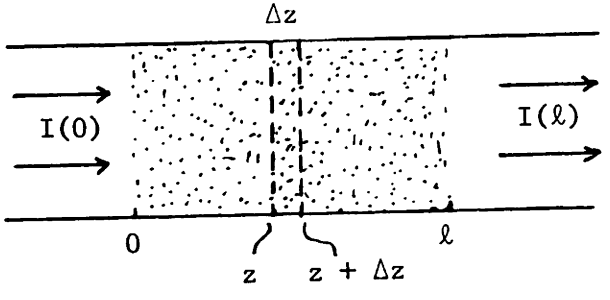

Light extinction model

(b)

Figure 4.2

I_o, I_1, and I_2 are all related to the scope measurements by the same constant of proportionality. By taking three measurements - I_o corresponding to no exhaust (n=0), I_2 corresponding to exhaust without a field on and I_1 corresponding to bed operation at a given applied field strength - the bed collection efficiency can be determined. By varying the supply voltage, I_1 varies, yielding the collection efficiency as a function of field strength. With the measurements on the scope represented by figure 4.3 it can be seen that the value of I_o does not matter, all the pertinent readings are relative ones.

The advantage to this method is that it provides a real-time measurement of bed operation. However, it should be remembered that these are rough measurements due to the assumptions required for the theory to work, especially the requirement of a monodisperse size distribution. Also, due to the necessity of measuring I_2 after the exhaust has passed through the bed, the mechanical collection efficiency of the bed has been eliminated. Thus, all efficiencies derived from this method should be higher by 2%-6% assuming a mechanical collection efficiency of 10%-15% .

Impactor Sampling

Impactor sampling was performed upstream and downstream of the bed using Andersen 2000 INC Air Samplers. The upstream sampling probe was located after the exhaust had passed through the water bath. The sampling probes were made

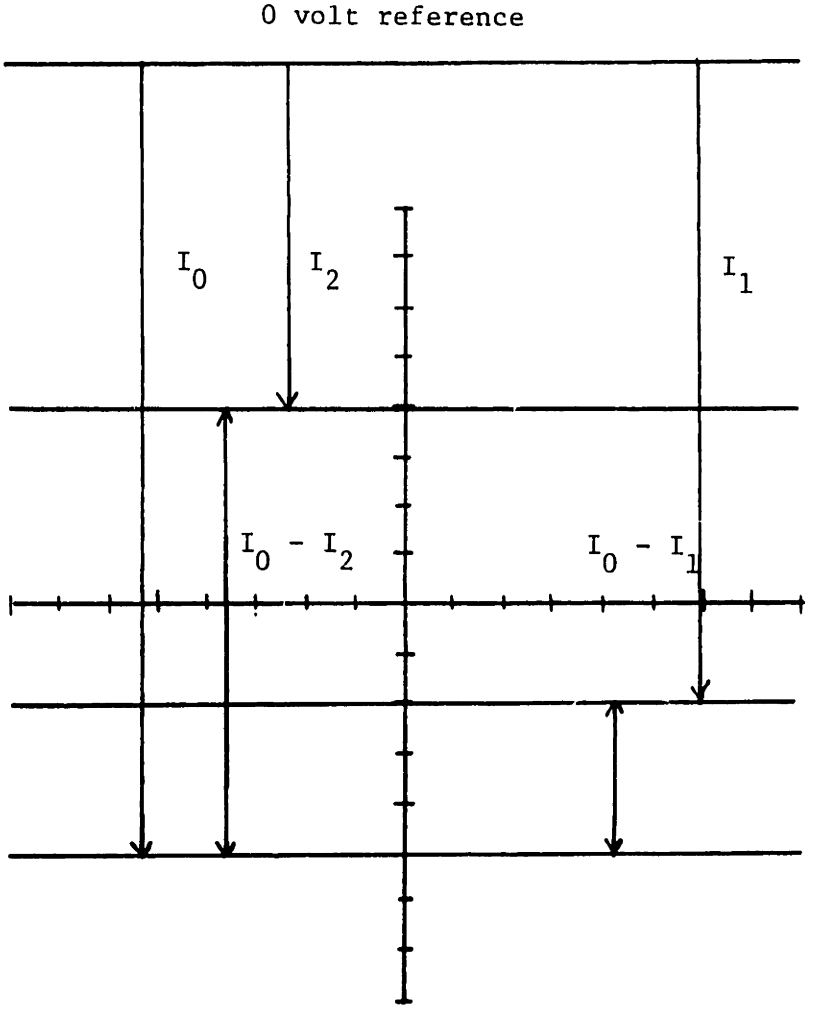

Efficiency

$$\eta = 1 - \frac{I_0 - I_1}{I_0 - I_2}$$

i.e. here $\eta = 66\frac{2}{3}\%$

Light extinction measurements

Figure 4.3

of $\frac{3}{16}$" ID brass tubes designed to isokinetically remove approximately 1 scfm. The copper tubing leading from the probes to the impactors were heated using electrical heating tape and the impactors were heated using heat lamps. Most of the time an absolute mass measurement was all that was required so only a standard fiberglass filter, with 100% retention down to .3 micron, was used. The final stage of the impactor, with the fiberglass filter, was placed above the first stage.

The EPA testing procedure requires the exhaust to be passed through a dilution tunnel meeting several criteria - among them is the requirement that the diluted exhaust must be less than 52°C (125°F) at the sampling point (27). Anything collected on glass filters at this temperature, except for condensed water, is called diesel particulate. Thus, hydrocarbons which are in vapor form and will condense or adsorb onto the soot particulate will constitute a percentage of the collected material. The amount will depend upon the temperature at the sampling point. Samples are divided into extractable and non-extractable fractions - the extractable fraction is generally associated with the adsorbed and condensed hydrocarbons. Many studies have documented the increase in extractables as the sampling temperature decreases and therefore, the dilution ratio increases (42-44). The extractable fraction may vary between 10%-90% but it is typically 15%-30%. It is more dependent upon the vehicle than the operating conditions (27).

The above discussion bears directly upon the measurements made here. Since no dilution tunnel was used, sampling was at a much higher temperature, closer to 180°F due to the heat lamps and lack of dilution. Much less mass is expected to be collected, even upstream of the bed, due to less adsorption and condensation of hydrocarbons at higher temperatures. The downstream impactor is a long distance from the upstream one. If the exhaust has cooled appreciably during that distance, hydrocarbons may have condensed or adsorbed onto the soot. Volatilization of this extractable fraction is probably not exactly reversible (see thermogravimetric analysis presented in reference 27) so reheating the cooled exhaust will not drive off these hydrocarbons. Sampling conditions may result in a higher extractable fraction downstream than upstream - leading to calculations of reduced, or even negative, efficiencies from those that actually exist.

A soot particle will probably produce essentially the same light-extinction measurements, whether or not it is coated with hydrocarbons. Cases of impactor samplings implying lower efficiencies than those obtained by light-extinction did arise and are interpreted in this manner.

4.2 Results

There were many variables with which to contend with in examining the performance of the LEEFB. Some factors that

come into play are volume flow rate, bed temperature, applied voltage, bed content - liquid mass loading and type of liquid, not to mention the modifications to the original design of the LEEFB such as the protruding lip bubble-cap and intensified charger. All reported experiments were performed at volume flow rates produced by the full output of the single cylinder. The same cooling by water-bath was used - resulting in temperatures of 170°F-200°F in the bed. Collection efficiency as a function of applied voltage was recorded and the types of liquids as well as their relative mass loadings were variable. Graded sand of either .1 or .2 mm mean diameter was used in amounts of $5\frac{1}{2}$ lbs. (2494.8 g) per bed.

Data taken from the last generation of LEEFB's (figure 4.4) using a bed mixture of #2 (2mm) sand and a Shell 10W-40 (7.1% by mass) is shown in figures 4.5-4.7. In figure 4.5 is shown the efficiency, as determined by light-extinction, at the beginning of the run with a fresh bed and 10 minutes into the run. The drop in efficiency with time is due to the collected soot coating surfaces such as the charger resulting in a steady state operation that is not as efficient as when the bed is 'new'. Looking at figure 4.6 it appears that the decline in efficiency with time has slowed considerably. It has reached a steady state - or would if the collected soot was removed from the bed using the oil as the transport medium. Also shown in figure 4.6 is a fairly stable power consumption level. The doubling in 75 minutes

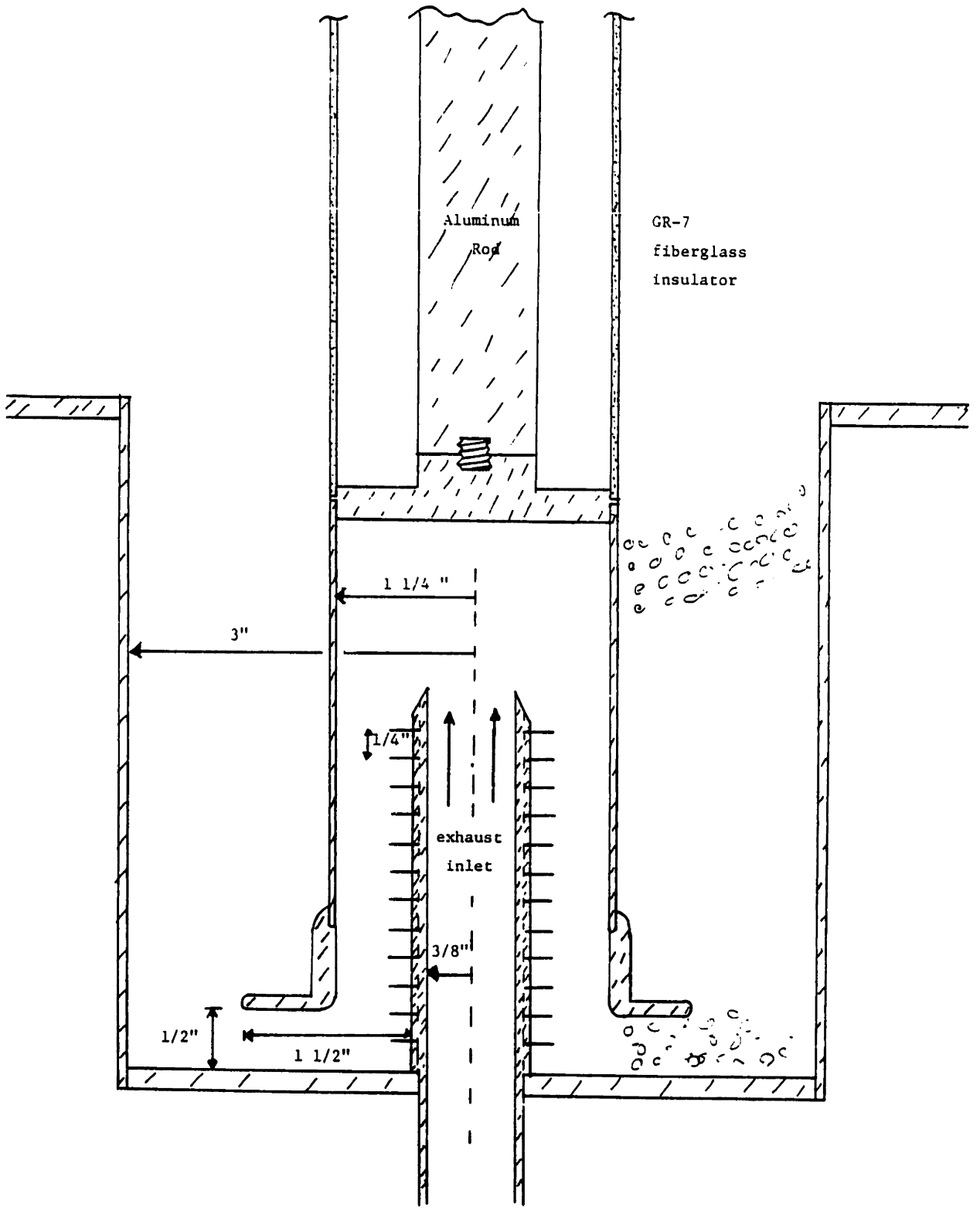

LEEFB with modified bubble-cap and charger

Figure 4.4

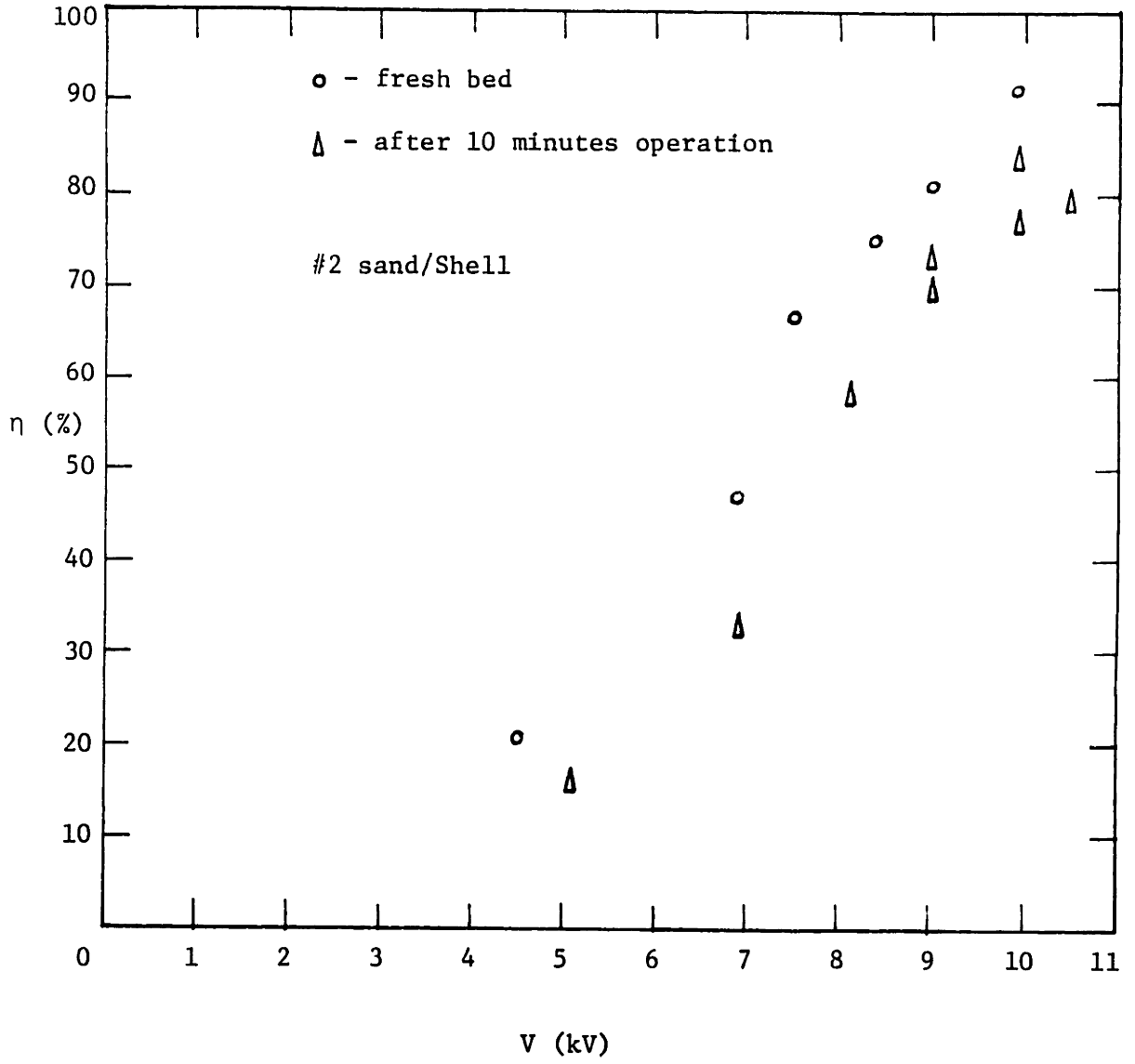

Efficiency vs. Applied Voltage

Figure 4.5

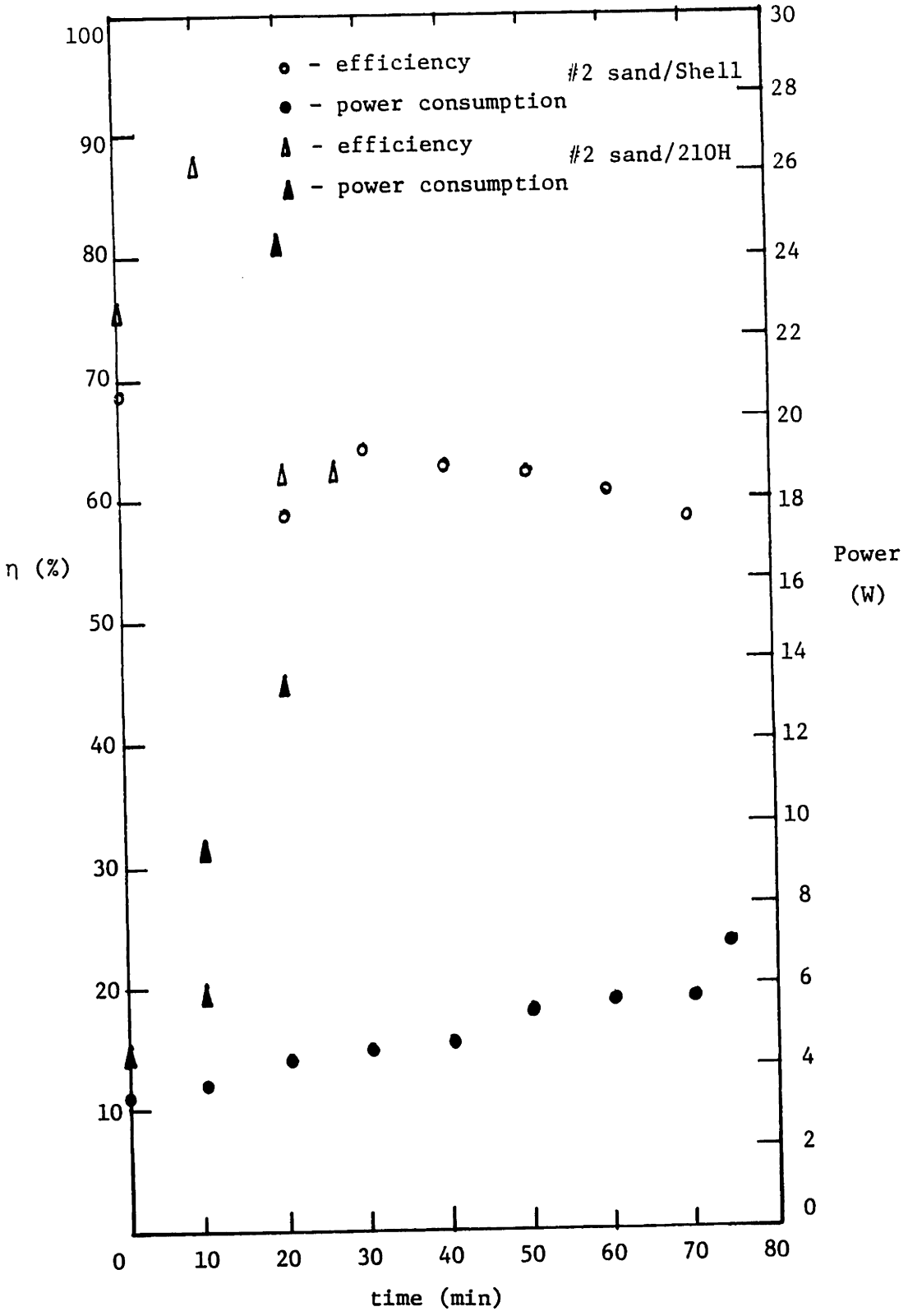

Efficiency and power consumption vs. time

Figure 4.6

could also be reduced significantly by a cycling through of the oil. In figure 4.7 is shown the V-I characteristics of the packed bed obtained by cutting off the exhaust flow. This measurement was taken after 75 minutes, when problems in maintaining bed operation at the steady state conditions occurred. It is clear that the soot loading has increased bed conductivity to the point where the power consumption in the bed affects the amount of voltage that can be applied across it without current overload.

Differences of bed performance using the 2 mm and 1 mm sand were not observed. Although efficiency should increase as R decreases in eq. 2.3.2, the increase in elutriation due to a larger percentage of fines apparently counteracted this effect.

It was desirable to use various liquids in the hope of finding one that would be useful at higher exhaust temperatures with less of a need for cooling. An obvious choice was the Dow Corning silicone fluids because of their thermal stability. Conductivity problems with a 100 cs, 200 series silicone fluid, even when initially collecting soot, severely affected the amount of voltage that could be applied across the bed. Silicone oil samples dirtied with soot, obtained from running the LEEFB, did not disperse the soot well. After several hours the soot would precipitate out of the colloid and settle to the bottom of a container. Apparently, the soot did not disperse well in the silicone oil and therefore, conducting paths could more readily form

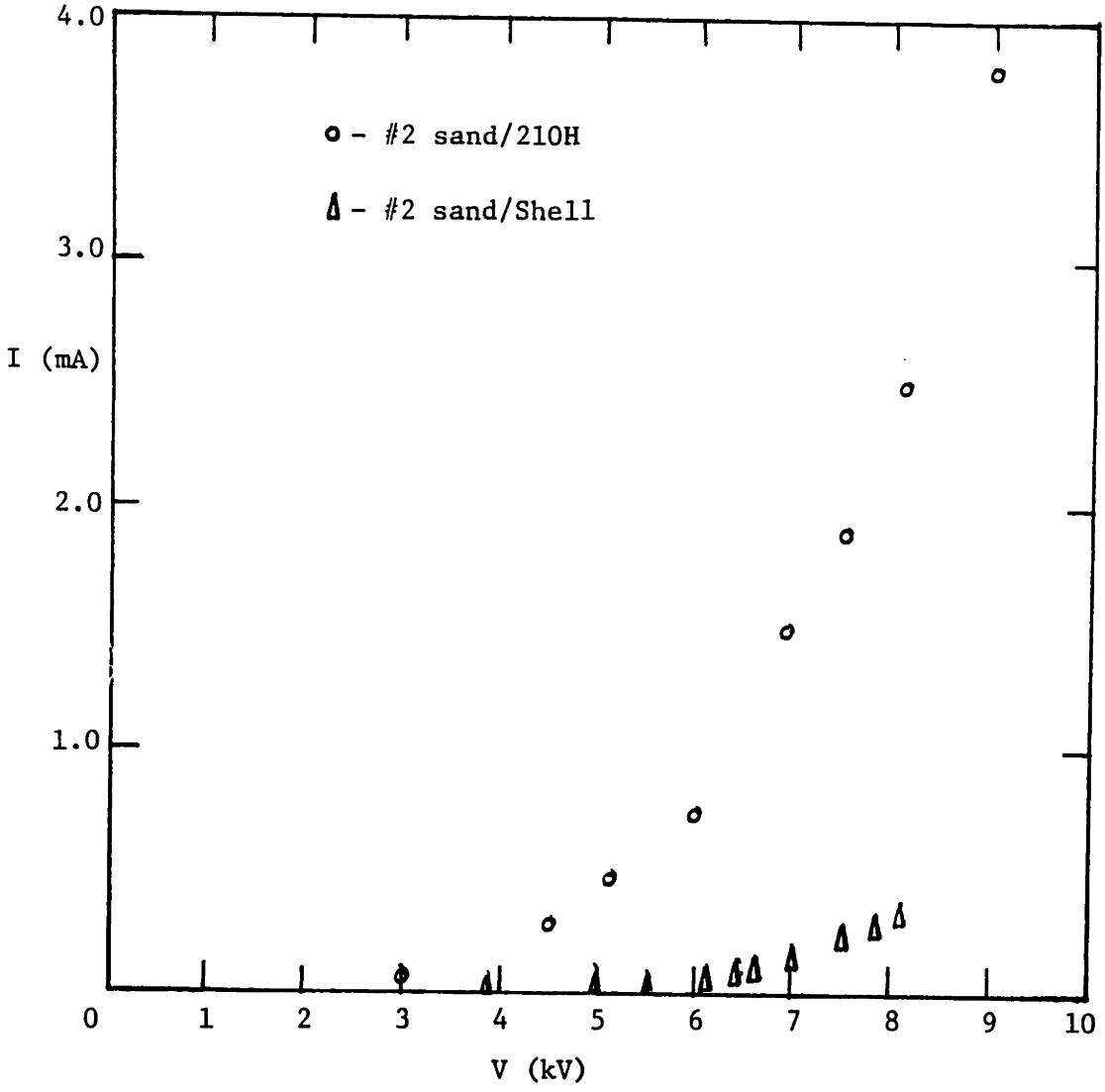

V-I characteristic of packed dirty bed

Figure 4.7

across the bed than with a mineral oil.

In the search for a silicone oil, possibly enhanced with additives, that would disperse the soot better, it was suggested that a graphite wetting agent, such as a fluorocarbon, would work well i.e. a polyflouro alcohol or a polyflouro hydrocarbon ester (45). The Dow Corning 200 series silicone fluids are a dimethyl siloxane polymer. Another Dow Corning silicone specialty fluid, 210H, is a dimethyl polysiloxane polymer with additives that make it more shear resistant and inhibit oxidation. It has a usable temperature range of -40°F to 600°F. When used in the LEEFB at a 7.1% mass loading, bed operation was stable for 26 minutes. The collection efficiencies (figure 4.8) are comparable to those obtained with the Shell oil (figure 4.5) and have the same general shape as a function of applied voltage. Power consumption (figure 4.6) is a problem, doubling every 10 minutes. For comparison, the packed bed conductivity (no exhaust) after 26 minutes is also shown in figure 4.7. The bed conductivity is much higher than that with the Shell oil (figure 4.9) . Even though there are additives which disperse the soot better (it did not settle out of oil samples taken from the bed) the silicone oil still does not insulate well enough. Physically, the dispersion is thought to be accomplished through electrical double layer formation around a soot particle immersed in the oil. The strength of the ambient electric field necessary to cause breakdown of this double layer will

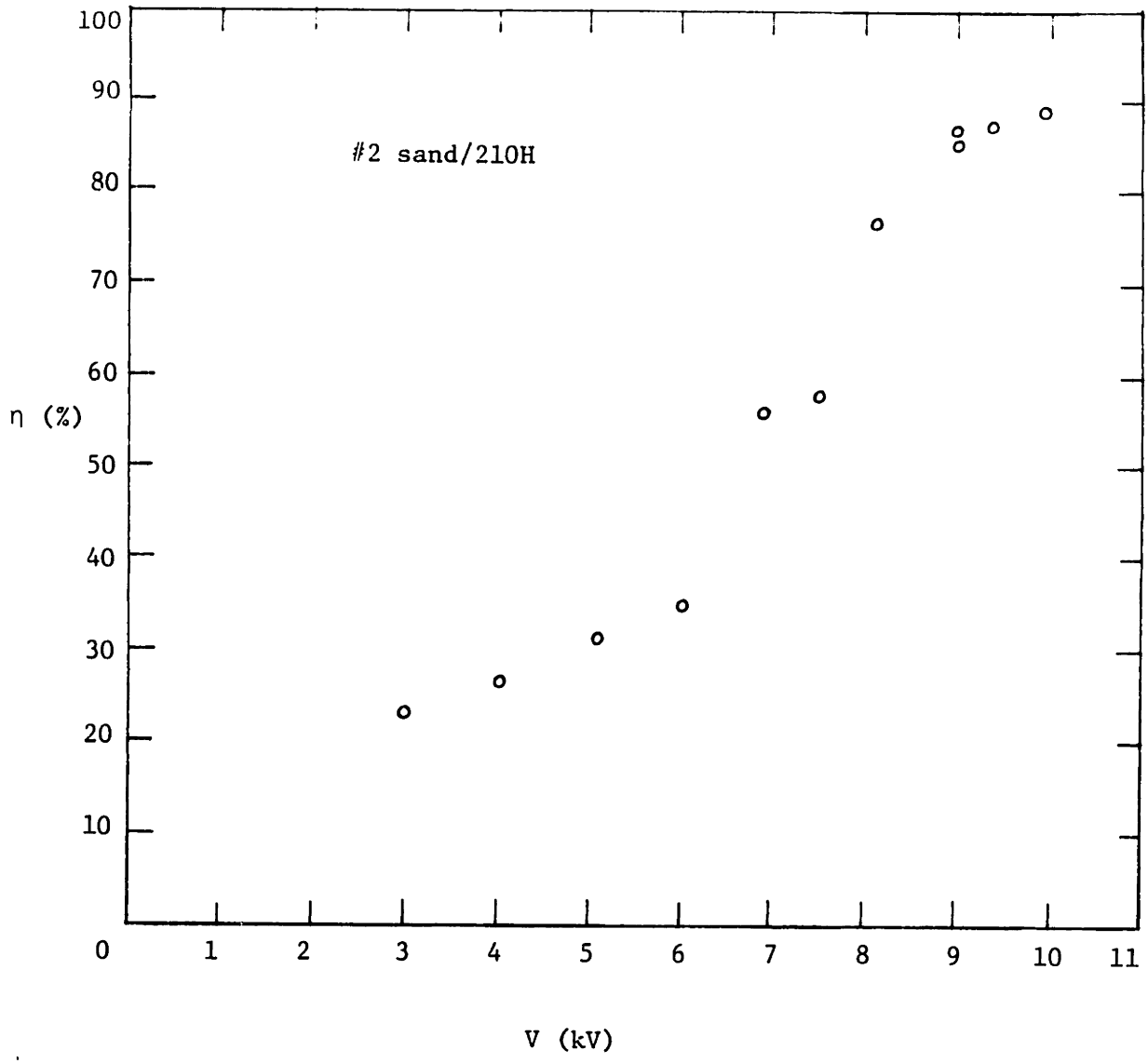

Efficiency vs. Applied Voltage

Figure 4.8

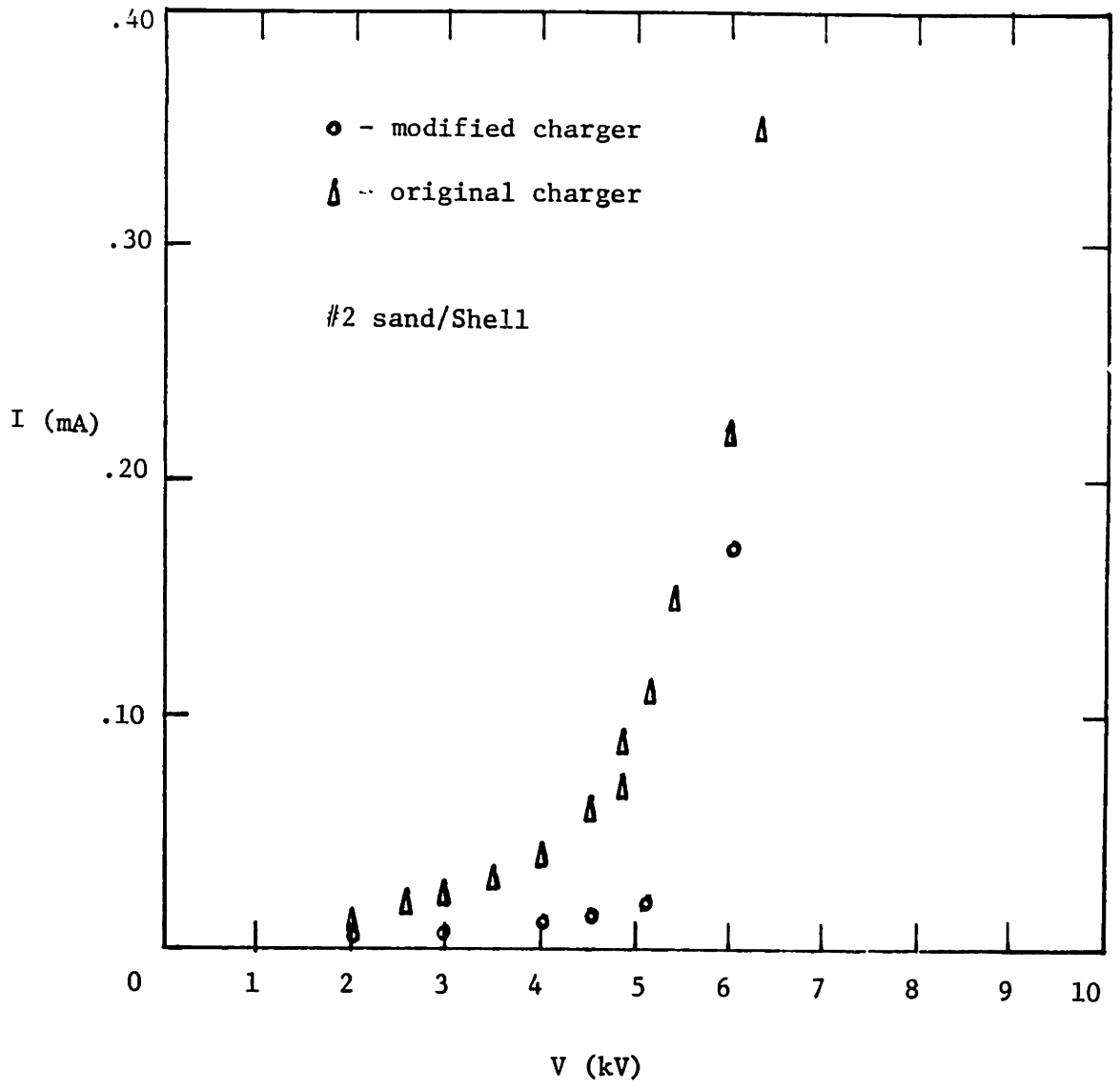

V-I characteristic of packed dirty bed

Figure 4.9

depend upon the value of the zeta potential, the potential across the double layer. Thus, zeta potentials with silicone oil as the liquid medium are considerably less than the potentials associated with the Shell oil. This would also be reflected in a lower electrophoretic mobility of the soot in the silicone oil, because mobility is proportional to the zeta potential.

The effectiveness of the modified charger is reflected in the fact that bed operation was stable for 60 minutes as opposed to 160 minutes with the original charger. Both beds used Shell oil but the mass loading was higher, 7.1% to 4.6%, with the new charger. After 35 minutes the LEEFB was operating at 9 kV, .15 mA and a 61% efficiency with the original charger. With the new charger, operating conditions after 30 minuter were 9 kV, .75 mA and a 66% efficiency. The relative efficiencies were not 2-3 times higher thus there is some doubt as to why there is such a difference in stable bed operation times. It should be noted that at the beginning of the run comparable collection efficiencies were 10%-15% higher with the new charger i.e. at 9 kV it was 95% as opposed to 82% with the original one. Packed bed conductivities indicate a higher soot loading with the original charger run for 160 minutes (figure 4.9). Possibly the definition of stable bed operation needs reworking. It was taken to exist when an applied voltage of 9 kV was not current limited. Generally, once the point was reached where there were problems applying those high voltages - it became

difficult to apply even 7 kV for any length of time.

An interesting phenomena was initial bed operation as a packed bed due to cool oil being too viscous to allow fluidization of the bed. Much higher efficiencies, 10%-15%, were obtained in this regime of operation (figure 4.10) . Of course, it is not feasible to operate in this regime unless transport of the soot out of the bed could be effected at a sufficient pace. It is anticipated that packed bed conductivities will increase faster than fluidized bed conductivities, given equivalent efficiencies.

As an attempt to increase collection efficiency an after-charger was slid into the bed. The after-charger was a brass tube onto which 9 rows of needles were soft-soldered. Each row had 22 needles equally spaced around the circumference (figure 4.11) . The thoughts motivating this were that the needles would break up bubbling to some extent but, more importantly, would penetrate bubbles, charge the soot entrained in them and help precipitate the soot onto surrounding bed particles. In figure 4.12 is shown efficiencies with and without the after-charger using beds of 2 mm diameter sand with Shell oil mass loadings of 2.4% and 4.6% respectively. Efficiencies are slightly higher with the after-charger but operation with it was curtailed after 1 hour as opposed to 3 hours of stable operation without it. The same characteristics are observed with the new charger and Shell oil mass loadings of 7.1% (figure 4.13) . Here, the after-charger curtails operation after 15 minutes as

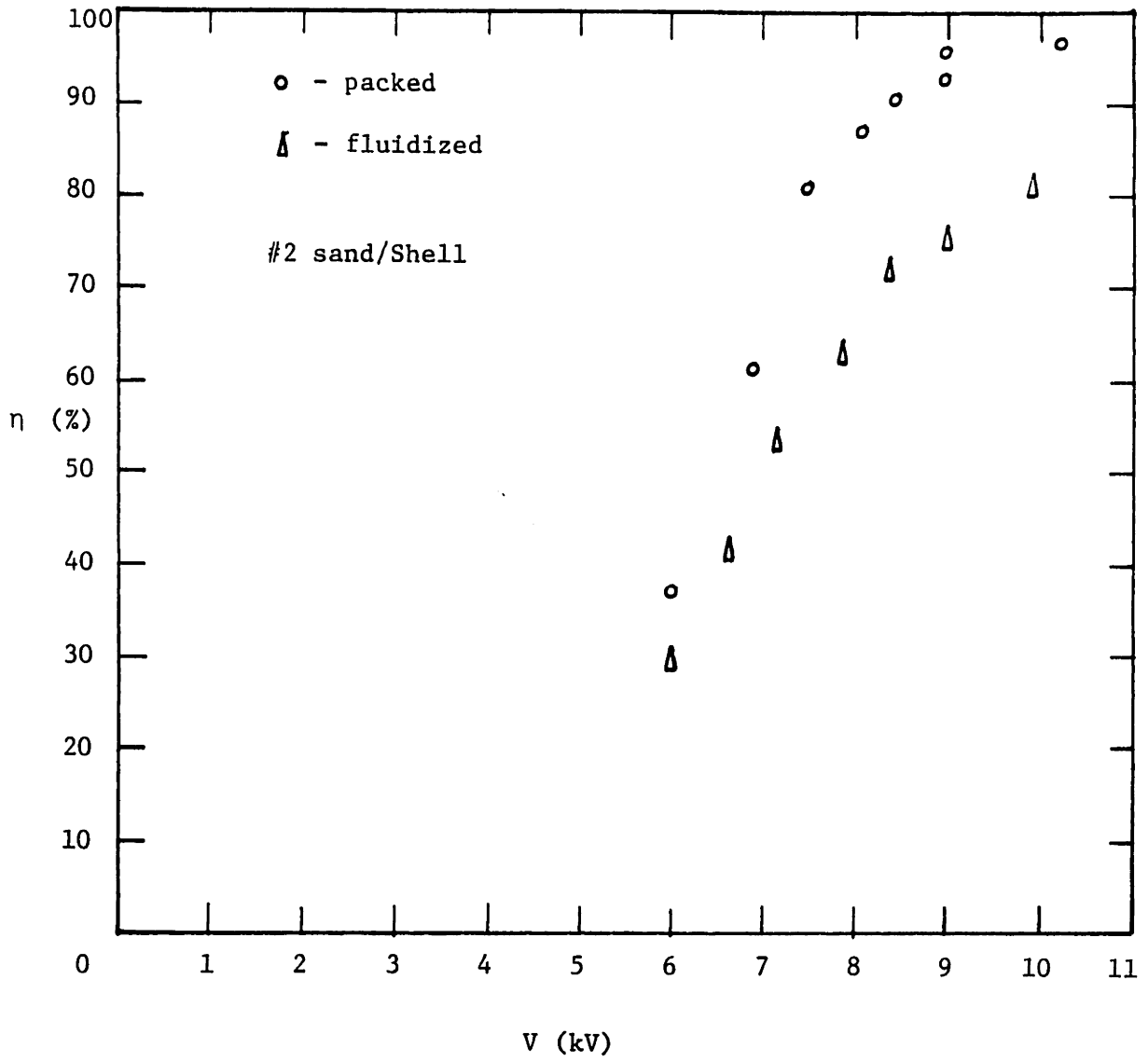

Efficiency vs. Applied Voltage

Figure 4.10

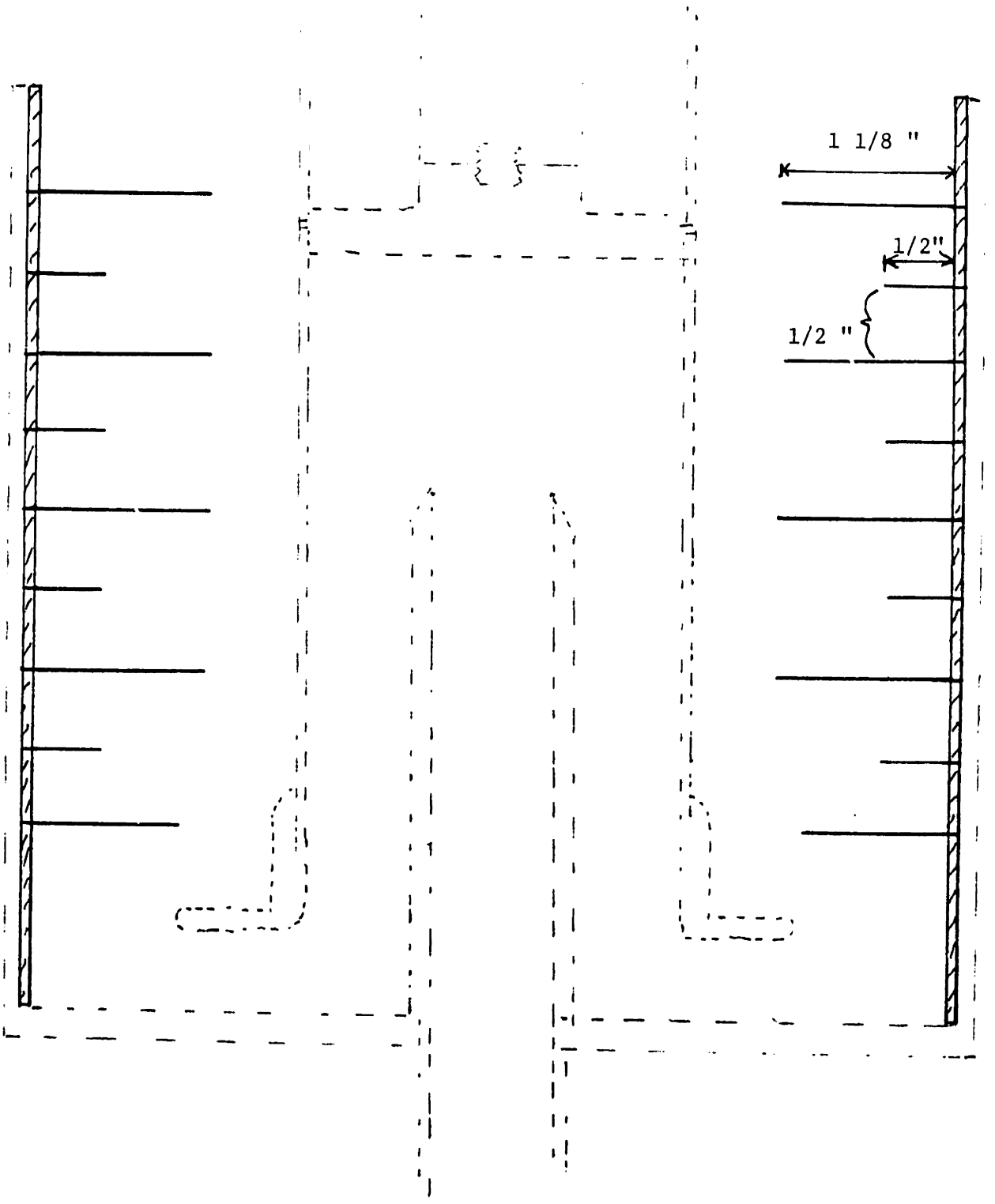

Dimensions of After-charger (to scale)

Figure 4.11

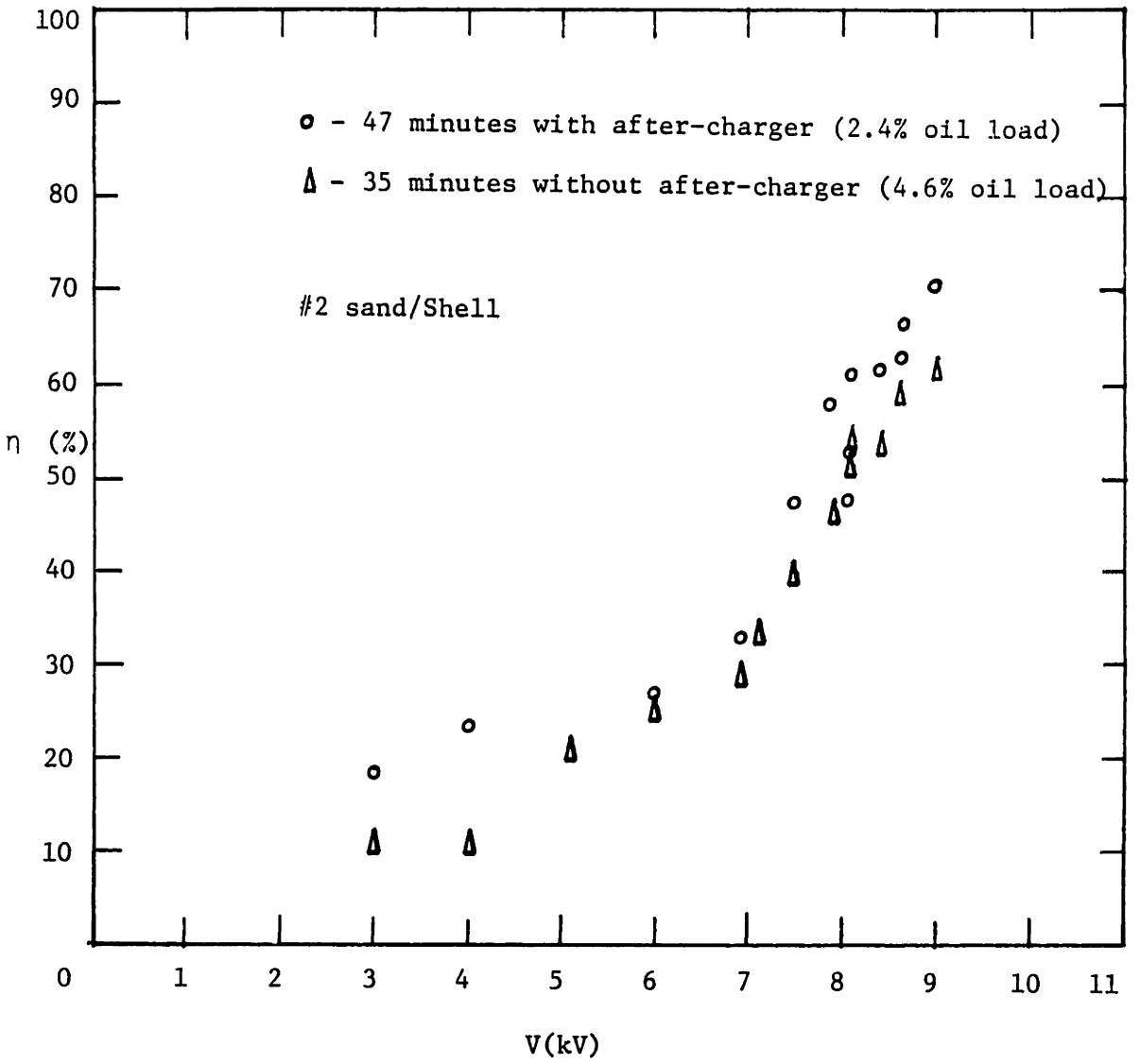

Efficiency vs. Applied Voltage

Figure 4.12

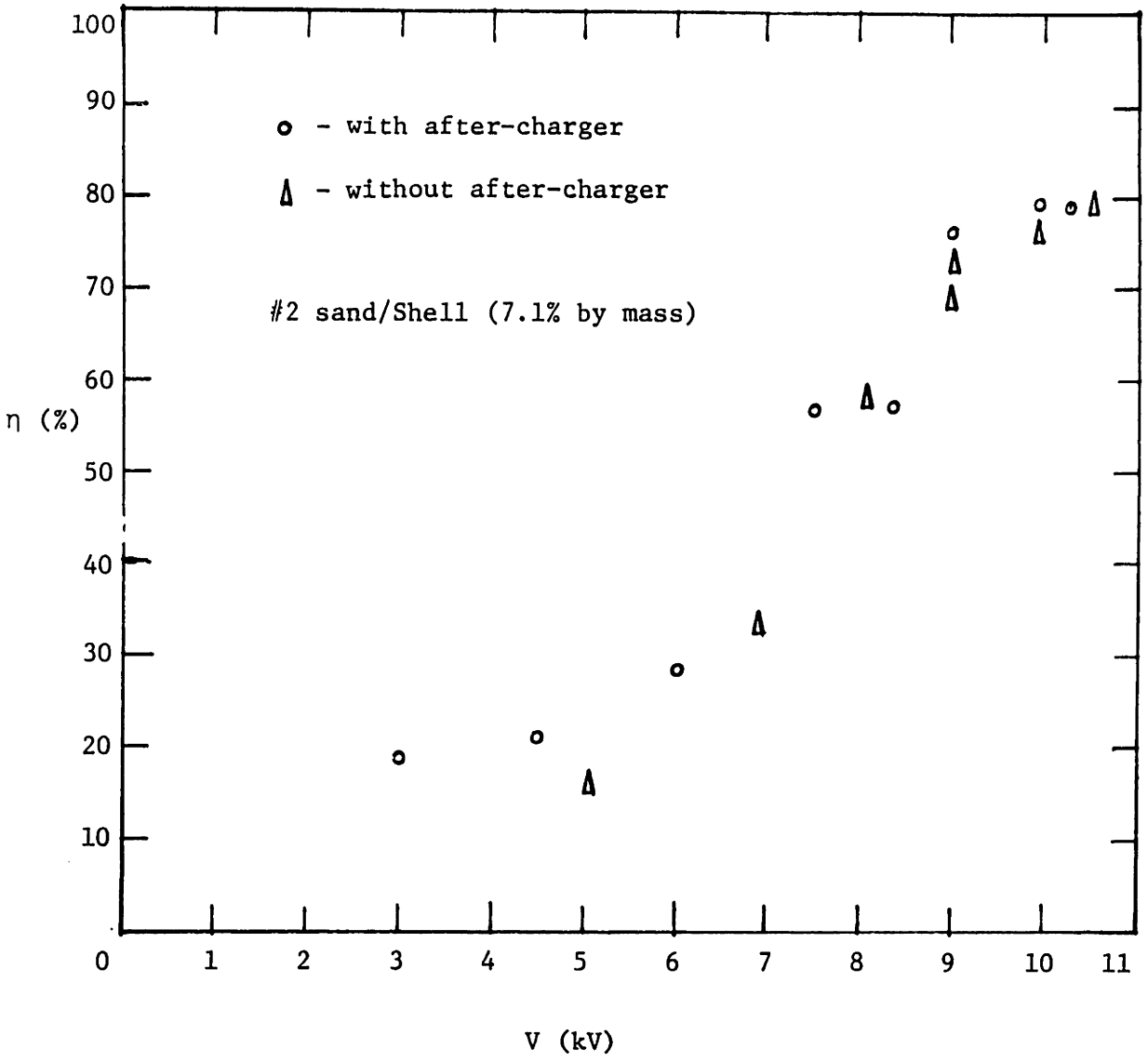

Efficiency vs. Applied Voltage

Figure 4.13

opposed to 60-75 minutes without it. The problem is the added structure introduced into the bed by the needles of the after-charger. Conducting path lengths from high voltage to ground are greatly reduced and there are many opportunities for those paths to develop with so many needles.

To determine how much of the operating current is attributable to the corona, the LEEFB was run without a bed - in a sense it was a two-stage ESP. The V-I characteristic of the corona at various times is shown in figure 4.14 . The LEEFB was operated this way for $1\frac{1}{2}$ hrs. The stability of the supply current demonstrates the validity of charger cleaning by the high velocity exhaust. Referring to the packed bed V-I characteristics of figures 4.7 and 4.9, the current is composed of both bed and corona currents. From figures 4.7 and 4.14 it can be seen that the corona current accounts for $\frac{1}{3}$ - $\frac{1}{2}$ of the packed bed current when the bed with Shell oil has voltages greater than 6 kV applied across it. The corona currents are insignificant compared to bed currents with the silicone oil - this is due to its poor dispersion property. The corona currents do not enter into the V-I characteristics of figure 4.9 because these beds are so dirty that they short out before the corona turns on significantly. Judging from the shapes of the V-I curves, the Shell oil seems to have a sharper transition to breakdown than the silicone oil. Bed currents rise slowly until some critical value is reached and then they shoot up.

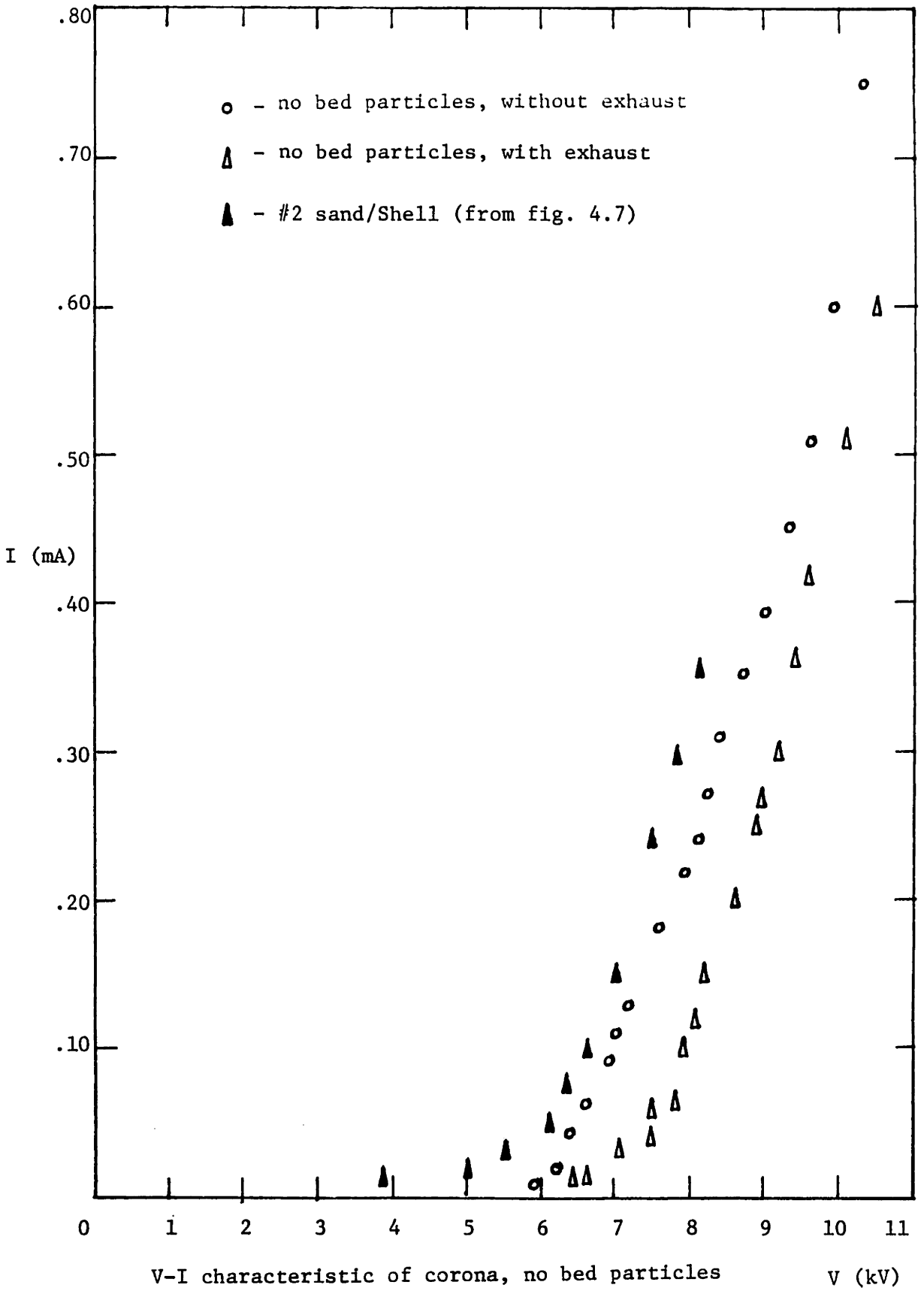

V-I characteristic of corona, no bed particles

Figure 4.14

A more steady increase is indicated with beds using silicone oil. Curiously, light-extinction measurements showed efficiencies of 50%-60%. This is probably due to the same amount of material passing through as with no applied field but, since the soot is now agglomerated one or two orders of magnitude in size, the density of particles decreases, more than compensating for the increased scattering cross-section.

What has been demonstrated by this bed in relation to the basic criteria described in section 2.2? Fouling of the charger has been completely eliminated by high velocity cleaning of the exhaust. Figure 4.15a shows the condition of the needles after 1 hour of bed operation with 7.1% mass loading of Shell oil. Only a thin coating of fine soot is visible. This is also true of the inside surface of the bubble-cap facing the corona points (figure 4.15b).

Reentrainment has been solved by the addition of a liquid to the bed. The collection efficiencies could be improved - but the improvement would have to be in terms of gas distribution throughout the bed. Figure 4.16 provides compelling proof that most of the gas is passing through one section of the bed. The picture was taken looking down at the bottom of the LEEFB after the bed contents had been dumped out. A large, black, oval shaped region of soot deposits bordering the inlet duct indicates the region through which most of the exhaust exited through. This was soot that had been precipitated out and not reentrained,

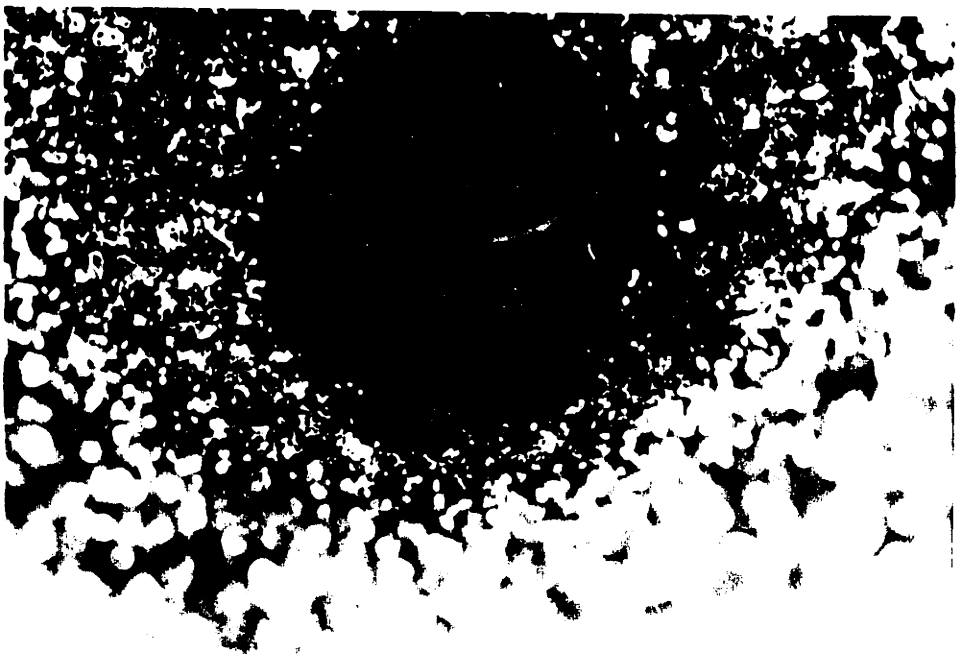

Clean needles surrounded by oil and sand bed mixture

(a)

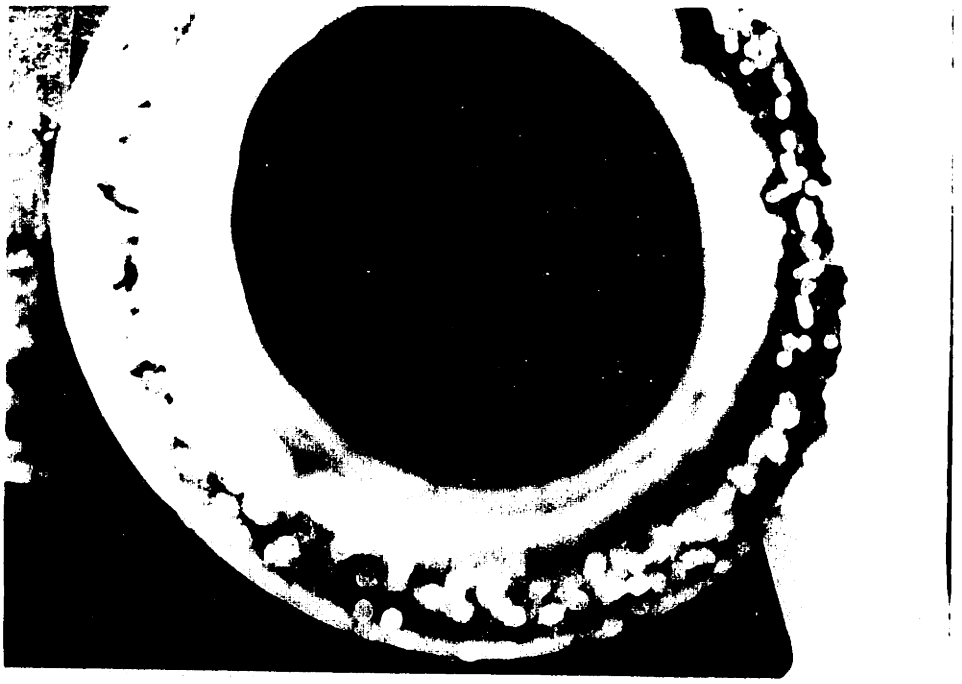

Inner surface of high voltage electrode (bubble-cap)

(b)

Figure 4.15

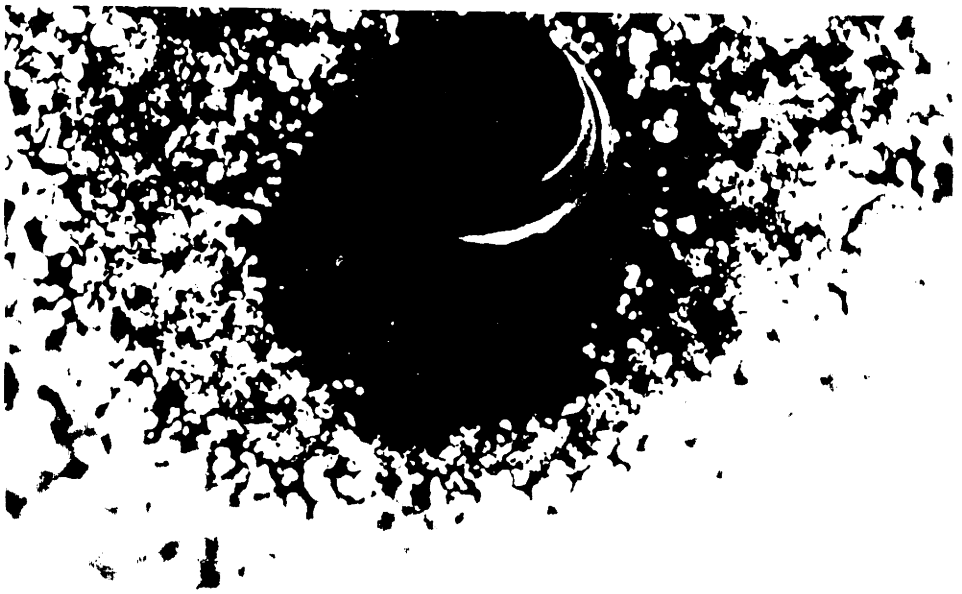

Clean needles surrounded by oil and sand bed mixture

(a)

Inner surface of high voltage electrode (bubble-cap)

(b)

Figure 4.15

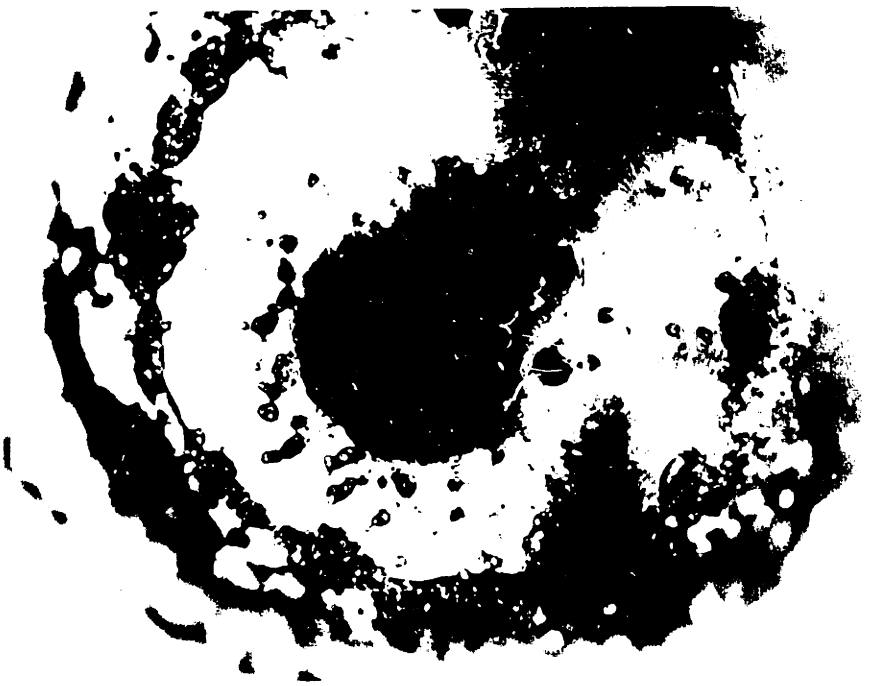

Looking down into the LFPB

Note region of black deposits bordering center duct

Bed contents removed

Figure 4.16

INTENTIONAL DUPLICATE EXPOSURE

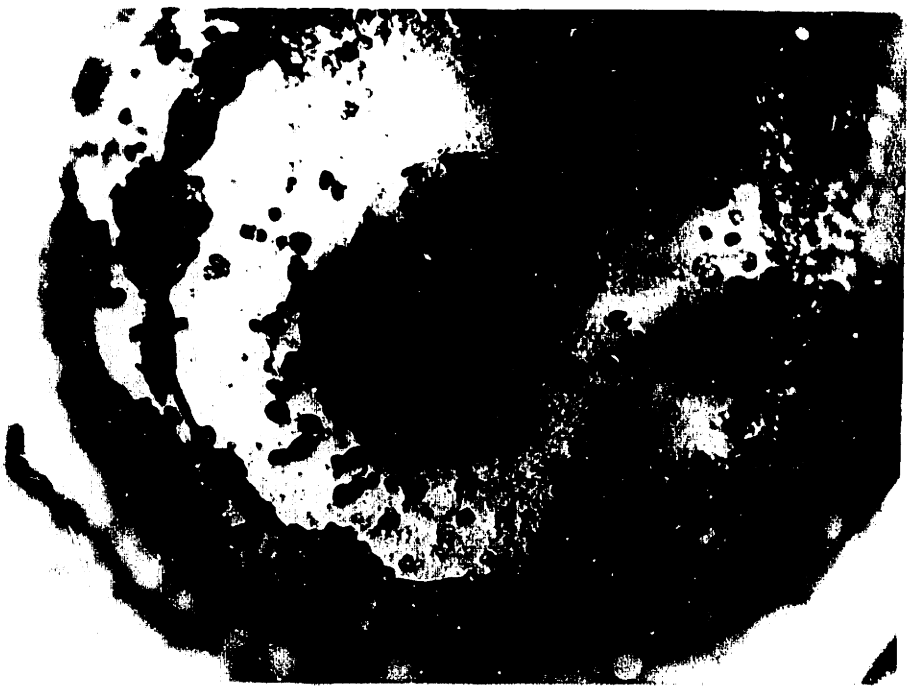

Looking down into the LEEFB

Note region of black deposits bordering center duct

Bed contents removed

Figure 4.16

probably due to a layer of oil on the bottom of the bed. A reasonable estimate as to how much of the bed comes into contact with the exhaust might be $\frac{1}{3}$ based upon this picture.

The other advantages of the liquid have proved themselves too. That a bed of sand and liquid could collect soot for an appreciable length of time without shorting out the power supply is a tribute to the insulating property of the oil. For comparison, a bed of sand particles without a liquid was run. It collected soot for 11 minutes before shorting out completely. In that time power consumption increased from 3.4W to 25.7W, a factor of almost 8! As demonstrated by the Shell 10W-40 versus the Dow Corning 210H specialty silicone fluid, the degree of insulation depends greatly upon the ability of the liquid to disperse the soot and prevent conducting paths. Up until a critical soot mass loading both liquids maintained a stable power consumption level of 3W-5W. Multiplied by eight units yields a consumption of 24W-40W, well under the 100W limit.

Prevention of fouling of the high voltage insulation was not accurately tested here. One problem, mentioned earlier, was that the length of the insulator did not allow appreciable leakage currents to develop. The top of the insulator was far enough removed from the exhaust to remain clean. Another problem was that the surface of the fiberglass insulator was rough and pitted - ideal for soot to remain embedded in. A smooth, glazed surface would allow bed particle scrubbing to have an effect.

The pressure drop across a fluidized bed is normally the bed height in inches H_2O ($5\frac{1}{2}$") plus the nominal drop through the bubble-cap. While actual numbers are not known, it should be noted that the engine load was measured to be slightly less with the exhaust passing through the bed and its plumbing than through the alternate exhaust train which was a muffler and plumbing. Also, this pressure drop was constant with time, it did not rise as soot was collected. In fact, it probably decreased slightly with time as the liquid warmed up.

Chapter 5.1: Experiments With Trapping

5.1 Experiments and Results

As noted in section 2.2, reentrainment of the highly conducting soot is a serious problem. An alternative to a wet-wall approach, trapping, has been studied to some extent. The electrostatic precipitator unit is shown in figures 5.1 and 5.2 . Flanges at either end of the ESP allowed easy attachment to and removal from the exhaust train. The corona element, either a hacksaw blade or needles, was insulated from ground by embedding it in a piece of teflon which also served as a removable top. No attempt was made to prevent fouling i.e. no air-injection. The brass side walls were also at ground potential and thus collected soot too. The traps were held in place by runners and rods and were constructed from steel shimstock, 8 mil thick. The particular shape was chosen for its ease of construction and with an intuitive guess as to the size of the trap space versus bounce surface (the top surface of the traps directly below the corona element).

Upstream of the ESP was plumbing leading to the ball valves. Heating tape and fiberglass insulation were wrapped around the pipe so that experiments could be conducted at realistic temperatures. Generally, the exhaust entering the ESP was 400°F-440°F. Downstream of the ESP was an orifice plate designed to measure flow velocities on the order of 2 m/s (standard). Impactor probes were placed upstream and

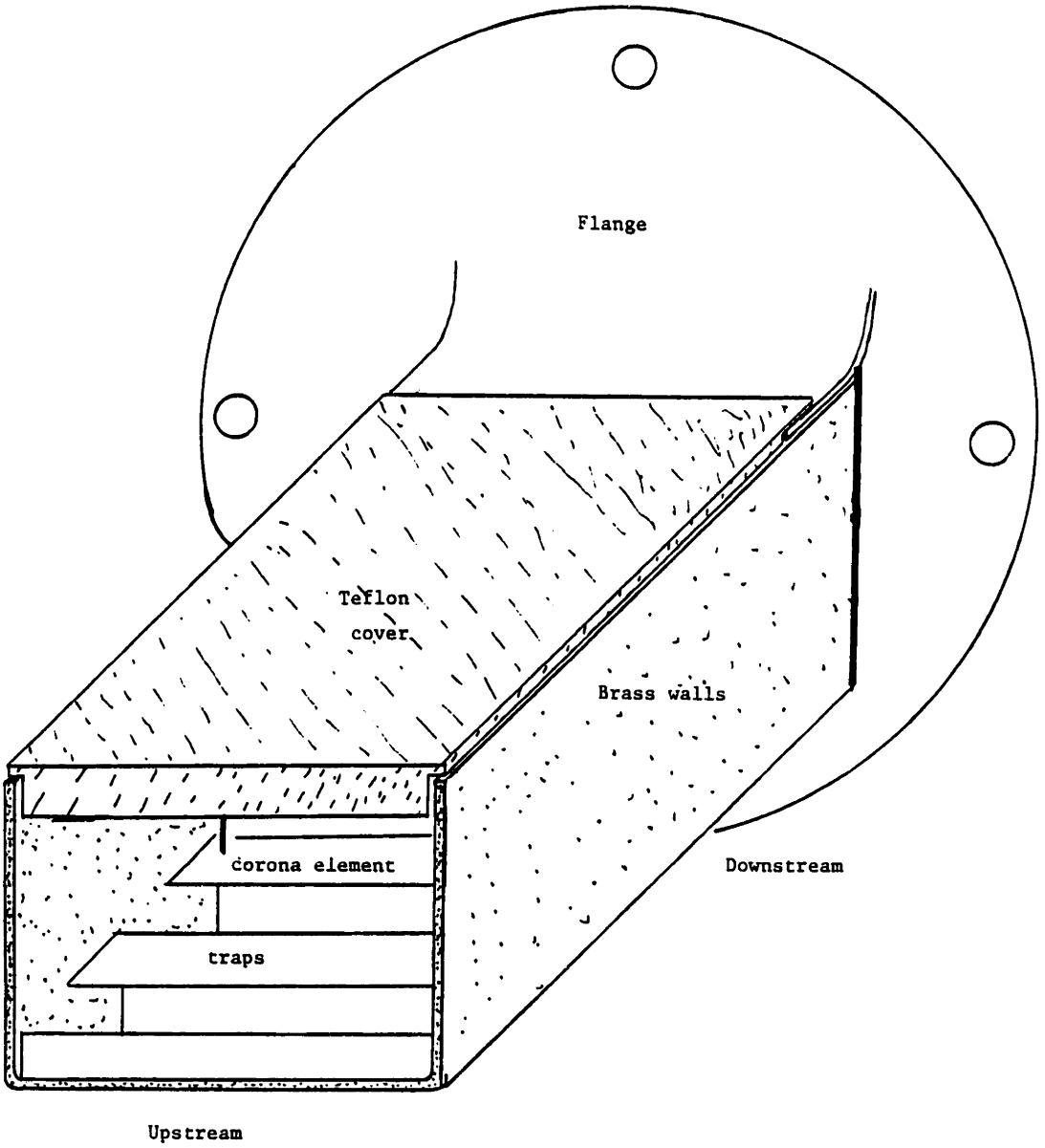

Cutaway view of ESP with traps

Figure 5.1

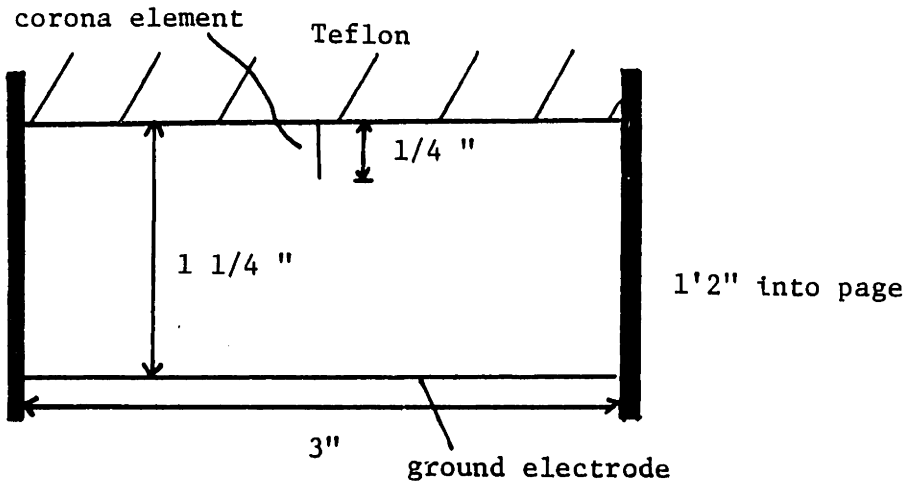

Cross-sectional View

ESP with traps

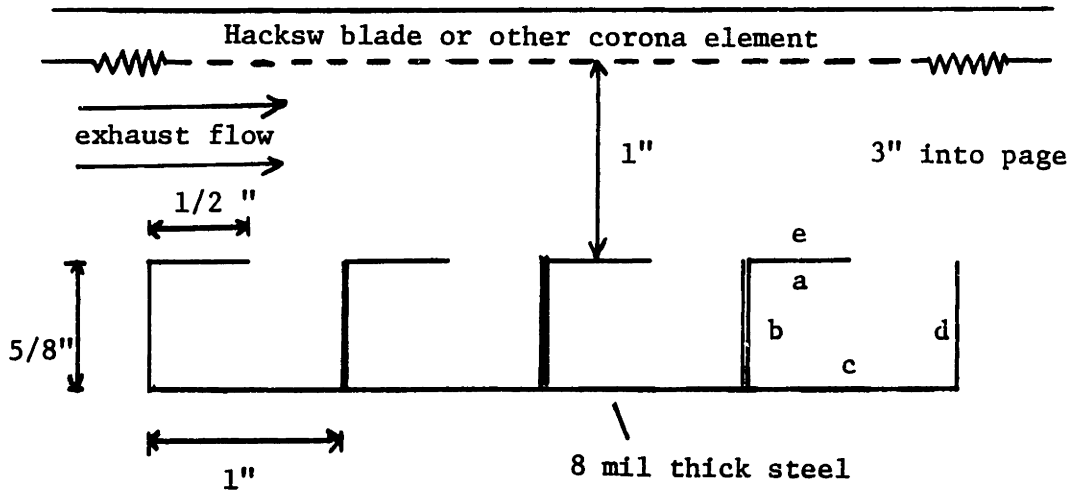

Cut-away side view

Figure 5.2

downstream of the ESP and were constructed to remove 1 scfm from an exhaust volume flow rate of 4 scfm (not ideal sampling situation).

The steady state engine conditions were close to those for the LEEFB. Engine RPM was 1890 and the air-to-fuel ratio was 38 (a fuel rate of .334 g/s), slightly higher than before. All experiments but two were conducted with an exhaust flow velocity of 1.6 m/s (at temperature). The impactor sampling duration was $\frac{1}{2}$ hr. due to the reduced flow rate.

With the traps as the collection electrode and a hacksaw blade as the corona element, the ESP was run for $4\frac{1}{2}$ hrs. After the first 45 minutes the power supply levels were stable at 9 kV and 2-3 mA. The collection efficiency was 95.3% for the first $\frac{1}{2}$ hr. and 80% after $3\frac{1}{2}$ hrs. of operation. Both impactor samplings are shown in figure 5.3 . The ESP with traps removed large particles well, it was basically the small, unagglomerated particulate that did not get collected. The increase in large particulates downstream in the later sample was probably due to flaking of large agglomerates off of the brass side walls - this partially accounted for the decrease in efficiency. Fouling of the charger was also responsible for this decrease.

Another run, at higher exhaust flow velocities and with a different corona element, produced comparable results. The exhaust flow velocity was 3.2 m/s (actual) as opposed to 1.6 m/s (actual) earlier. The corona element was composed of 7

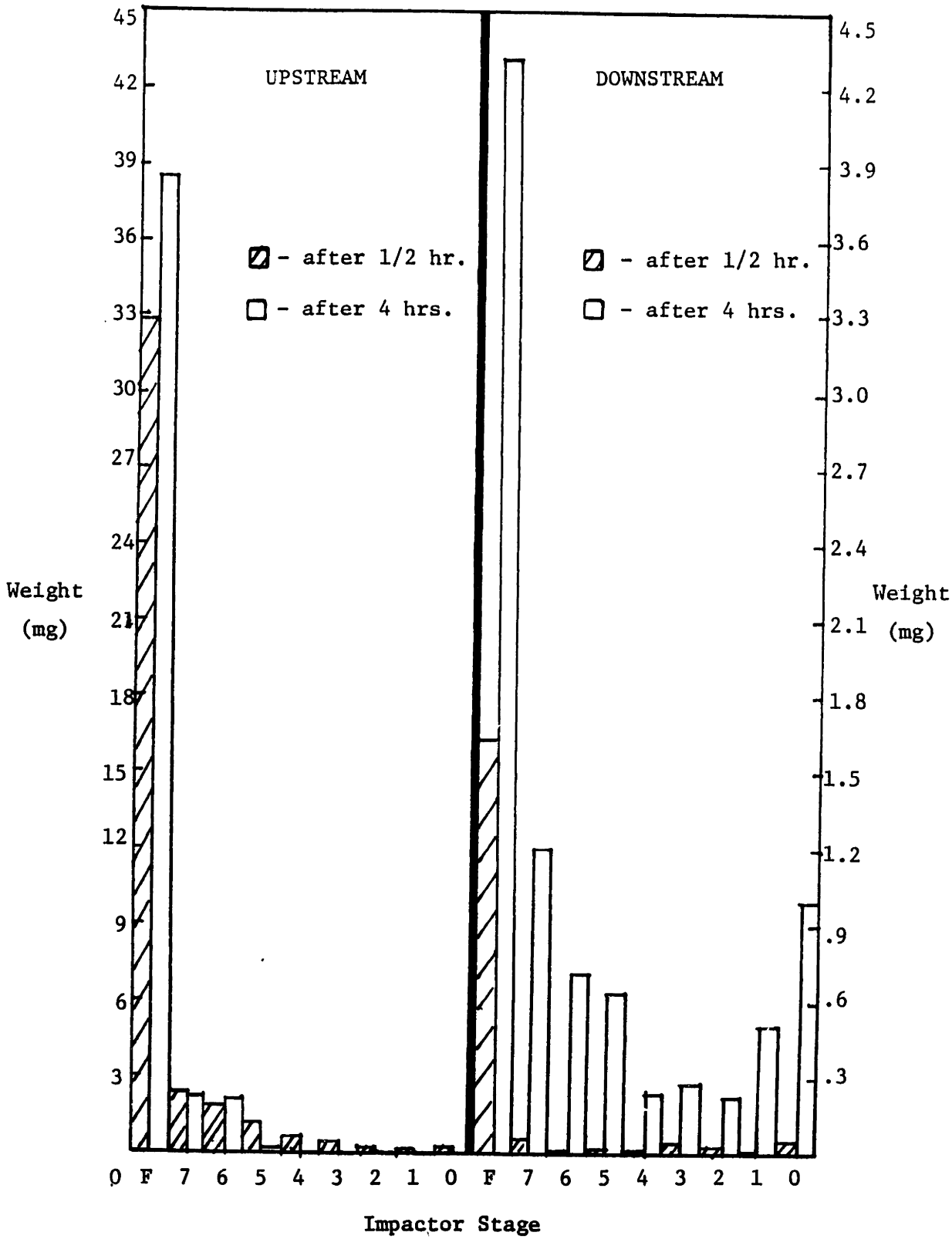

Impactor Sampling, hacksaw blade charger, flow velocity 1.6 m/s (actual)

Figure 5.3

needles stuck through the teflon at $1\frac{1}{2}$" intervals. Again the length of the run was $4\frac{1}{2}$ hrs. The power supply levels began at 9 kV, .5 mA but for the majority of the run were at 5 kV and 3 mA. For the first $\frac{1}{2}$ hr. of operation the collector efficiency was 92.5% but it was down to 76.9% by $3\frac{1}{2}$ hrs. into the run. Looking at the impactor sampling in figure 5.4 it was again evident that agglomerated particulate was being removed while some small particulate was making it through.

It appears that the idea of trapping works. Most of the particulate entering the device was agglomerated and collected. The trapping scheme operated well even at exhaust volume flow rates of 13.1 acfm. How high a volume flow rate can this device efficiently handle? Judging from figure 5.5 it appears that 13.1 acfm is rapidly approaching that limit. Each trap was weighed before and after a run thus yielding the distribution of soot trapped as a function of distance downstream. For the higher volume flow rate, the amount trapped tapers off much less with distance and is interpreted as follows. The surface area necessary for a collection efficiency comparable to the lower volume flow rate experiments' efficiency was approaching the total surface area of the device.

The distribution of soot within the trap was also obtained by carefully brushing and weighing the soot off of each surface. The trap surfaces and orientation to the exhaust flow are shown in figure 5.2. Several patterns emerged from these measurements, independent of the

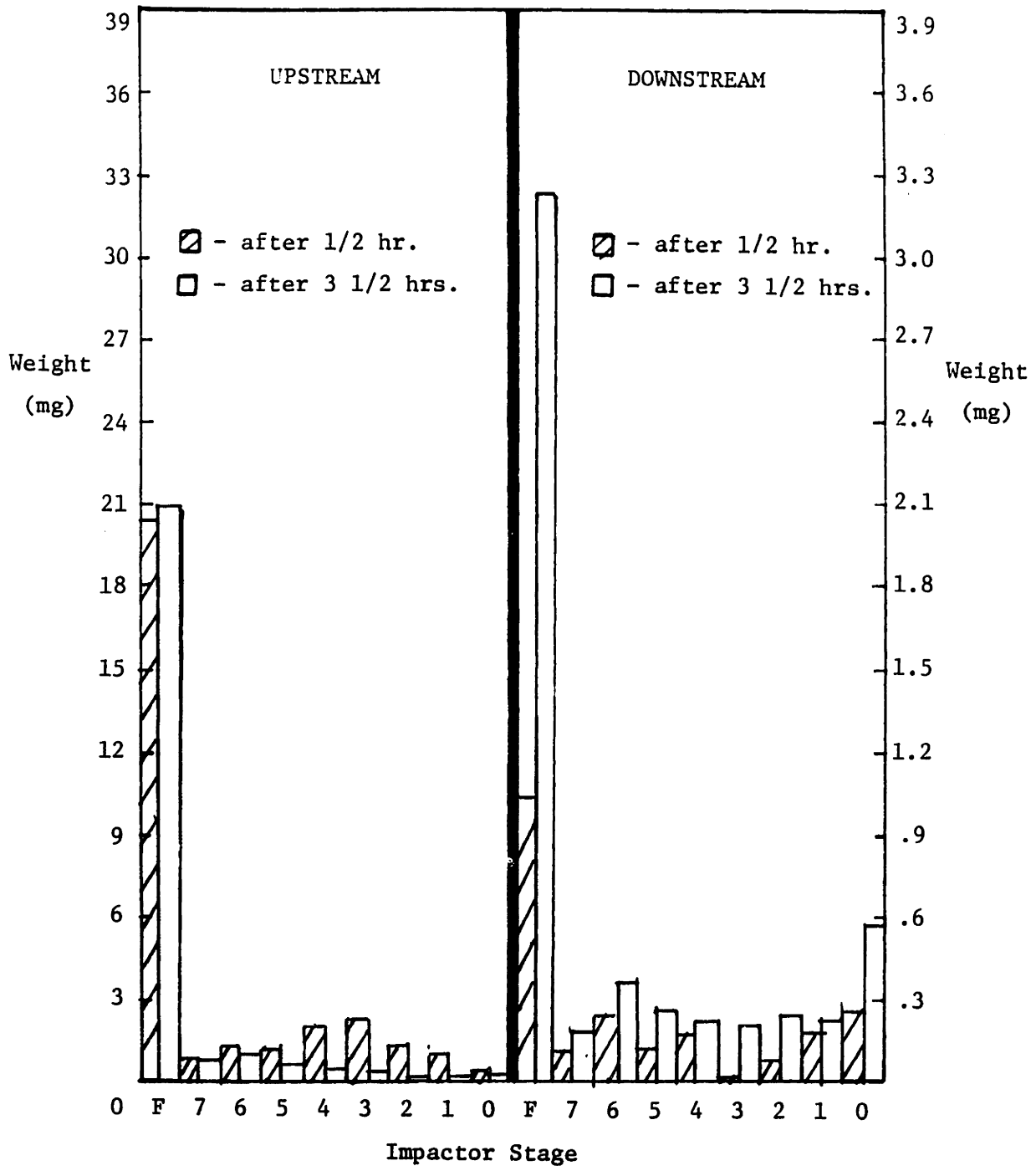

Impactor Samplings, 7 needle charger, flow velocity 3.2 m/s (actual)

Figure 5.4

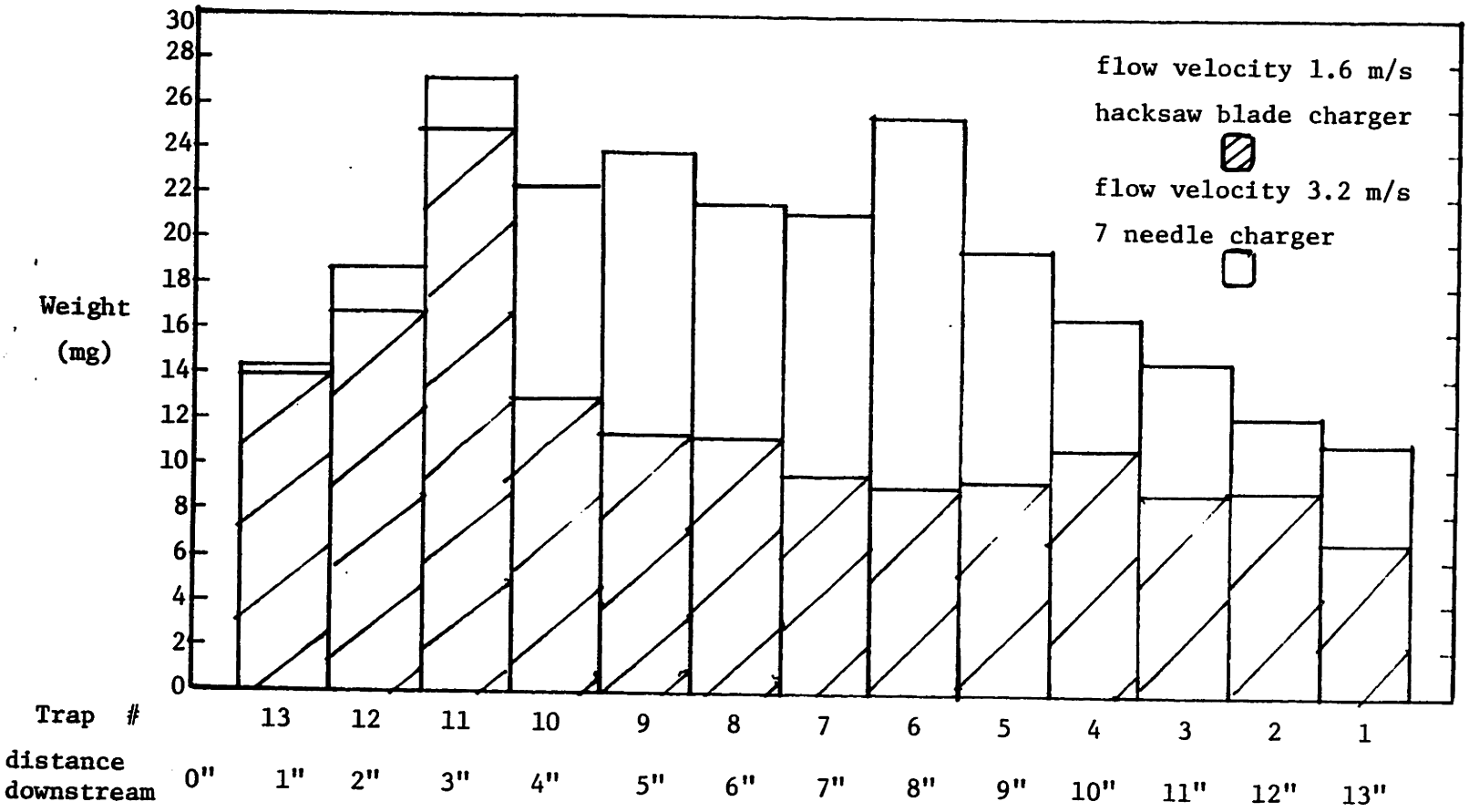

Trapped Soot Distribution Along Length of ESP, comparison of chargers

Figure 5.5

downstream location of the traps. The greatest amount of soot was deposited on surface c, the least on surface a and the amount on surface b was always less than that on surface d. This is contrary to the pattern that would be produced if electric forces dominated within the traps (in other words, if the particulate were large and highly charged). What is to be considered large and highly charged in this case? Pictures of soot inside the traps, figures 5.6 and 5.7 , show large agglomerates of soot. Did they arrive in the traps that way or did they agglomerate inside of the traps? This question will be addressed later on.

A curious phenomena resulted from the fouling of the charger. Some soot would reentrain from the bounce surface of the traps and the side walls, precipitate onto the teflon and adhere. The teflon surface soon became coated with soot in such a way as to leave two gaps, clean zones. One was between the high voltage corona element and the soot deposits and the other was between the grounded side walls and the soot deposits. In figures 5.8 and 5.9 these clean zones are shown with the hacksaw blade and with the needles. The high currents drawn from the power supply are attributed to breakdown and the resulting arc discharges across these gaps, perhaps triggered by particulate entering the clean zone. After a couple of hours the clean zones around the needles, or hacksaw blade, were getting smaller and dirtier - the fouling was shutting off the corona points. The electric field stresses in the region were reduced and this

Traps 12 11

Traps 10 9

Soot collected in traps after 1 hr. of operation

Figure 5.6

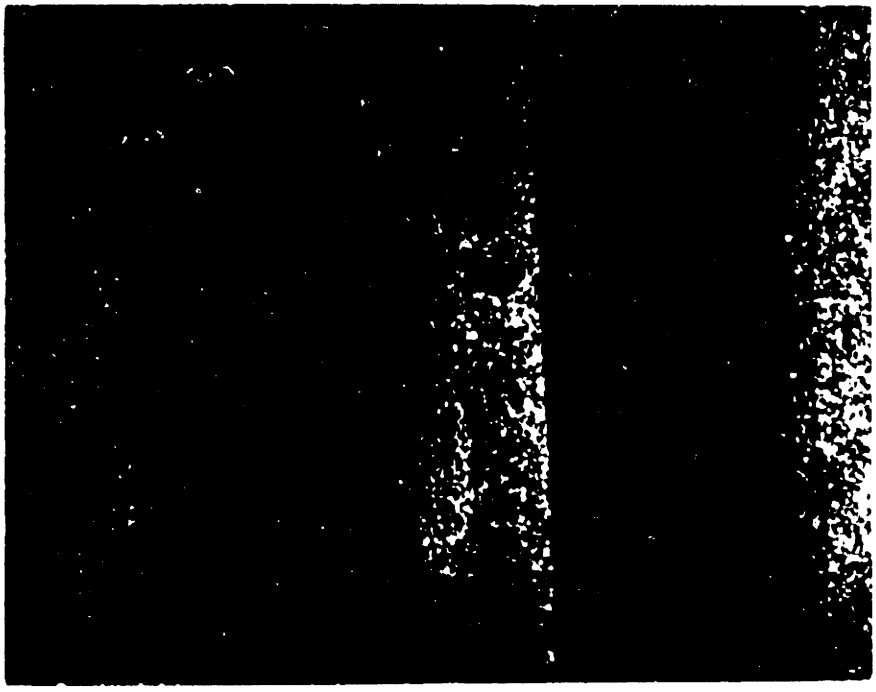

Traps 12 11

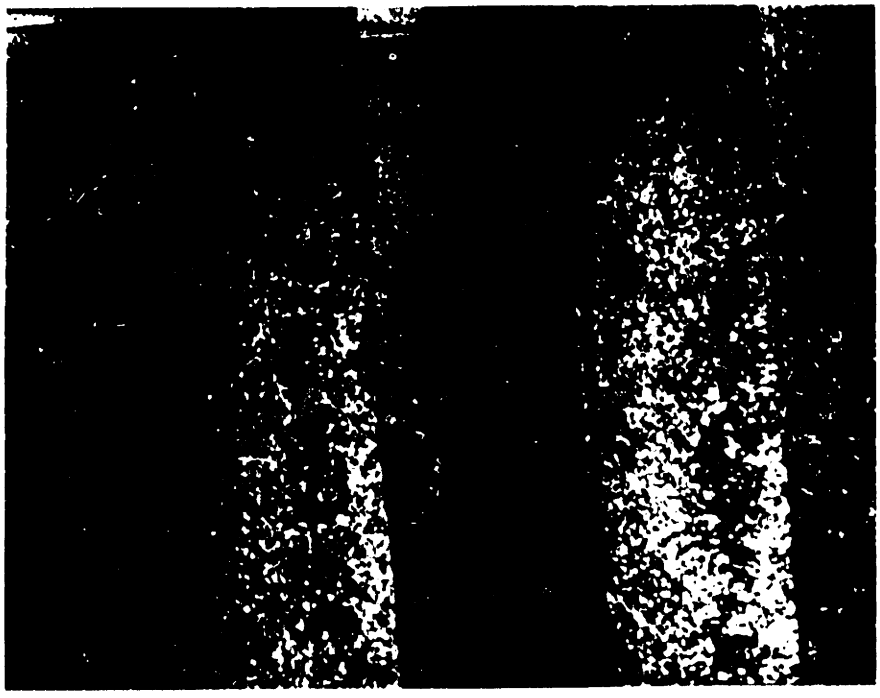

Traps 10 9

Soot collected in traps after 1 hr. of operation

Figure 5.6

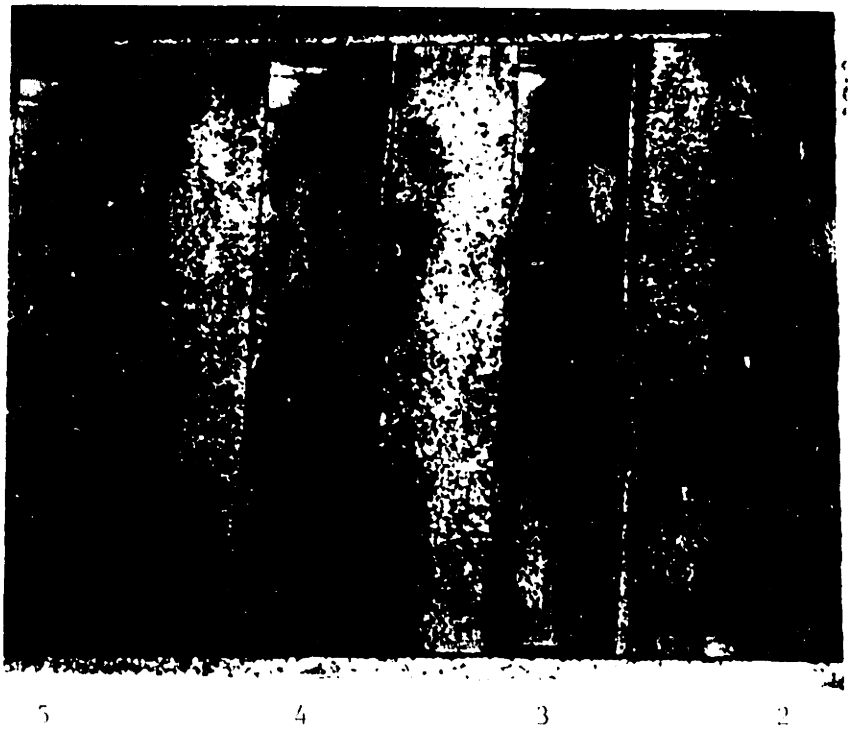

Soot collected in traps after 1 hr. of operation

Figure 5.7

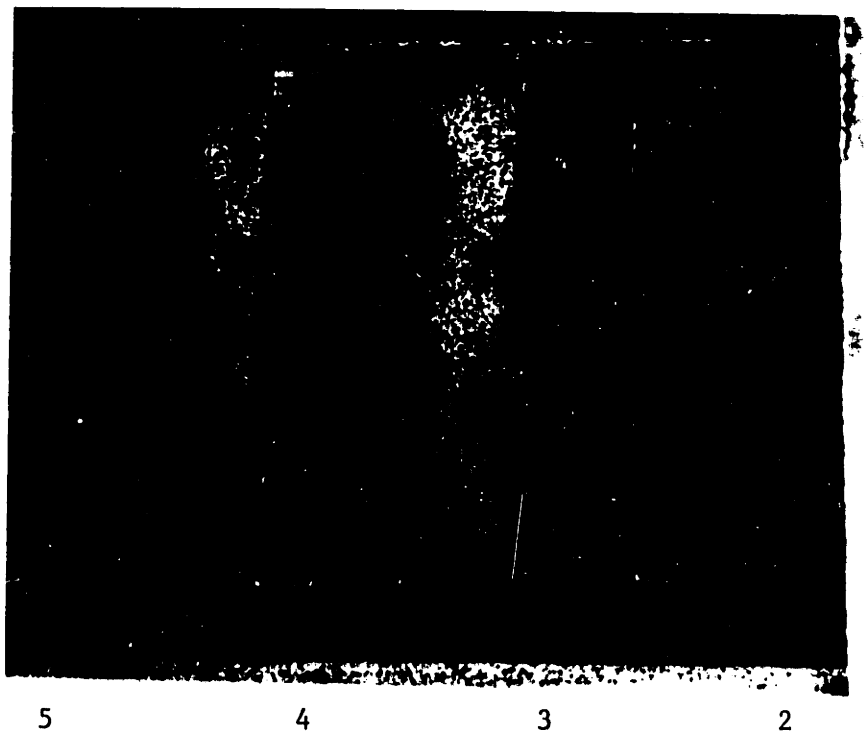

Soot collected in traps after 1 hr. of operation

Figure 5.7

INTENTIONAL DUPLICATE EXPOSURE

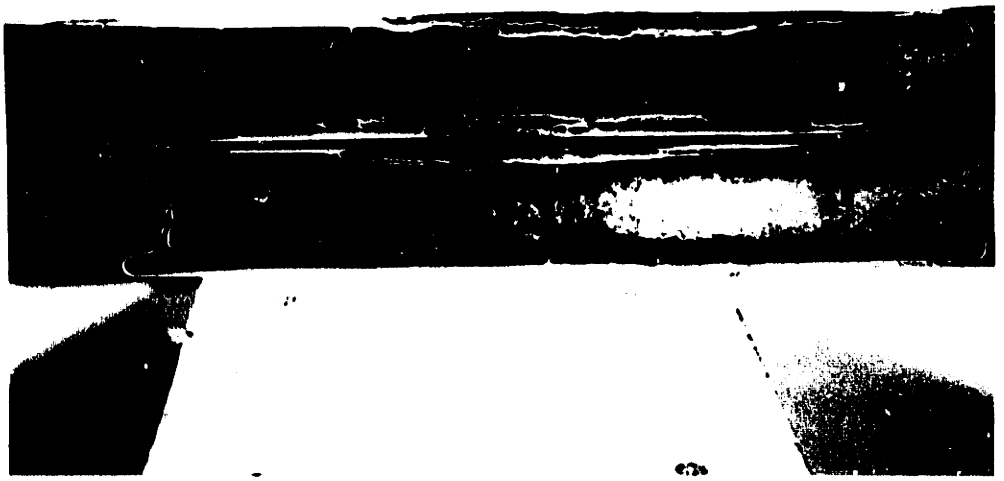

Hacksaw blade charger (perpendicular to page)

Upstream charger needles

Fouling of corona elements and surrounding clean zones

Figure 5.8

Hacksaw blade charger (perpendicular to page)

Upstream charger needles

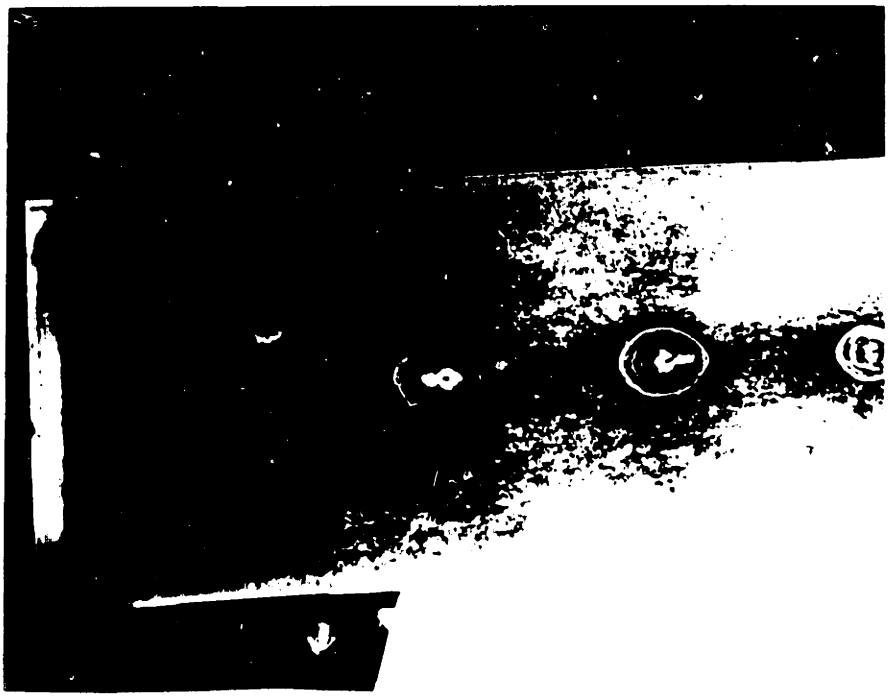

Fouling of corona elements and surrounding clean zones

Figure 5.8

INTENTIONAL DUPLICATE EXPOSURE

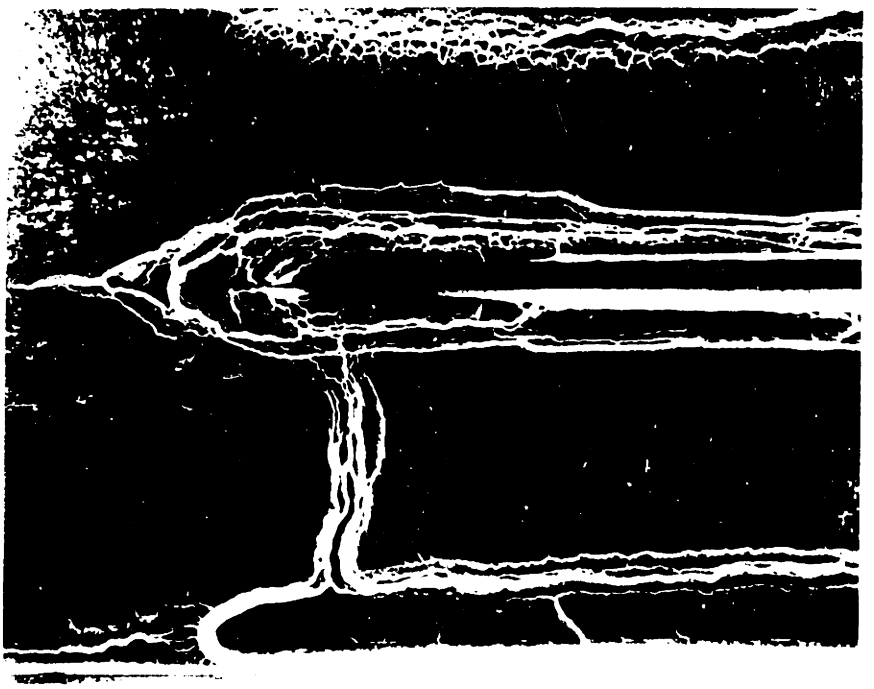

Close-up of hacksaw blade and clean zones

Figure 5.9

INTENTIONAL DUPLICATE EXPOSURE

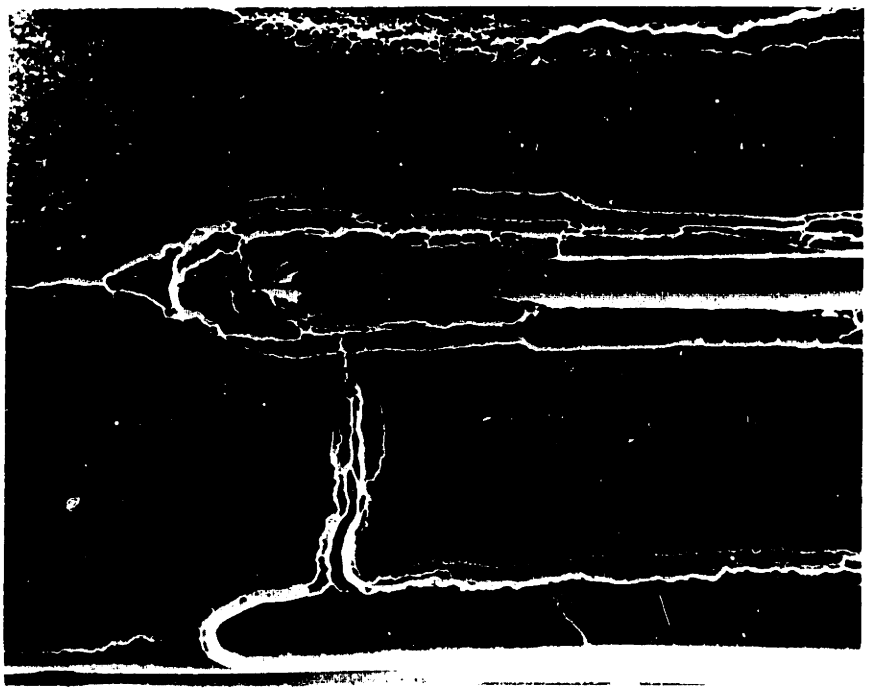

Close-up of hacksaw blade and clean zones

Figure 5.9

decreased the scouring action of the discharges. When the dirty teflon piece was removed and placed over a ground electrode - supported on either side by blocks of wood - the current readings were negligible, indicating that the corona points were completely turned off. Yet a large current of 2-3 mA was recorded while the corona element was still in the ESP. Not only were the leakage currents quite high due to fouling but the space charge that charges the incoming particulate must have been produced by the discharges taking place across the clean zone regions. This is not unreasonable since the electric stresses are very high and the soot-clean zone boundary is fairly sharp.

All the above experiments were conducted using the ESP in a single stage mode. In order to better isolate the issue of bouncing a two stage mode of operation was investigated. The charging stage was a needle, the collection stage was a flat plate electrode and both were opposite the traps (figure 5.10) . Two experiments were performed, one with a dry wall collector and one with a wet wall collector. For the wet wall collector, a thin layer of Dow Corning 200 series 60,000 cs silicone fluid was applied. At exhaust flow velocities of 3.2 m/s (actual) the gas residence time was too short for the physics of proper charging and agglomeration to occur. This judgement was based upon the visual evidence of no noticeable accumulation of soot in the traps or on the charger. Therefore, the experiments were conducted at flow velocities of 1.6 m/s (actual). The

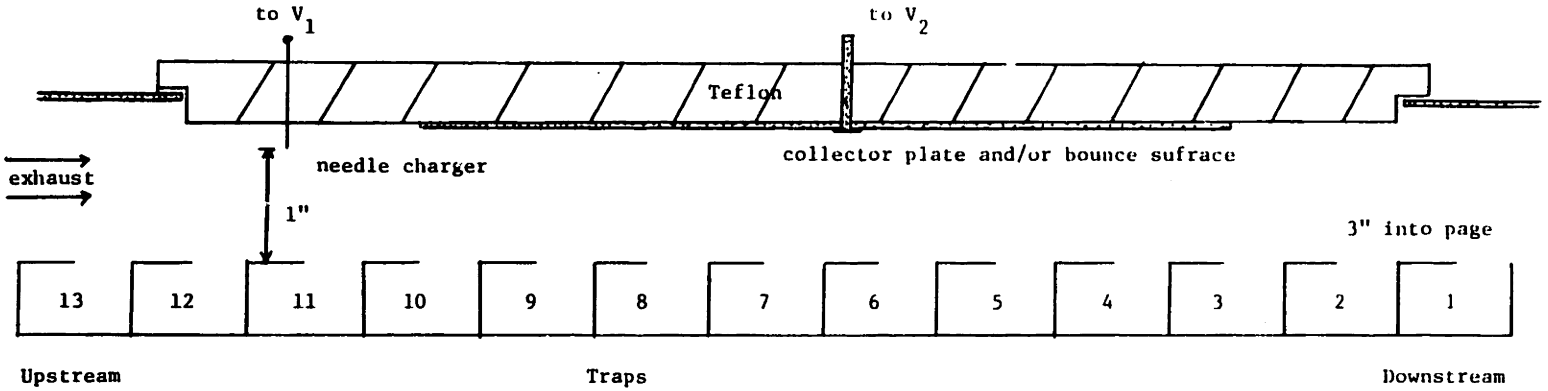

Two stage ESP layout

Figure 5.10

collection efficiency was 72.6% for the dry wall and 68.6% for the wet wall after 2 hrs. of operation. There are several factors that must be taken into account when comparing the devices' efficiencies. The mass loading for the wet wall run was 80.4% that of the dry wall run's mass loading. However, balancing that out was the reduced electric field that could be applied. It was harder to prevent conduction paths with the silicone oil present - this resulted in reduced applied voltages, 1.3 kV as opposed to 2.5 kV with a dry wall.

The trapped soot distribution downstream for both runs is shown in figure 5.11 . There is considerably more soot in the traps for the dry wall run, 2.6 times as much whereas the mass loading factor is only 1.2. The biggest differences are in traps 8-13, most of which are in the charger section. Coupled with the pictures of figure 5.12 this leads to an interesting thought. Does the particulate migrate against the flow? The wet wall collector is full of soot while the dry wall only has a fine coating. The charger region of the wet wall is fairly clean while the dry wall charger is fouled and has developed the clean zones and agglomerated soot coating characteristic of earlier runs. Since the difference between the two precipitators is in the collector stage and the silicone oil will prevent reentrainment of precipitated soot it is concluded that the soot does bounce between electrodes and, in fact, agglomerates to a large enough size where the electrical force dominates viscous

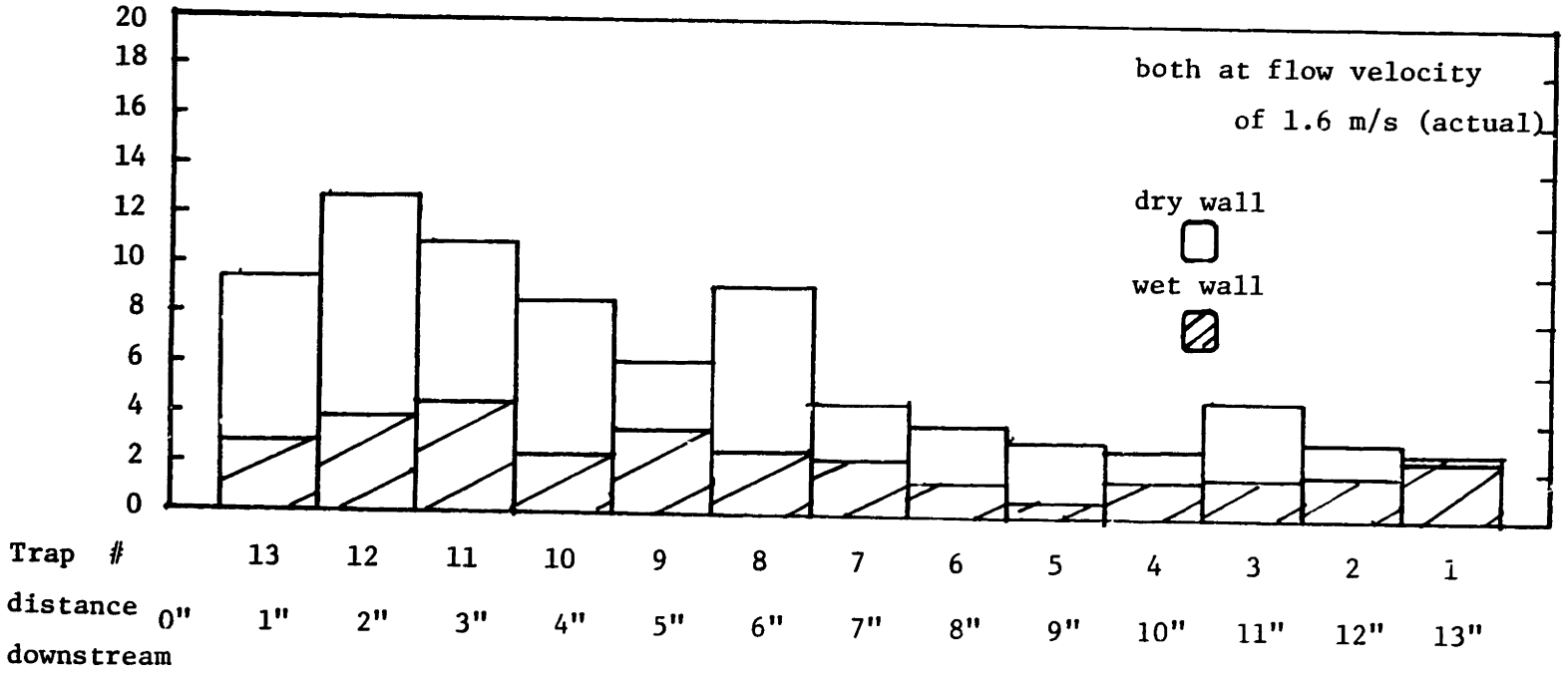

Trapped Soot Distribution Along Length of ESP, wet wall vs. dry wall

Figure 5.11

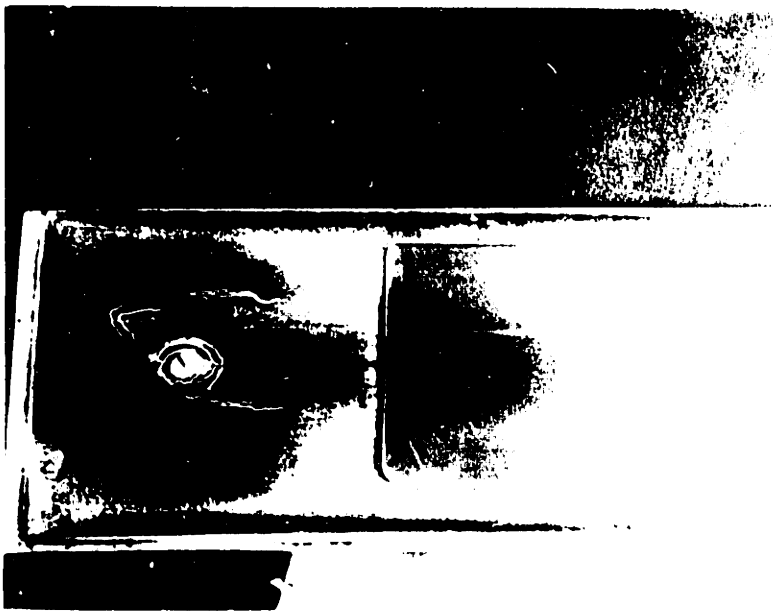

dry wall

after 1 3/4 hrs.
ESP operation

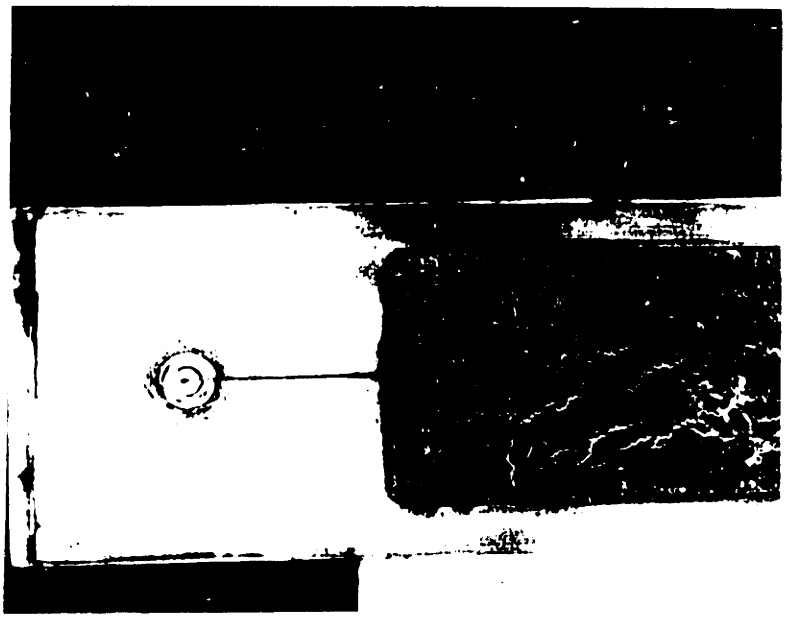

wet wall
(silicone oil)

Two stage ESP: charger and upper collection electrode

Figure 5.12

INTENTIONAL DUPLICATE EXPOSURE

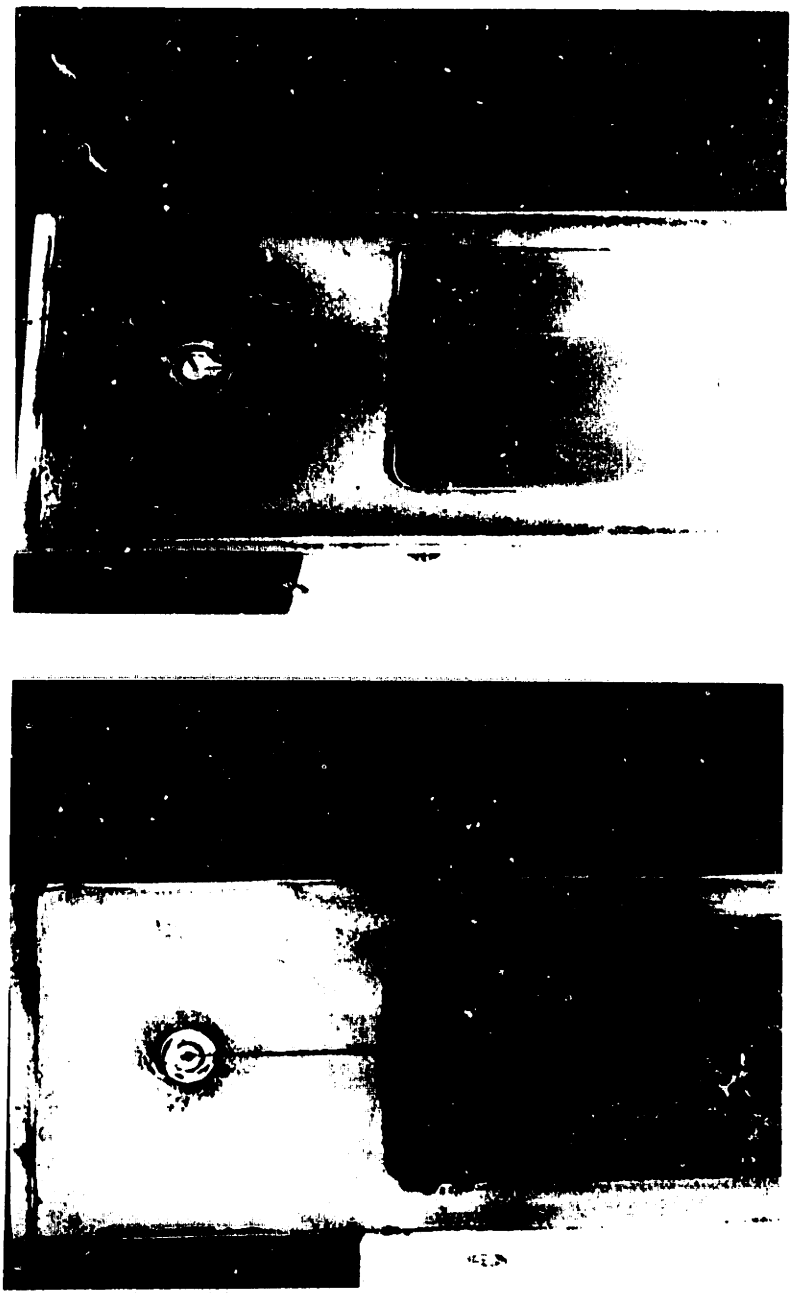

dry wall

after 1 3/4 hrs.
ESP operation

wet wall
(silicone oil)

Two stage ESP: charger and upper collection electrode

Figure 5.12

drag forces. This occurs when

$$\frac{bE}{U} > 1 \ . \qquad 5.1.1$$

With U = 1.6 m/s and E ≈ 10^5 V/m this implies mobilities on the order of 10^{-4} m^2/V-s or agglomerates of 1000 micron in diameter! This last result comes from a force balance between coulombic forces and Stokes drag on a sphere,

$$b = \frac{2a\varepsilon_o E}{\mu} \qquad 5.1.2$$

where μ is the viscosity of air at 400°F, $2.5x10^{-5}$ in MKS units (46). Using higher fields, $5x10^5$ V/m and allowing for the low bulk density of the soot particles reduces the estimate to something more reasonable, say 10-50 micron in size. Thus, it is conceivable for agglomerates to reach this size and migrate against the flow to foul the charger.

5.2 Discussion

What does determine the size to which precipitated soot agglomerates before reentraining? This is a hard question to answer, even qualitatively. There are many surface forces at work which are not easily accounted for. The lift-off force is due to the repulsion of a charged particle (sphere) resting on an infinite ground plane (calculated by Lebedev (47)) combined with a "kick" provided by the drag force of the exhaust in a boundary layer adjacent to the surface. Balancing these forces is the adhesion of the soot to the

surface, both mechanically and electrically. The London van der Waal's force, a time average force due to quantum electromechanical effects, has been calculated by Hamaker for the case of a sphere on a plane (48). Equating the electrical repulsive force ($E \simeq 5 \times 10^5$ V/m),

$$F_E = 1.37(4\pi\epsilon_o a^2 E^2) \qquad 5.2.1$$

to the van der Waal's force,

$$F_H = \frac{A\ 2a}{12\ z_o^2} \qquad 5.2.2$$

where A is the Hamaker constant, 10^{-20} J and z_o is the sphere-plane separation distance at the point of closest contact, 4×10^{-10} m, yields the unsettling conclusion that particles smaller than a diameter of 547 micron will stick. This calculation neglects any electrical double layer effects, irregularities in contact surfaces and the influence of adsorbed layers on the soot particles. In particular, electrical double layer forces can be quite important (49,50,51). Another factor to be included is the effect of a boundary layer. Clearly, the larger a particle the further it extends into the layer and the more of a drag force it experiences. Viewing this force as a catalyst, supplying sufficient energy to gain some separation between the particle and surface, the adhesive forces will drop rapidly once this initial separation occurs and the electrical force, combined with the exhaust flow, will then

dominate the reentrainment process.

Clearly the picture on a microscopic scale is very complex. The trapping process is not straightforward either. Writing a force balance equation for a soot particle in an electric and velocity field allows a comparison of the relative importance of each term.

$$F_{inert.} = F_{elect.} + F_{grav.} + F_{drag} \qquad 5.2.3$$

Substituting in for the forces yields,

$$m_s \frac{d^2\vec{r}}{dt^2} = q\vec{E} + m_s\vec{g}\cdot\vec{r} - 6\pi\mu a(\vec{v}_g - \frac{d\vec{r}}{dt}) \qquad 5.2.4$$

where m_s - mass of particulate $= \frac{4}{3}\pi a^3 \rho_s$

$\vec{r}$ - position of particulate

$\vec{v}_g$ - gas velocity $= U\vec{i}_z$

Dividing by $6\pi\mu a$ yields

$$\frac{2}{9}\frac{a^2\rho_s}{\mu}\frac{d^2\vec{r}}{dt^2} = b\vec{E} - \frac{2}{9}\frac{a^2\rho_s}{\mu} g\vec{i}_z - (U\vec{i}_z - \frac{d\vec{r}}{dt}) \qquad 5.2.5$$

where $b = \frac{q}{6\pi\mu a} = \frac{2a\epsilon_o E_o}{\mu}$ assuming saturation charging of the particulate. Plugging in known parameter values:

ρ_s - $.1\text{x}10^3$ kg/m^3

μ - $2.5\text{x}10^{-5}$ kg/m-s (at 400°F)

$$U - 1.6 \text{ m/s}$$

$$g - 9.8 \text{ m/s}^2$$

$$E_o - 5x10^5 \text{ V/m}$$

yields the following conclusions. Even for particles as large as 10 micron in diameter the inertial and gravitational forces are five and four orders of magnitude smaller than the drag force, respectively. The electrical force is within two orders of magnitude of the drag force for .1 micron sized particulate and it increases to the same magnitude for 10 micron diameter agglomerates. Thus, it is concluded that the inertia of the particle and gravitational effects can be neglected with respect to the acting electrical and viscous drag forces. Particle trajectories are determined by the field and flow patterns due to the specific geometry of the traps. As a first guess, assuming the velocity field is curl free implies that only the field need be determined. The boundary conditions, electrical and fluid, match up so the relationship between the individual field and flow vectors satisfy the Cauchy-Reimann conditions for complex variables. Finding the electric field for the specific trap geometry used requires a conformal mapping solution which results in an elliptic integral due to the necessity of having a minimum of 5 points to transform from one space to another.

Rather than go through this complex piece of math which would model only one trap in space and require much hypothesizing, a computer generated plot of a numerical

solution for the equipotentials, using a finite element relaxation method, is examined (figure 5.13) . Using a curvilinear squares technique to sketch in field lines leads to the following conclusions. Almost half the field lines entering the trap terminate on side d and most of the other half is divided among sides a and b, leaving very few field lines to terminate on side c. This is contrary to all the observations of deposition in a trap as noted in the previous section. Hence, the majority of the entering particulate are not very large - the electrical forces are subdominant to the viscous drag. This will tend to skew the deposition pattern downstream. Only particles with a high mobility will precipitate on sides a and b. Lower mobility particles will deposit on side c, tending towards the downstream direction, and on side d, which benefits from both the large number of field line terminations and the flow velocity pattern.

Agglomerates visible to the eye are observed in the traps (figures 5.6 and 5.7) - these are much larger than 10 micron. This deposition pattern, a mottled pattern where the trap bottom can be seen even in regions of thick deposits, has occurred elsewhere. When the LEEFB was run without a bed, as a two stage ESP, these patterns were seen on the high voltage insulator (figures 5.14 and 5.15) . This mottling is attributed to an increase in localized fields around a particle sitting on the surface. Modeling the situation as a perfectly conducting half-sphere atop an

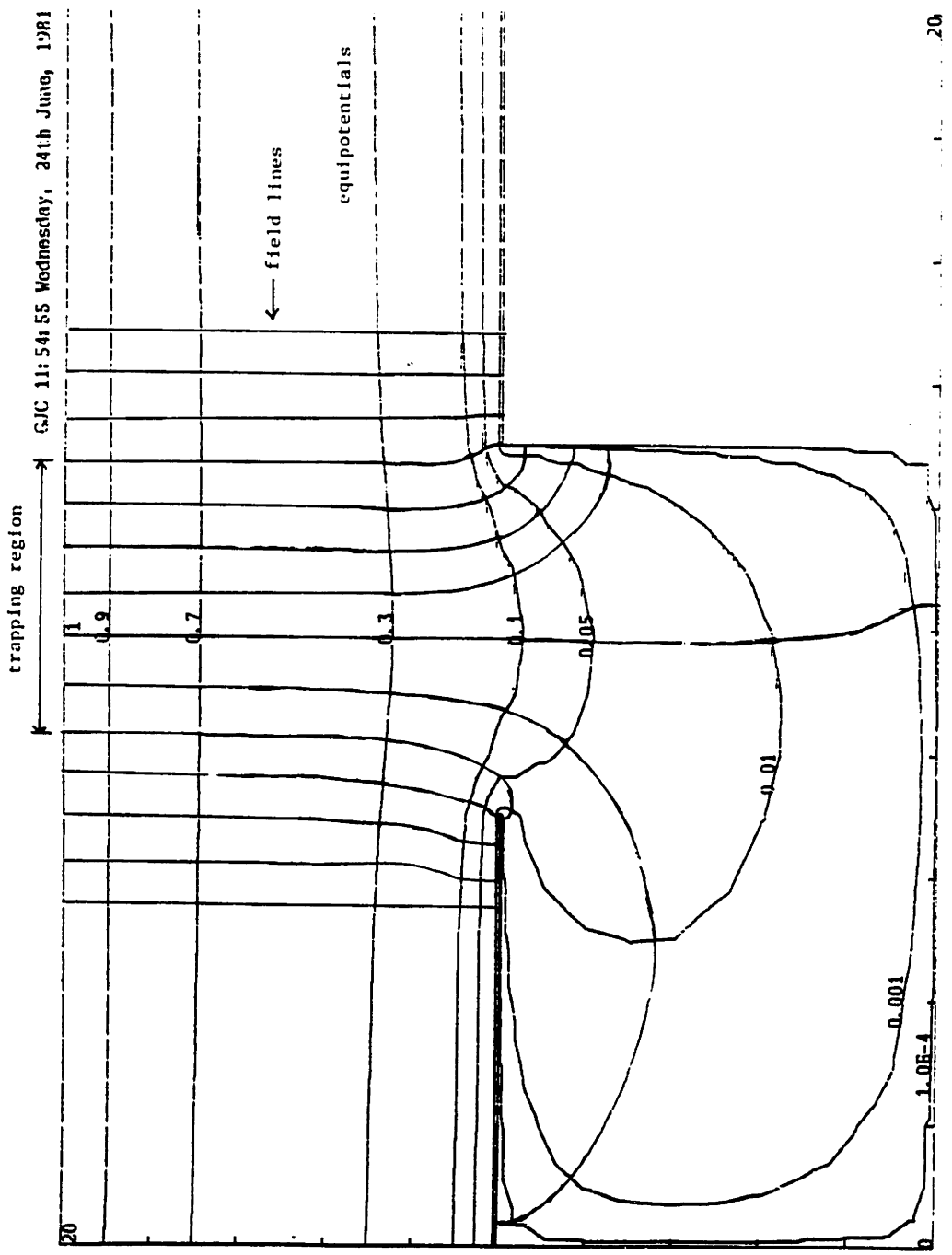

Figure 5.13

Plot of field lines inside a trap

Figure 5.14

Soot deposits on high voltage electrode and on insulator

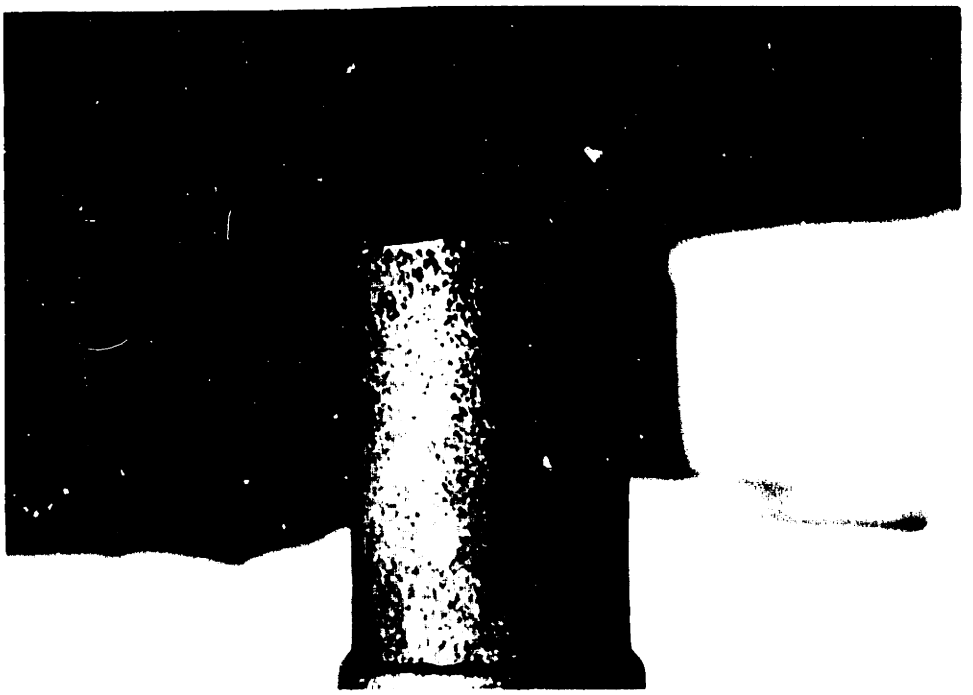

Soot deposits along length of insulator

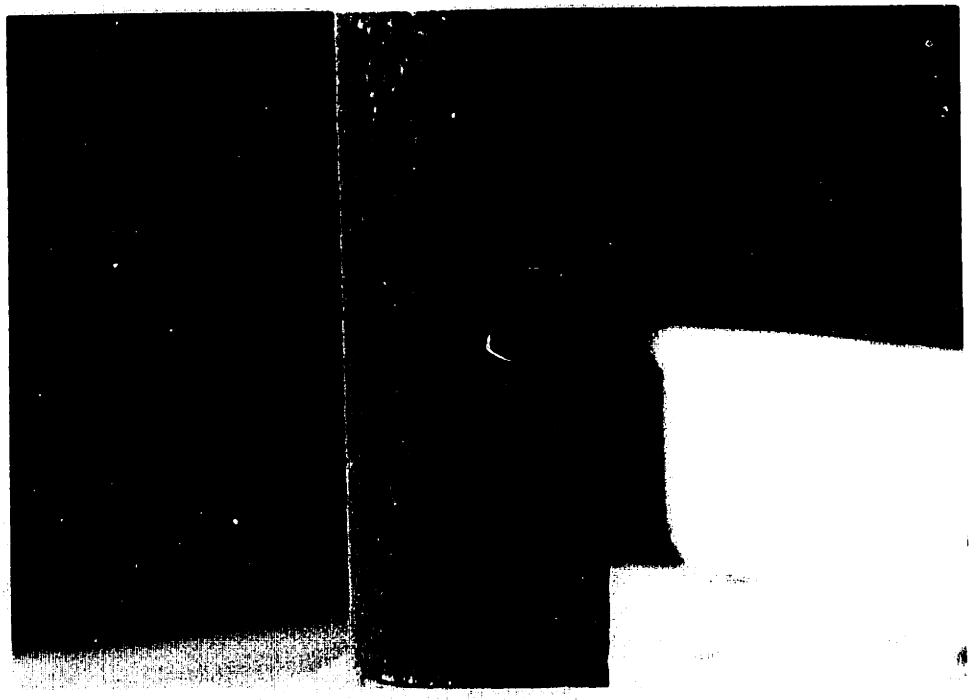

INTENTIONAL DUPLICATE EXPOSURE

Figure 5.1.

Soot deposits on high voltage electrode and on insulator

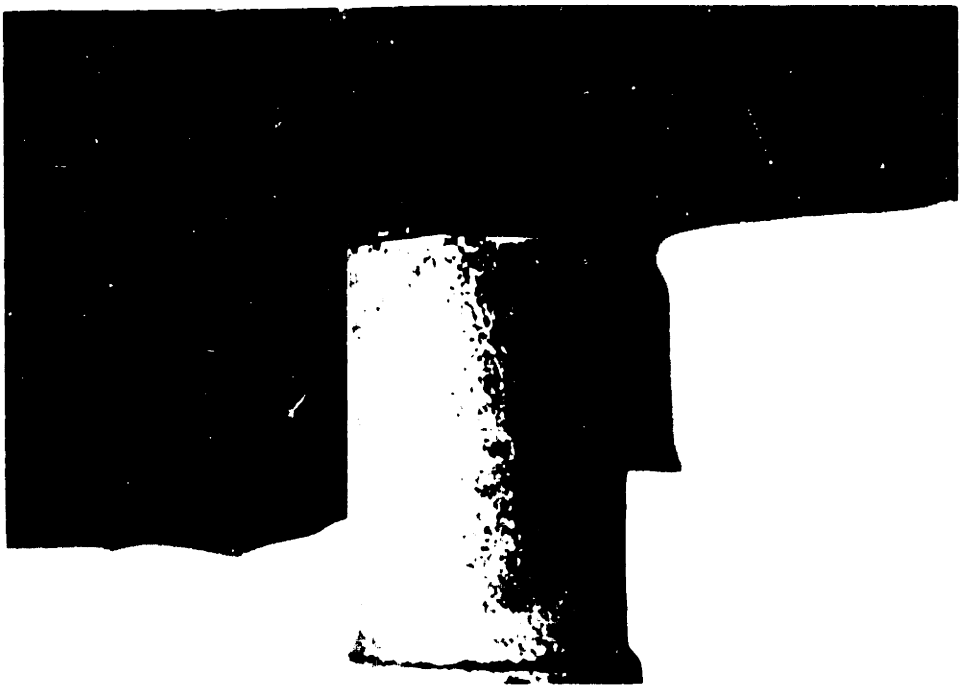

Soot deposits along length of insulator

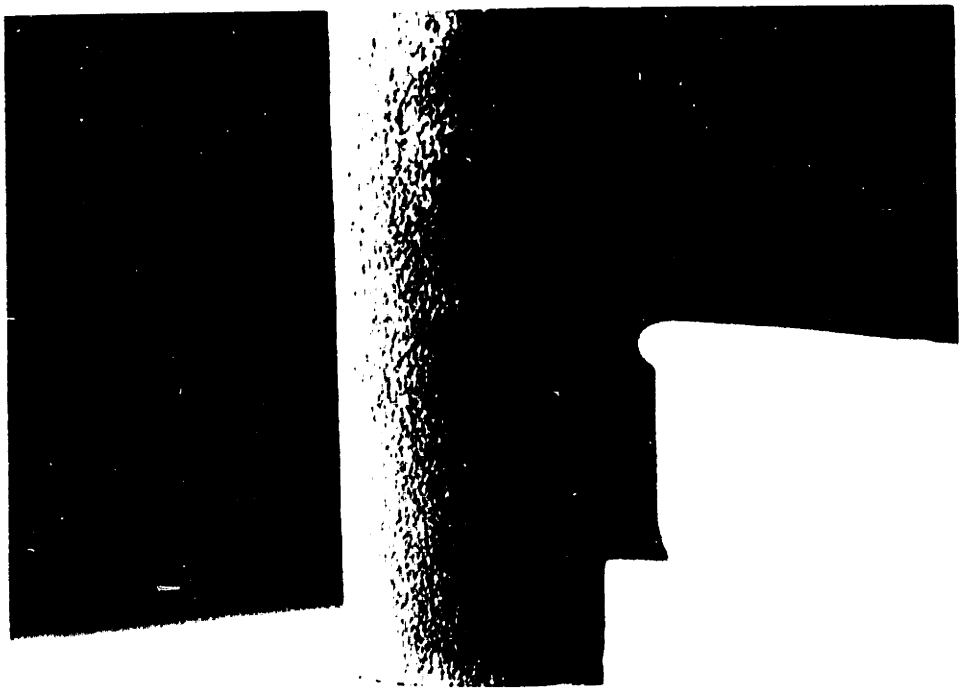

INTENTIONAL DUPLICATE EXPOSURE

Figure V.15

Close-up of soot deposition on insulator

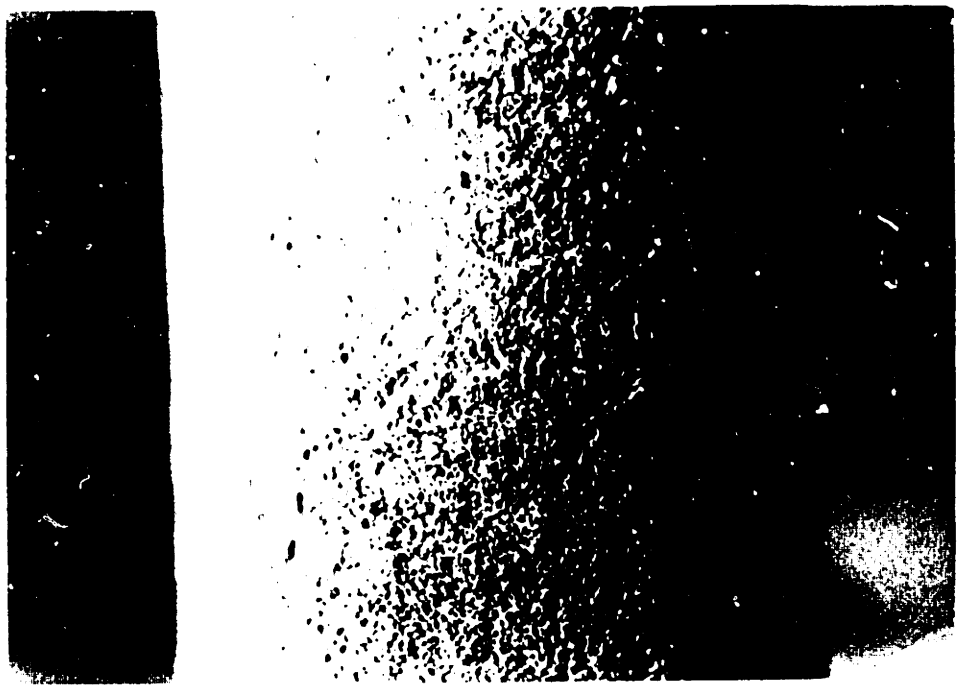

Surface of insulator exposed by scraping soot off

INTENTIONAL DUPLICATE EXPOSURE

Figure 5.15

Close-up of soot deposition on insulator

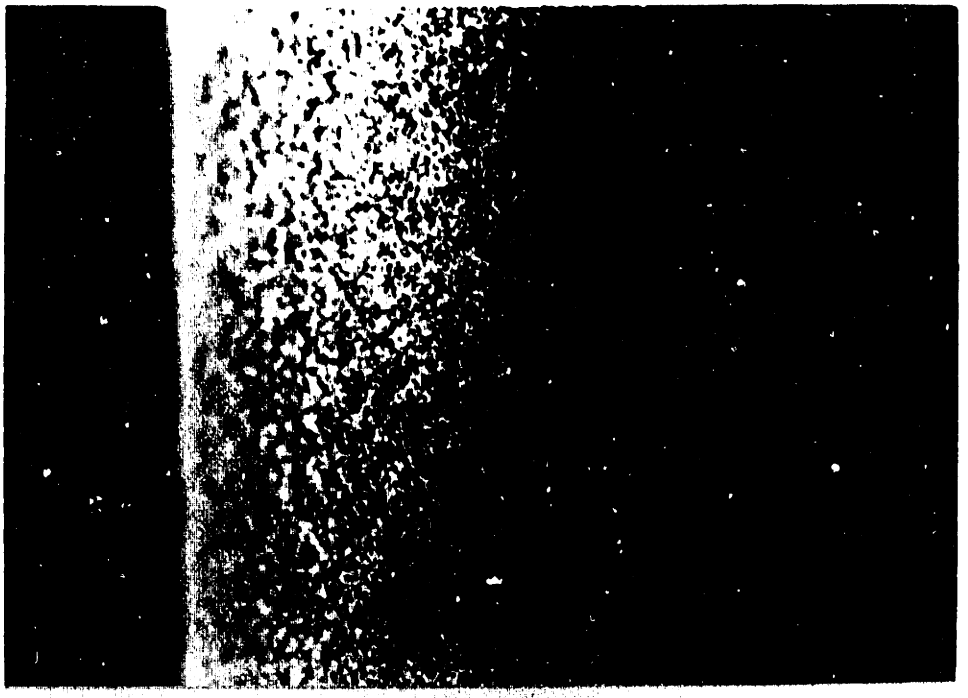

Surface of insulator exposed by scraping soot off

INTENTIONAL DUPLICATE EXPOSURE

infinite ground plane, it is easy to show that the radial field strength at the top of the hemisphere is a factor of three time greater than at the plane's surface. Particulate precipitating out within a neighborhood of deposits are more likely to end up on a deposit already there as opposed to starting a new deposit. This process further distorts the fields in the deposit's favor, so the process enhances the growth of previous deposits thus producing gaps through which the plane surface can be seen. Note also the marked difference between deposits on the insulator and on the metal. This is a demonstration of surface roughness playing a very important role in determining the adhesion of particles to a surface.

The last comparisons to be made are between experimental and theoretical efficiencies using a completely-mixed model for the ESP (equation 2.3.3). This can be rewritten as

$$\eta = 1 - e^{\frac{-A}{Q_v} bE} \qquad 5.2.6$$

where A is the surface area available for collection. For this ESP, A is 70 sq. in. or .486 sq. ft., if the side walls are included and the traps are taken to be flat plates. Using $E = 5 \times 10^5$ V/m, the lower exhaust volume flow rate of 6.6 acfm at an efficiency of 90% yields a mobility of 3.18×10^{-7} $m^2/V\text{-}s$,

$$b = -\frac{Q_v}{AE} \ln(1-\eta) \ . \qquad 5.2.7$$

Setting this equal to equation 5.1.2 yields particles with a diameter of 1.8 micron. This is reasonable and agrees well with previous conclusions. For the higher volume flow rate of 13.1 acfm and corresponding efficiency of 85% the particle diameter turns out to be 3 micron. It is doubtful that particles are agglomerating to a larger size when the exhaust velocities are higher. If anything, reentrainment of smaller particles than before should be the case.

Chapter 6: Conclusions And Future Work

6.1 Improvements To LEEFB

Two major obstacles stand in the way of practical application of the LEEFB to diesel cars. The easier of the two to be resolved is the increased power consumption due to soot buildup in the bed. Removal of soot from the bed can be accomplished by two mechanisms. As shown in section 3.2, electrophoretic removal can keep up with the incoming rate of collected soot. With proper electrode polarities the soot will migrate towards the outer wall and bottom of the bed. No large accumulation of soot or sludge in these regions was noticed but this is attributed to the scrubbing action of the recirculating bed particles. What is required is a sponge type material for an outer wall which will allow only soot to migrate through.

A solution which seems easier to realize is a cycling through of the oil. The thought here is very similar to the oil and oil filter in a car. Clean oil would be introduced from the top of the bed, possibly through a gap between the insulator and high voltage electrode. Dirty oil would drain through the bottom of the bed into a region where cleansing of the oil would take place. This cleansing could also be accomplished by electrophoresis, using the same power supply that is used for the bed. The cleansed oil would then be pumped back up to the top of the device and the cycle begun again. A low volume flow rate pump is required. This is

based upon the observation of excess pools of oil remaining in the device after the bed contents had been dumped out. These excesses indicate that the initial oil content (7.1% by mass) is large enough to expect a drain off of oil. If this amount of oil could be cycled through every hour then it is reasonable to believe that continuous, stable bed operation would be achieved. Of course, improvements in bed design resulting in increased efficiencies will also increase the rate of oil cycling.

Using 190 ml of oil as an estimate as to the amount of oil actually in a bed at a given instant in time, multiplied by 8 beds, yields a grand total of 1.6 quarts of oil. If the total reservoir of oil is twice that again, the total oil requirement for the device is 4.8 quarts.

The larger obstacle is the temperature limitation due to the volatility of the oil. This problem can be attacked from either end, cooling the exhaust or finding an oil that can withstand higher temperatures. Silicone oils are very attractive due to their good thermal stability. Lack of additives such as detergents, viscosity improvers and oxidation reducers, which serve as dispersing agents for soot immersed in oil, are a serious drawback to the silicone oils. The Dow Corning 210H specialty fluid was a step in the right direction. Soot remains dispersed in the oil for long periods of time but this is a macroscopic observation. Judging from the experiments performed, conduction paths occur at a much lower soot to oil mass loading with the

silicon oil than with the Shell oil. Perhaps there are other additives which could be blended in with the silicone oil which would disperse the soot better. Mineral oils such as the Shell oil will volatilize in significant amounts at temperatures above 300°F.

Another consideration is economical, the silicone oil costs at least four times as much as petroleum based oils. This, of course, depends upon the supply and demand of the product. If demand should go up dramatically with the use of the LEEFB, the supply must be altered too.

Directly cooling the exhaust down to temperatures of 300 F is very difficult given the constraints of size and cost. Using a water jacket heat exchanger would require a larger radiator and more durable water pumps. Cooling accomplished by air dilution requires a rather large fan in order to feed air at a pressure greater than the back pressure of the LEEFB, on the order of 6"-7" H_2O. Air cooling by conduction from pipes appears to work well. Typical exhaust temperatures are 1100°F at the exhaust manifold but cool down to 500°F after several feet of exhaust pipe.

Furthermore, the alteration of diesel exhaust temperatures, either up or down, is imminent. Regeneration studies of particulate filters invove raising engine exhaust temperatures so that soot oxidation can take place. On the other hand, certain strategies offer benefits in diesel engine performance and result in cooler exhaust

temperatures. An SAE paper entitled, "Trends in Diesel Engine Charge Air Cooling" takes just this approach (52). Basically, the idea is to have cooler air at the intake manifold. The cooler the air, the denser it is and thus, the higher a compression ratio that can be achieved by the turbocharger compressor. With more air available, and at a higher pressure, the more fuel that can be burned, resulting in increased power. NO_x emissions are reduced due to lower peak cycle temperatures in the pistons. Reduced fuel consumption and increased altitude capability are also mentioned. It is stated that the intake manifold temperatures required would be about 100°F lower than it is presently and that this would result in at least a 100°F drop in exhaust temperatures. Two basic cooling schemes are suggested, an air-to-air charge air cooling system and a low water flow system. The air-to-air cooling system uses the engine fan to blow air over the cooler. A water jacket is utilized with the low water flow system. This system also requires either two regular sized radiators or one oversized radiator.

It appears that operation at lower exhaust temperatures is not altogether out of the question. Several papers have suggested cooling engine exhaust so as to reduce hydrocarbon emissions. The cooler the exhaust, the more hydrocarbons that are adsorbed or condensed onto soot particles. Referring to the earlier discussion on impactor sampling techniques, it would appear that significant increases in

efficiency would result (see section 4.1).

Based on this discussion the middle road seems to be the correct one. Combine a system which will cool the exhaust some with a liquid that has better thermal stability. A target temperature might be 400°F, one which is well within the range of the silicone oils (assuming an additive that can disperse soot well can be found) or synthetic oils, as well as one which does not appear to require too much added machinery to accomplish the necessary heat transfer. There is always the bypass option if, under certain load conditions or accelerations, the exhaust temperature goes significantly above 400°F for a noticeable length of time.

As noted before, the gas distribution in the bed, even with the protruding lip, was very uneven (figure 4.16) The bed was not used to its full capacity and results in lower efficiencies than otherwise might be expected. The problem boils down to one of structures. How can structures be put into the bed without increasing the likelihood of conducting paths shorting out the bed - as occurred with the addition of the aftercharger? Possibly a combination of an outwardly sloped bubble-cap and a finned inlet tube would better distribute the exhaust. If some bed particles remained in the neighborhood of the fins during operation then their scrubbing action could help keep the fin surfaces clean, thus maintaining the high electric field breakdown requirement. The key points are how far out must the fins

extend to sufficiently break up the exhaust flow and is that distance compatible with the high electric fields required for corona discharge.

6.2 Status of LEEFB

The LEEFB is an important step in developing electrostatic devices to control highly conducting, submicron particulate. It is remarkable in that it can collect an appreciable amount of material which is essentially carbonaceous, having a conductivity on the order of 10^4 mhos/m, and maintain electric fields on the order of $2x10^5$ V/m throughout the bed for a reasonable length of time. As a test, the bed was run without a liquid. It shorted out within ten minutes of operation and operation was by no means stable, the current limited voltage was continually decreasing with time. The basic design and construction of the device is fairly simple, there are no fragile or finely tuned parts that require special design or must be protected. As presented in chapter 3, it is a complete system, not just one stage in the removal proceess.

The problems noted in section 6.1 are not specific to diesel engine applications only. The temperature limitation is placed by the particular liquid used in the bed and the choice of liquid depends upon the material to be collected. The particulate must be well dispersed by the liquid so that high bed conductivities are avoided. Higher efficiencies,

through better gas distribution and optimal bed design, will emphasize the need for a good method for removal of the collected particulate. This necessitates a careful study of the dynamics of cycling a liquid through the bed. A linear modeling of the problem would be a capacitor in parallel with a conductance. This would imply that a DC input of liquid would result in a rising exponential output similar to the charging of a capacitor. However, physical intuition says the output would be zero until a saturation level of liquid is present. This level, as well as the values of the capacitance and conductance, would depend upon many parameters: bed size, degree of fluidization, the nature of the liquid films surrounding the bed particles and possibly the volume flow rate of liquid into the bed. Thus the problem has turned into a complex one. Development of a material which would allow electrophoresis to remove the particulate from the bed would reduce the emphasis placed on cycling of the liquid.

6.3 Alternative Schemes

If the temperature restriction proves to be an insurmountable obstacle then EFB's must, in general, be ruled out. Without proper insulation, bed conductivities will rapidly approach the maximum current output levels of the power supply and operation will be curtailed. Only by feeding in clean bed particles and removing dirty ones can this be avoided.

An alternative is to use a spouting bed as an agglomerator. Recent work indicated collection efficiencies of up to 90%-95% when collecting DOP on #2 sand particles (53). Experimental volume flow rates were 16-18 scfm with a bed height of 20 cm. The spouted bed setup looked much like figure 3.4 with both plexiglass tubes removed and a corona wire suspended down the center of the bed. Spouting of the aerosol is centered about the corona wire. A wall of stable bed particles defined the width of the spout. The bed surrounding the spout can be treated as packed, resulting in much of the potential drop to be across the spout, depending upon bed conductivity. If the spout can sustain bed conductivities typical of a bed loaded with soot, then the spouted bed would be attractive as an agglomerator, part of a two stage system, to be followed by an inertial separator. In a spouted bed, proper location of the high voltage insulator can result in prevention of fouling of both the corona element and insulator by bed particle scrubbing within the spout. A possible danger is the initiation of arc discharges across the spout by the soot laden bed particles within the spout. Collection of particulate within the packed bed will be reduced due to the small potential drop across it resulting from high bed conductivity. The size to which the soot particles agglomerate to before reentraining is also unknown. A point in this favor is the relatively low degree of fluidization outside of the spout. The less bed particles jostle each other, the less impetus there is to

reentrain.

Another approach is to combine electrostatic agglomeration and inertial impaction in one unit. Such a device, called an electrocyclone, is under investigation (54). A corona electrode (rod) is suspended down the center of the cyclone and gas is introduced tangentially into the unit. Contrary to ESP's, collection of smaller particulate implies smaller devices - this increases inertial separation forces. The price paid is an increase in pressure drop. Proper introduction of dirty gas into the cyclone will result in a large percentage of the particulates being located adjacent to the outer wall where a strong collection field exists. Eventually, soot would flake off of the wall and down into a hopper for storage. Fouling of the charger and high voltage insulation is prevented by the exiting clean gas blowing over the suspended corona element. The main problem here appears to be the pressure drop required to provide sufficient collection efficiencies of small particulate. All other problems (as outlined in section 2.2), appear to be resolvable.

Bibliography

1. "General Motors Response to EPA Notice of Proposed Rulemaking on Particulate Regulation for Light-Duty Diesel Vehicles," Attachment 4, General Motors, submission to EPA, April 19, 1979.

2. Williams, D.S.D., ed., The Modern Diesel, Development and Design ,Butterworth Co., London (1972), p. 22.

3. Amano, M., Sami, H., Nakagawa, S. and Yoshizaki, H., "Approaches to Low Emission Levels for Light-Duty Diesel Vehicles," SAE paper 760211, 1976.

4. Springer, K., Stahman, R., "Diesel Car Emissions - Emphasis on Particulate and Sulfate," SAE paper 770254, 1977.

5. Notice of Proposed Rulemaking, Particulate Regulation for Light-Duty Diesel Vehicles, Federal Register, Vol. 44, No. 23, Feb. 1, 1979.

6. Amann, C.A., Stivender, D.L., Plee, S.L. and MacDonald, J.S., "Some Rudiments of Diesel Particulate Emissions," SAE paper 800251, 1980.

7. Federal Register - Vol. 45, No. 45 - Wednesday, March 5, 1980.

8. Marshall, E., "Safe to Delay 1985 Diesel Rule, Study Says," Science, vol. 215, Jan. 15, 1982, p. 268.

9. "Deposition and Retention Models For Internal Dosimetry Of The Human Respiratory Tract," Task Group On Lung Dynamics, Health Physics, Vol. 12, 1966, pp. 173-207.

10. Faulkner, M.G. Dismukes, E.B., McDonald, J.R., Pontius, D.H. and Dean, A.H., NTIS PB 80-128655 Oct. 1979.

11. Kaden, D.A., "Mutagenicity Of Soot And Polycyclic Aromatic Hydrocarbon Soot Components To S. Typhimurium," S.M. Thesis MIT Nutrition May, 1978.

12. Hagstrom, R.M., Sprague, N.A. and Landau, E., "The Nashville Air Pollution Study: VII. Mortality From Cancer in Relation to Air Pollution," Archives of Environmental Health, Vol. 15 Aug. 1967, p. 237.

13. White, H.J., Industrial Electrostatic Precipitation , Addison-Wesley Pub. Co., Reading, MA 1963.

14. Masuda, S. and Moon, J.D., "Moving Belt Type Electrostatic Precipitator for Control of Diesel Engine Particulates," Scientific Bulletin, Dep't Of The Navy

Office Of Naval Research Tokyo, Vol. 6, No. 2, April-June 1981, p. 39.

15. Hoenig, S.A., "New Application of Electrostatic Technology to Control of Dusts, Fumes, Smoke and Aerosols," IEEE Trans. on Industry Applications, Vol. IA-17, No. 4, July/Aug. 1981, p. 386-391.

16. private communication, Stuart Hoenig, Unniv. of Ariz.
17. Springer, K. and Stahman, R., "Removal of Exhaust Particulate from a Mercedes 300D Diesel Car," SAE paper 770716, 1977.

18. "Particulate Control Highlights: recent developments in Japan" NTIS PB 80-148802 May-July 1979.

19. Howitt, J.S., and Montierth, M.R., "Cellular Ceramic Diesel Particulate Filter," SAE paper 810114, 1981.

20. Wade, W.R., White, J.E. and Florek, J.J., "Diesel Particulate Trap Regeneration Techniques," SAE paper 810118, 1981.

21. "Particulate Filters: a 'must' for light-duty diesels?", Automotive Engineering, Vol. 89, No. 3, March 1981.

22. Murphy, M.J., Hillenbrand, L.J., Trayser, D.A. and Wasser, J.H. "Assessment of Diesel Particulate Control-Direct and Catalytic Oxidation," SAE paper 810112, 1981.

23. Wade, W.R., "Light-Duty Diesel NO_x-HC-Particulate Trade-Off Studies," SAE paper 800335, 1980.

24. "Diesel Exhaust Filter uses steel wool," Automotive Engineering Vol. 90, No. 4, April 1982, p.57 based on SAE paper 820183.

25. Sittig, Marshall, Automotive Pollution Control Catalysts and Devices , Noyes Data Corp., Park Ridge, NJ, 1977.

26. Campanile, A., "Soot Removal and Heat Recovery From Diesel Engine Exhaust By Means Of A Fluidized Bed Filter/Agglomerator and Heat Exchanger," Proceedings International Symposium on Automotive Technology and Automation, Vol. 1, Torino Sept. 8-12 1980, p. 165.

27. Amann, C., and Siegla, D., "Diesel Particulates-What They Are and Why," GMRL publication 3672, 1981.

28. Stoy, W.S. and Garret, M.D., "Carbon Black," ch. 5 from Treatise On Coatings, Vol. 3, Pigments, Part I ed. by Myers, R.R. and Long, J.S., Marcel Dekker, Inc., NY, NY, 1975.

29. Pinheiro, G., "Precipitators for Oil-Fired Boilers," Power Engineering, Vol. 75, No. 4, April, 1971, p. 52.

30. Walker, A.B., "Enhanced Scrubbing of Black Liquor Boiler Fume by Electrostatic Pre-Agglomeration: A Pilot Plant Study," JAPCA, Vol. 13, No. 12, Dec. 1963, p. 622.

31. Drogin, J., "Carbon Black," JAPCA, Vol. 18, No. 4, Dec. 1963, p. 216.

32. Melcher, J.R., Sachar, K. and Warren, E.P., "Overview of Electrostatic Devices for Control of Submicron Particles," Proceedings of the IEEE, Vol. 65, No. 12, Dec. 1977, p. 1659.

33. Zahedi, K. and Melcher, J.R., "Electrofluidized Beds in the Filtration Of a Submicron Aerosol," JAPCA, Vol. 26, No. 4, April, 1976, p.345.

34. Kunii, D. and Levenspiel, O., Fluidization Engineering Kreiger Pub. Co., Huntington, NY, 1977, p. 76.

35. Melcher, J.R., "Continuum Electromechanics," MIT Press, Cambridge, MA,1981, p. 5.9.

36. Zieve, P.B., Zahedi, K., and Melcher, J.R., "Electrofluidized Bed in Filtration of Smoke Emissions from Asphaltic Pavement Recycling Process," Envir. Sci. and Tech., Vol. 12, No. 1, Jan. 1978, p. 96.

37. Alexander, J.C., " Electrofluidized Beds In The Control Of Flyash," PhD. Thesis, MIT EECS May, 1978.

38. private communication, Kevin G. Rhoads.

39. private communication, James Spearot, GMRL.

40. Simpson, H.B.D. III, "Effect of Operating Conditions On The Particulates From A Single Cylinder Diesel Engine," SM Thesis MIT Mech. E Dec. 1980, p. 96.

41. Rouse, H., Elementary Mechanics of Fluids , Wiley NY, NY, 1946.

42. Frisch, L.E., Johnson, J.H. and Leddy, D.G., "Effect of Fuels and dilution Ratio on Diesel Particulate Emissions," SAE paper 790417, 1979.

43. Lipkea, W.H., Johnson, J.H. and Vuk, C.T., "The Physical and Chemical Character of Diesel Particulate Emissions- Measurement Techniques and Fundamental Considerations," SAE paper 780108, 1978.

44. Khatri, N.J., Johnson, J.H., and Leddy, D.G., "The

Characterization of the Hydrocarbon and Sulfate Fractions of Diesel Particulate Matter," SAE paper 780111, 1978.

45. private communication, David Ripple, Cleveland Research Center, Lubrizol Corp.

46. op. cit., Melcher, p. 5.4.

47. Lebedev, N.N., and Skal'skaya, I.P., Sov. Phy. Tech. Phy. Vol. 7, No. 3, Sept. 1962, p. 268.

48. Hamaker, H.C., Physica, Vol. 4, 1937, p.1058.

49. Gregory, J. and Wishart, A.J., "Deposition of Latex Particles On Alumina Fibers," Colloids and Surfaces, Vol.1, 1980, pp. 313-334.

50. Deryaguin, B.V., Muller, V.M. and Toporov, Y.P., "Effect of Contact Deformation on the Adhesion of Particles," J. of Col. and Int. Sci., Vol.53, 1975, p. 314.

51. Aleinikova, I.N., Deryaguin, B.V. and Toporov, Y.P., "The Electrostatic Component Of Adhesion Of Dielectric Particles To A Metal Surface," Colloid Journal, Vol. 30 1968, p. 128.

52. Sekar, R.R., "Trends in Diesel Engine Charge Air Cooling," SAE paper 820503, 1982.

53. MacGinitie, L., "Electromechanics and Filtration Efficiency Of Spouted Beds With Corona Discharge," SM Thesis, EECS, May, 1982.

54. Giles, W.B., "Electrostatic Separation in Cyclones," Proc. First Symp. on the Transfer and Utilization of Particulate Control Technology, Vol. 3, 1979, p. 291.